Squeezing flows in the non-Newtonian fluids
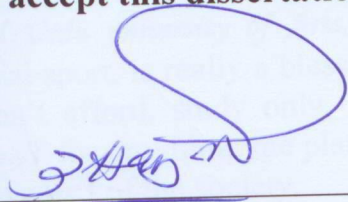
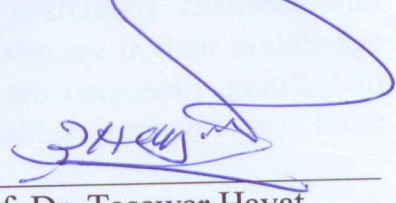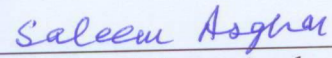## By

Abdul Qayyum

CERTIFICATE

A THESIS SUBMITTED IN THE PARTIAL FULFILLMENT OF THE REQUIREMENTS FOR THE DEGREE OF THE DOCTOR OF PHILOSOPHY

We accept this dissertation as conforming to the required standard

1. _____
   Prof. Dr. Tasawar Hayat
   (Supervisor)

2. _____
   Prof. Dr. Tasawar Hayat
   (Chairman)

3. _Saleem Asghar_
   Prof. Dr. Saleem Asghar
   (External Examiner)

4. _____
   Dr. Muhammad Salahuddin
   (External Examiner)

Department of Mathematics
Quaid-i-Azam University
Islamabad, Pakistan
2014

Acknowledgement

All praise and appreciations are for the omnipotent **ALLAH**, the most merciful and generous that knows better the hidden truths of the universe and HIS **Holy Prophet Muhammad (Peace be upon Him)** who declared it an obligatory duty of every Muslim to seek and acquire knowledge.

My sincerest appreciation goes to my supervisor **Pro. Dr. Tasawar Hayat**, for his patience, advice, guidance, valuable suggestions and extraordinary experiences throughout my study and research work. He provided me the valuable material and background information. His unique perspective was essential to bring the project to successful completion.

Federal Urdu university of Arts, Science and Technology (FUUAST), Islamabad with financial sport, is really a blessing for many, like me, who are in their middle age and can't afford, study only, with family bounds. I am personally gratified to FUUAST for providing me platform to enhance my qualification and to be a more effective part of the society.

I gratefully acknowledge my research group mates, Dr. Muhammad Awais and Muhammad Farooq for the wonderful moments, we spent together. Thank you for all these moments, filled with wishes, dreams, secrets, tension and laughter. I am really impressed by the memory that Muhammad Farooq is gifted by GOD. He is really a sincere fellow and helped me a lot throughout this journey of crest and trough.

I would like to extend my gratitude to all members of fluid mechanics group (FMG). I always feel honor to be the part of the group. I would like to thank my respected teachers Dr. Sohail Nadeem, Dr. Malik Muhammad Yousaf and Dr. Rehmat Ellahi. I would also like my special thanks to friends and colleagues specially Humaira Yasmin, Sadia Asad, Anum shafiq and Dr. Ramzan.

Finally, I thank my parents and wife (Shagufta Batool) for the infinite support, direction and tireless sacrifies; my brothers Muhammad Shafiq and Muhammad Sarfraz; sister Iram Siddiqa and my loving daughter Ammara Qazi for their constant support and cheerful encouragement. I owe my heartiest gratitude to

father in law Haji Baz Khan and brother in law colonel Muhammad Akram for their support, prayers and moral encouragement.

May Allah bless all those who pray for me (Ameen).

Abdul Qayyum
Date: July 11, 2014

Dedicated

To

My loving family

(especially my wife

And

Loving

daughter)

Abstract

The present thesis models the squeezing flows in the regime of non-Newtonian fluids. Mathematical modeling is based upon the constitutive equations of Jeffrey, couple stress, second grade and third grade fluids. These fluid models have been employed to predict the relaxation and retardation times, polar effect, body couples normal stress and shear thinning/shear thickening features. It addition heat and mass transfer is considered. The modeled nonlinear mathematical problems are computed by a modern technique namely the homotopy analysis method (HAM). Comparison of developed convergent series solutions with previous numerical solutions in limiting situation is shown. Discussion to important parameters in the solutions is given.

Preface

The curiosity to understand the flows of fluids obeying nonlinear rheological paradigm is increasing due to vast industrial and engineering applications. The examples include material plasticizing and solidification processes for manufacturing parts, oil-well drilling, fossil fuel combustion, paper production and many others. Spirited researchers endeavoring in assorted domains have been experimentally testing, mathematically modelling and developing algorithms for analyzing flow problems through different constitutive relationships and geometric configurations. Resulting equations in such flow problems are generally more nonlinear and higher order than the Navier-Stokes equations. These equations offer interesting challenges to the researchers in the field. Mathematicians are particularly exposed to challenging mathematical riddles, for instance, related to solvability and thermodynamic compatibility of constitutive relations, their solutions and analysis. The present thesis in this direction models and examines the flow problems of Jeffrey, couple stress, second and third grade fluids. The considered fluid models definitely predict the effects of relaxation and retardation times, polar, normal stress and shear thinning/shear thickening respectively. On the other hand the study of squeezing flow between two disks has attracted the interest of recent researchers because of its numerous applications in engineering, biology and bioengineering. For example compression moulding processes of metals and polymers represents squeeze flows. Valves and diarthroidial joints are examples of squeezing flow in biology and bioengineering. Even some phenomena occurring during food intake can be modeled using squeezing flow. In fact compression of food between the tongue and the palate can be approximated as a squeezing flow. Further chemical reaction can be codified as either homogeneous/heterogeneous process. Such situation depends on whether they occur at an interface/single phase volume reaction. Mechanism of cooling towers is perhaps the cheapest way that can be used for the cooling of large quantities of water. Importance of chemical reaction in the nuclear industry is also quite obvious. Its applications range from smoke detectors to nuclear reactors and even from gun sights to nuclear weapons. The Soret and Dufour effects are very important when the temperature and concentration gradient are high. The thermal-diffusion or Soret effect corresponds to species differentiations in an initial homogeneous mixture submitted to a thermal gradient and diffusion-thermo or Dufour effect corresponds to the heat flux produced by a concentration gradient. Motivated by all such facts we organized the present thesis as follows.

Chapters two to five address the unsteady axisymmetric flow of Jeffrey fluid between two parallel disks. Relevant problems are modeled. Appropriate transformations reduced the resulting partial differential system into ordinary differential system. The nonlinear problems are solved for the convergent series

solutions by homotopy analysis method (HAM). Contributions reflecting the influence of pertinent parameters into each problem are explored. The following problems are analyzed in these chapters.

- ❖ Unsteady squeezing flow of Jeffery fluid between two parallel disks.
- ❖ Thermal radiation effects in squeezing flow of Jeffery fluid.
- ❖ Soret-Dufour effects in magnetohydrodynamic (MHD) squeezing flow of Jeffrey fluid with Joule heating.
- ❖ Squeezing flow of Jeffrey fluid with chemical reaction.

The purpose of chapters six and seven is to examine the squeezing flows of couple stress fluids. This fluid model sustains couple stresses and the body couples. The stress tensor in present model is not symmetric. Main interest here is to introduce a size dependent effect through body couple. In particular the effects of heat transfer and chemical reaction are analyzed in these chapters. The series solutions are derived and main findings of these two chapters have been pointed out. Squeezing flow problems in regime of magnetohydrodynamics and porous surface are studied in the chapters eight and nine. Thermal-diffusion and diffusion-thermo effects are also investigated. The second grade fluid is chosen for the interest to capture the normal stress feature. Convergent solutions are developed. Physical insights is described by plots. Chapter ten models the time-dependent flow of third grade fluid between two squeezed disks. The third grade fluid model can predict the shear thinning and shear thickening effects even in the steady unidirectional flow due to a rigid surface. The formulated problem is nonlinear. Computations are made and examined.

Contents

Chapter 1

Review and some fundamental laws

1.1   Introduction

This chapter consists of review regarding the background of the considered flow problems. Brief idea of homotopy analysis method (HAM) is also summarized.

1.2   Background

Newtonian fluids reflecting a linear between the stress and the rate of strain do not explain many materials occurred in diverse applications of industry. The constitutive equations of such liquids vary considerably in complexity. Different models have been discussed in context of these fluids. A special category of viscoelastic fluid attracted many researchers in the recent years. Exact/approximate solution can be expected in case of second grade fluid which is considered as a subclass of viscoelastic fluids. The rheologists have been able to provide a theoretical foundation in the form of a constitutive equation which can in principle, have any order. For applied mathematicians, modelers and computer scientists the challenge comes from a different quarter. The constitutive equations of even the simple viscoelastic fluids, namely, second grade fluids are such that the differential equations describing the motion have, in general, order higher than those describing the motion of the Newtonian fluids but apparently there is no corresponding increase in the number of boundary conditions. Applied mathematicians and computer scientists are thus forced with the so-called ill-posed boundary value problems which,

in theory, would have a family of infinitely many solutions for flows confined for finite domain. The task then becomes to select one of them under some plausible assumption. However for different flow configurations, the stated assumptions take different forms. Taking all such complexities in view, even various recent researchers are engaged in the advancement of flows of second grade fluids (see [1 − 10]). Further, geophysicists encounter MHD aspect through interaction of conducting fluids. The MHD concept is useful for the engineers in the design of heat exchangers, MHD pumps and flow meters, in space vehicle propulsion, control and reentry problems, in metallurgical process and polymer industry; in creating novel power generating systems and in controlling fusion process. The flows of second grade fluids in the presence of magnetic field have been addressed by the very recent investigations [11 − 15]. No doubt, the model of second grade fluid describes the normal stress effects but important features of shear thinning/ thickening cannot be explained through its implementation. In such situation, the model of third grade fluid is more appropriate. This fluid model even in steady flow predicts the shear thinning/ thickening properties. With this awareness, Feiz-Dizaji et al.[16] examined the flow of third grade fluid in the annulus. Some fundamental flows of third grade fluid in the presence of partial slip effects are discussed by Ellahi et al.[17]. Abelman et al. [18, 19] investigated such analysis in a rotating frame. Flow of third grade fluid over a stretching surface with heat transfer and partial slip is analyzed by Sahoo and Do [20]. They used the regular perturbation method for the solution analysis. The series solution to unsteady boundary layer equations in a special third grade fluid is presented by Abbasbandy and Hayat [21]. Convergent series solutions are developed by homotopy analysis method. Narain and Kara [22] made the analysis of conservation laws in third grade fluid. Keimanesh et al. [23] employed multi-step differential transform method for flow of third grade fluid between two parallel plates. Hayat et al. [24] constructed mathematical model for peristaltic flow of third grade fluid in a curved channel with heat and mass transfer. Ellahi and Afzal [25] studied the effect of variable viscosity on the flow of third grade fluid in a porous space. The convergent solutions of the governing equations are obtained via homotopy analysis method. The second grade and third grade fluid models can not explain the relaxation and retardation times effects. Among the several models which have been employed to describe the rheological parameters exhibited by certain real fluids, the Jeffrey fluid has gained much support from the experimentalists and theoreticians.

This is due to the reason that the Jeffrey fluid model can predict the ratio of relaxation to retardation effects. Many researchers discussed the Jeffrey fluid model in different situation. Kothandapani and Srinivas [26] investigated peristaltic transport of a Jeffrey fluid under the effect of magnetic field in an asymmetric channel. Peristaltic motion of Jeffrey fluid under the effect of magnetic field in a tube was studied by Hayat and Ali [27]. Hayat et al. [28] found the series solution for MHD channel flow of a Jeffery fluid. Boundary layer flow of Jeffrey fluid with convective boundary conditions is discussed by Hayat et al. [29]. Hayat et al. [30] examined the effects of an endoscope and magnetic field on the peristalsis involving Jeffrey fluid. Ellahi et al. [31] investigated magnetohydrodynamic peristaltic flow of a Jeffrey fluid in eccentric cylinders. They found the series solution. Very recently the Karman flow of Jeffrey fluid has been discussed by Siddiqui et al. [32]. The couple stress fluid model proposed by Stokes [33] can predict various features of couple stresses in the fluids caused by the mechanical interactions that occur inside a deforming continuum. A prominent feature of this model is that it takes into account the polar effects. Having such preference in mind, Lakshmana and Iyengar [34] presented analytical and computational studies for flow of couple stress fluid. Stokes flow of an incompressible couple stress fluid past an approximate sphere has been studied by Srinivasacharya [35]. Ramanaiah [36] analyzed the squeezing films between finite plates lubricated by fluids with couple stresses. Analysis of couple stresses lubricant in hydrostatic thrust bearings has been reported by Gupta and Sharma [37]. Very recently Hayat et al. [38] presented the unsteady three dimensional flow of couple stress fluid over a stretching surface with chemical reaction.

Heat and mass transfer effects play a key role in extensive applications of engineering, physiology and industry. In particular these effects with the chemical reaction have essence in chemical and hydrometallurgical processes. Some interesting fields where heat and mass transfer phenomena subject to chemical reaction are significant include formation and dispersion design of chemical processing equipment, food processing and cooling towers, temperature distribution and moisture over agriculture fields and groves of fruit trees, damage of crops due to freezing, oxygenation and dialysis processes, crossurgery, hyperthermia etc. Effects of mass transfer are very important in the evaporation of water from a container to the atmosphere, the blood distillation in the kidneys and liver and purification of alcohol [39 − 43]. Also Shehzad et al. [44] studied the Soret and Dufour effects in the stagnation point flow of Jeffrey fluid with

6

convective boundary condition. Unsteady flow of third grade fluid with Soret and Dufour effects was discussed by Hayat et al. [45]. Islam and Alam [46] investigated the Soret and Dufour effects in free convection rotating flow. Shooting iteration technique is used to solve the system of governing equations. Rashidi et al. [47] addressed the simultaneous effects of partial slip and Soret and Dufour effects in flow of viscous fluid induced by rotating disk. Soret and Dufour effects in mixed convection boundary layer flow over a stretching vertical surface was studied by Hayat et al. [48]. Here viscoelastic fluid fills the porous space. Tsai and Huang [49] presented a theoretical study of the steady stagnation point flow over a stretched vertical surface in the presence of species concentration and mass diffusion under Soret and Dufor's effects. They concluded that for some kinds of mixtures with the light and medium molecular weight, the Soret and Dufor's effects should be considered as well. Afify [50] discussed the effects of thermal diffusion and diffusion thermo in MHD free convective flow over a stretching surface with suction or injection. He used Shooting and fourth order Runge Kutta method. The initial study on squeezing flow through lubrication approach was presented by Stefan [51]. Reynolds [52] obtained solution for elliptic plates and Archibald [53] studied this problem for rectangular plates. Many researchers [54 − 63] discussed the theoretical and experimental studies of squeezing flows. Landlois [64] represented the results for isothermal squeezed films. Numerical solution for a squeezed flow between two plates is developed by Verma [65]. Influence of suction/blowing on the squeezed flow is analyzed by Hamza [66]. Rajagopal and Gupta [67] discussed the squeezed flow in a second grade fluid. Analytic solution for squeezed flow problem is constructed by Rashidi et al. [68]. Homotopy perturbation solution (HPM) for magnetohydrodynamic (MHD) squeezed flow between parallel disks is developed by Domairy and Aziz [69]. Mahmood et al. [70] examined the heat transfer characteristics in the squeezed flow over a porous surface. Mustafa et al. [71] studied heat and mass transfer characteristics in a viscous fluid which is squeezed between parallel plates. They found that the magnitude of local Nusselt number is an increasing function of both Prandtl and Eckert numbers. Heat transfer effect in squeezing flow of Newtonian fluid between two disks has been studied by Hayat et al. [72]. Hussain et al. [73] developed the analytical and numerical solutions for squeezing flow and heat transfer with velocity slip and temperature jump. Khaled and Vafai [74] studied the magnetohydrodynamic effects in the squeezed flow and heat transfer over a

sensor surface. Heat transfer of Cu-water nanofluid flow between parallel plates was explored by Sheikholeslami et al. [75]. Duwairi et al. [76] investigated heat transfer effects of viscous fluid squeezed and extruded between the two parallel plates. Unsteady MHD flow between two disks with heat transfer was explored by Hamza [77]. He found the results by using Shooting and Maching technique. Bhattacharyya and Pal [78] studied unsteady MHD squeezing flow between two parallel rotating disks. Sweet et al. [79] discussed the unsteady MHD flow of viscous fluid between moving parallel plates.

1.3   Homotopy analysis method

Liao [80] proposed the homotopy analysis method (HAM) to solve ordinary and partial differential equations. The method separates itself from other methods in the following manner.

- HAM is not dependent on physical parameters. Therefore the technique can be used for both strong/weak nonlinear problems.

- Other methods like the delta expansion method, Adomian decomposition method and the Lyapunov artificial small parameter method are special cases of HAM (Homotopy analysis method).

- The HAM facilitates a simple way to control and adjust the convergence of the series solutions and allow to select required base functions in different situations with freedom.

- This method can be coupled with many other mathematical methods such as integral transform methods, series expansion methods, numerical methods and so on.

This technique is applicable in the development of results to numerous problems $[81 - 100]$. Idea behind the HAM is as follows.

We consider the nonlinear differential equation in the form

$$\mathcal{N}\left[u\left(\eta\right)\right] = 0, \tag{1.1}$$

where $\mathcal{N}$ is the nonlinear operator, u is an unknown dependent function and x denotes the independent variable. The homotopic equation is [82]

$$(1 - q) \mathcal{L} \left[\bar{u}(\eta; q) - u_0(\eta) \right] = q \hbar \mathcal{N} \left[\bar{u}(\eta; q) \right], \tag{1.2}$$

in which the embedding parameter q, $0 \leq q \leq 1$, the auxiliary parameter $\hbar \neq 0$, auxiliary linear operator $\mathcal{L}$ and initial guess $u_0(\eta)$ satisfying the boundary conditions. When $q = 0$ and $q = 1$ then

$$\bar{u}(\eta; 0) - u_0(\eta) = 0, \text{ and } \bar{u}(\eta; 1) - u_0(\eta) = 0, \tag{1.3}$$

respectively. Thus as q varies from 0 to 1, the solution $\bar{u}(\eta; q)$ ranges from initial guess $u_0(\eta)$ to the final solution $u(\eta)$. Writing $\bar{u}(\eta; q)$ in the Taylor series of parameter q we get

$$\bar{u}(\eta; q) = u_0(\eta) + \sum_{m=1}^{\infty} u_m(\eta) q^m, \quad u_m(\eta) = \frac{1}{m!} \left. \frac{\partial^m \bar{u}(\eta; q)}{\partial q^m} \right|_{q=0}. \tag{1.4}$$

The mth order equation is

$$L \left[u_m(\eta) - \chi_m u_{m-1}(\eta) \right] = \hbar \mathcal{R}_m \left(u_{m-1} \right), \tag{1.5}$$

with

$$R_m \left(u_{m-1} \right) = \frac{1}{(m-1)!} \left. \frac{\partial^{m-1} \bar{u}(\eta; q)}{\partial q^{m-1}} \right|_{q=0}, \tag{1.6}$$

$$\chi_m = \begin{cases} 0, & m \leq 1, \\ 1, & m > 1. \end{cases} \tag{1.7}$$

The solution of equation (1.5) can be obtained using a suitable software like MATHEMATICA or MAPLE. If the auxiliary parameter, the initial guess and the auxiliary linear operator is chosen accurately, the series (1.5) will converge at $q = 1$

$$\bar{u}(x) = u_0(\eta) + \sum_{m=1}^{\infty} u_m(\eta). \tag{1.8}$$

Chapter 2

Unsteady squeezing flow of Jeffery fluid between two parallel disks

This chapter addresses the unsteady axisymmetric flow of Jeffrey fluid between two parallel disks. The relevant partial differential equations are modeled. The modeled partial differential equations are reduced to the ordinary differential equations through appropriate transformations. The resulting ordinary differential system is solved for the series solution. Convergence of series solution is explicitly discussed. Effects of flow quantities due to different physical parameters are seen. It is found that the velocity profile is enhanced via larger porosity and squeezing parameters.

2.1   Mathematical formulation

We consider axisymmetric flow of an incompressible Jeffrey fluid. The flow is bounded between two parallel disks distant $H\left(1-at\right)^{\frac{1}{2}}$ apart. The upper disk has the velocity $-\frac{aH}{2}\left(1-at\right)^{-\frac{1}{2}}$ at $z=h\left(t\right)=H\left(1-at\right)^{\frac{1}{2}}$. The lower permeable disk at $z=0$ is stationary. In absence of body forces, the laws of conservation of mass and linear momentum are

$$\frac{\partial u}{\partial r}+\frac{u}{r}+\frac{\partial w}{\partial z}=0, \tag{2.1}$$

$$\rho\frac{d\mathbf{V}}{dt}=\text{div }\mathbf{T}, \tag{2.2}$$

10

where the Cauchy stress tensor ($\mathbf{T}$) in a Jeffrey fluid is defined by

$$\mathbf{T} = -p\mathbf{I} + \mathbf{S}, \quad \mathbf{S} = \frac{\mu}{1 + \lambda_1}\left(\dot{\mathbf{r}} + \lambda_2\ddot{\mathbf{r}}\right), \tag{2.3}$$

in which $\frac{d}{dt}$ is the material time differentiation, ($\mathbf{V}$) the velocity field, (u) the velocity component along radial direction (r) and (v) the axial component of the velocity in $z-$direction, (ρ) the fluid density, ($\mathbf{I}$) the identity tensor, (p) the pressure, (μ) the dynamic viscosity, (λ_1) the relaxation to retardation times ratio, (λ_2) the retardation time, dots over the quantities represent material time differentiation and

$$\dot{\mathbf{r}} = \nabla\mathbf{V} + (\nabla\mathbf{V})^T, \quad \ddot{\mathbf{r}} = \frac{d}{dt}\left(\dot{\mathbf{r}}\right). \tag{2.4}$$

The above fundamental equations give the following scalar expressions:

$$
\begin{aligned}
\rho\left(\frac{\partial u}{\partial t} + u\frac{\partial u}{\partial r} + w\frac{\partial u}{\partial z}\right) =\ & -\frac{\partial p}{\partial r} + \frac{\mu}{1 + \lambda_1}\left(\frac{\partial^2 u}{\partial r^2} + \frac{\partial^2 u}{\partial z^2} + \frac{1}{r}\frac{\partial u}{\partial r} - \frac{u}{r^2}\right) \\
& + \frac{\mu\lambda_2}{1 + \lambda_1}\left[\frac{\partial^3 u}{\partial t\partial z^2} + 2\frac{\partial^2 u}{\partial t\partial r^2} + \frac{2}{r}\frac{\partial^2 u}{\partial t\partial r} + \frac{\partial^3 w}{\partial t\partial r\partial z}\right. \\
& - \frac{2}{r^2}\frac{\partial u}{\partial t} + \frac{\partial u}{\partial r}\left(\frac{\partial^2 u}{\partial r^2} - \frac{2u}{r^2}\right) + \frac{\partial w}{\partial r}\frac{\partial^2 u}{\partial z\partial r} \\
& + u\left(\frac{\partial^3 u}{\partial r^3} + \frac{\partial^3 w}{\partial r^2\partial z} + \frac{\partial^3 u}{\partial r\partial z^2} + \frac{2u}{r^3}\right) \\
& + w\left(\frac{\partial^3 u}{\partial z\partial r^2} + \frac{2}{r}\frac{\partial^2 u}{\partial z\partial r} + \frac{\partial^3 w}{\partial z^3} + \frac{\partial^2 w}{\partial r\partial z}\right) \\
& + \frac{\partial u}{\partial z}\left(\frac{\partial^2 w}{\partial r^2} - \frac{2w}{r^2} + \frac{\partial^2 u}{\partial z\partial r}\right) \\
& + \left.\frac{\partial w}{\partial z}\left(\frac{\partial^2 u}{\partial z^2} + \frac{\partial^2 w}{\partial r\partial z}\right) + \frac{2}{r}\frac{\partial^2 u}{\partial r^2}\right],
\end{aligned}
\tag{2.5}
$$

$$\rho\left(\frac{\partial w}{\partial t}+u\frac{\partial w}{\partial r}+w\frac{\partial w}{\partial z}\right)=-\frac{\partial p}{\partial z}+\frac{\mu}{1+\lambda_1}\left(\frac{\partial^2 w}{\partial r^2}+\frac{\partial^2 w}{\partial z^2}+\frac{1}{r}\frac{\partial w}{\partial r}\right)$$

$$+\frac{\mu\lambda_2}{1+\lambda_1}\left[\frac{\partial^3 w}{\partial r\partial t\partial z}+\frac{\partial^3 w}{\partial t\partial r^2}+2\frac{\partial^3 u}{\partial r\partial z^2}+2\frac{\partial u}{\partial z}\frac{\partial^2 w}{\partial r\partial z}\right.$$

$$+\frac{\partial u}{\partial r}\left(\frac{\partial^2 u}{\partial r\partial z}+\frac{\partial^2 w}{\partial r^2}\right)+u\left(\frac{\partial^3 u}{\partial r^2\partial z}+\frac{\partial^3 v}{\partial r^3}\right)$$

$$+\frac{\partial w}{\partial r}\left(\frac{\partial^2 u}{\partial z^2}+\frac{\partial^3 u}{\partial t\partial z^2}\right)$$

$$+w\left(\frac{\partial^3 u}{\partial r\partial z^2}+\frac{\partial^3 w}{\partial r^2\partial z}+\frac{\partial^3 w}{\partial z^3}+\frac{1}{r}\frac{\partial^2 u}{\partial z^2}+\frac{1}{r}\frac{\partial^2 w}{\partial z\partial r}\right)$$

$$+\frac{u}{r}\left(\frac{\partial^2 u}{\partial r\partial z}+\frac{\partial^2 w}{\partial r^2}\right)+\frac{1}{r}\left(\frac{\partial^2 u}{\partial t\partial z}+\frac{\partial^2 w}{\partial t\partial r}\right)\right]. \tag{2.6}$$

The boundary conditions are given by

$$u = 0, \qquad w = \frac{\partial h}{\partial t}, \text{ at } \quad z = h(t),$$

$$u = 0, \qquad w = -w_0, \text{ at } \quad z = 0. \tag{2.7}$$

Defining [69]

$$u = \frac{ar}{2\left(1-at\right)}f'\left(\eta\right), \qquad w = -\frac{aH}{\sqrt{1-at}}f\left(\eta\right), \qquad \eta = \frac{z}{H\sqrt{1-at}} \tag{2.8}$$

equation (2.1) is readily satisfied and Eqs. (2.5) − (2.7) give

$$f^{(iv)}-S_q\left(1+\lambda_1\right)\left(\eta f'''+3f''-2ff'''\right)+\frac{\beta}{2}\left(\eta f^{(v)}+5f^{(iv)}+f''f'''-3f'f^{(iv)}\right)=0, \tag{2.9}$$

$$f\left(0\right)=S, \qquad f'\left(0\right)=0, \qquad f\left(1\right)=\frac{1}{2}, \qquad f'\left(1\right)=0, \tag{2.10}$$

where $S > 0$ and $S < 0$ respectively denote the suction and blowing effects at the lower static disk. The squeeze parameter S_q and Deborah number β are introduced via the following expressions:

$$S_q=\frac{aH^2}{2\nu}, \qquad \beta=\frac{\lambda_2 a}{1-at}. \tag{2.11}$$

12

Coefficient of skin friction in the present flow of Jeffrey fluid is

$$C_{fr} = \frac{\tau_{rz} \mid_{z=h(t)}}{\rho \left(\frac{aH}{2(1-at)^{1/2}} \right)^2}, \tag{2.12}$$

with

$$
\begin{aligned}
\tau_{rz} &= \frac{\mu}{1+\lambda_1} \left(\frac{\partial u}{\partial z} + \frac{\partial w}{\partial r} \right) \\
&+ \frac{\lambda_2}{1+\lambda_1} \left[\frac{\partial^2 u}{\partial t \partial z} + \frac{\partial^2 w}{\partial t \partial r} + u \left(\frac{\partial^2 u}{\partial r \partial z} + \frac{\partial^2 w}{\partial r^2} \right) + w \left(\frac{\partial^2 u}{\partial z^2} + \frac{\partial^2 w}{\partial z \partial r} \right) \right].
\end{aligned} \tag{2.13}
$$

Dimensionless form of skin friction coefficient is

$$\frac{H^2}{r^2} R_{er} C_{fr} = \left(1 + \frac{3}{2}\beta \right) f''(1), \tag{2.14}$$

where

$$R_{er}^{-1} = \frac{2\nu}{raH \left(1 + \lambda_1 \right) \left(1 - at \right)^{1/2}}, \quad \beta = \frac{\lambda_2 a}{1 - at}. \tag{2.15}$$

2.2 Solution for $f(\eta)$

We expressed the velocity profile $f(\eta)$ as the set of base functions

$$\left\{ \eta^k \mid k \geq 0 \right\}, \tag{2.16}$$

in the form of the following series

$$f(\eta) = \sum_{k=0}^{\infty} a_k \eta^k,$$

where a_k are the coefficients. The initial approximation (f_0) and linear operator $(\mathcal{L}_f)$ are presented as follows:

$$
\begin{aligned}
f_0(\eta) &= S + \left(\frac{3}{2} - 2S \right) \eta^2 + (2S - 1) \eta^3, \tag{2.17} \\
\mathcal{L}_f &= f^{(iv)}, \tag{2.18}
\end{aligned}
$$

13

where

$$\mathcal{L}_f \left(C_1 + C_2\eta + C_3\eta^2 + C_4\eta^3 \right) = 0, \tag{2.19}$$

and C_i $(i = 1 - 4)$ depict the arbitrary constants.

2.2.1 Zeroth order deformation problem

The zeroth order deformation problem can be written as

$$(1 - q)\,\mathcal{L}_f \left[\bar{f}\,(\eta; q) - f_0\,(\eta) \right] = q\hbar_f \mathcal{N}_f \left[\bar{f}\,(\eta; q) \right], \tag{2.20}$$

$$\bar{f}\,(0; q) = S, \ \ \bar{f}'\,(0, q) = 1, \ \ \bar{f}\,(1, q) = \frac{S_q}{2}, \ \ \bar{f}'\,(1, q) = 0, \tag{2.21}$$

where $\hbar_f \neq 0$ denotes the auxiliary parameter and $0 \leq q \leq 1$ indicates embedding parameter. It is observed that when q changes from 0 to 1, then $\bar{f}(\eta, q)$ varies from the initial solution $f_0\,(\eta)$ to the required solution $f(\eta)$. When $q = 0$ and $q = 1$, one can obtain

$$\bar{f}(\eta, 0) = f_0(\eta), \ \ \bar{f}(\eta, 1) = f(\eta). \tag{2.22}$$

The nonlinear operator is defined as follows:

$$\mathcal{N}_f \left[\bar{f}\,(\eta; q) \right] = \frac{\partial^4 \bar{f}\,(\eta; q)}{\partial \eta^4} - S_q\,(1 + \lambda_1) \left(\eta \frac{\partial^3 \bar{f}\,(\eta; q)}{\partial \eta^3} + 3\frac{\partial^2 \bar{f}\,(\eta; q)}{\partial \eta^2} - 2\bar{f}\,(\eta; q) \frac{\partial^3 \bar{f}\,(\eta; q)}{\partial \eta^3} \right)$$
$$+ \frac{\beta}{2} \left(\eta \frac{\partial^5 \bar{f}\,(\eta; q)}{\partial \eta^5} + 5\frac{\partial^4 \bar{f}\,(\eta; q)}{\partial \eta^4} + \frac{\partial^2 \bar{f}\,(\eta; q)}{\partial \eta^2}\frac{\partial^3 \bar{f}\,(\eta; q)}{\partial \eta^3} - 3\frac{\partial \bar{f}\,(\eta; q)}{\partial \eta}\frac{\partial^4 \bar{f}\,(\eta; q)}{\partial \eta^4} \right). \tag{2.23}$$

By applying the Taylor series on $f(\eta)$ one can write

$$f(\eta) = f_0(\eta) + \sum_{m=1}^{\infty} f_m(\eta)q^m, \tag{2.24}$$

$$f_m(\eta) = \frac{1}{m!}\frac{\partial^m \bar{f}(\eta, q)}{\partial q^m}\bigg|_{q=0}. \tag{2.25}$$

2.2.2 mth-order deformation problems

We differentiate Eq. (2.20) $m-$times with respect to q then divide by m! and setting $q = 0$ we get

$$\mathcal{L}_f \left[f_m \left(\eta \right) - \chi_m f_{m-1} \left(\eta \right) \right] = \hbar_f \Re_m^f \left(f_{m-1} \left(\eta \right) \right), \tag{2.26}$$

$$f_m \left(0 \right) = 0, \ f_m' \left(0 \right) = 0, \ f_m \left(1 \right) = 0, \ f_m' \left(1 \right) = 0, \tag{2.27}$$

in which

$$\chi_m = \begin{cases} 0, & m \leq 1, \\ 1, & m > 1, \end{cases}$$

$$\begin{aligned} \Re_m^f \left(f_{m-1} \left(\eta \right) \right) &= f_{m-1}^{(iv)} \left(\eta \right) - S_q \left(1 + \lambda_1 \right) \left[\eta f_{m-1}''' \left(\eta \right) + 3 f_{m-1}'' \left(\eta \right) \right] \\ &+ \frac{\beta}{2} \left[\eta f_{m-1}^{(v)} \left(\eta \right) + 5 f_{m-1}^{(iv)} \left(\eta \right) \right] + \sum_{n=0}^{m-1} \left[2 S_q \left(1 + \lambda_1 \right) f_n \left(\eta \right) f_{m-1-n}''' \left(\eta \right) \right. \\ &+ \left. \frac{\beta}{2} \left(f_n'' \left(\eta \right) f_{m-1-n}''' \left(\eta \right) - 3 f_n' \left(\eta \right) f_{m-1-n}^{(iv)} \left(\eta \right) \right) \right]. \end{aligned} \tag{2.28}$$

The general solution of boundary value problem given in Eq. (2.26) with boundary conditions (2.27) is

$$f_m(\eta) = f_m^*(\eta) + C_1 + C_2 \eta + C_3 \eta^2 + C_4 \eta^3 \tag{2.29}$$

in which $f_m^*(\eta)$ is the particular solution of the problem given in Eq. (2.29). The coefficients $C_i \ (i = 1 - 4)$ can be found through the boundary conditions expressed in Eq. (2.21).

2.2.3 Convergence of solution

The convergence of HAM solution (2.29) highly depends upon the auxiliary parameter $\hbar_f$ for the function f. This parameter is useful in adjusting and controlling the convergence of the obtained solution. To obtain the admissible values of auxiliary parameter, we have drawn Figs. $(2.1 - 2.4)$ at $\eta = 0$ and $\eta = 1$ respectively. The permissible values of auxiliary parameter $\hbar_f$ is $-1.0 \leq \hbar_f \leq -0.3$ in all cases. Further, convergence of the series solution exists through out

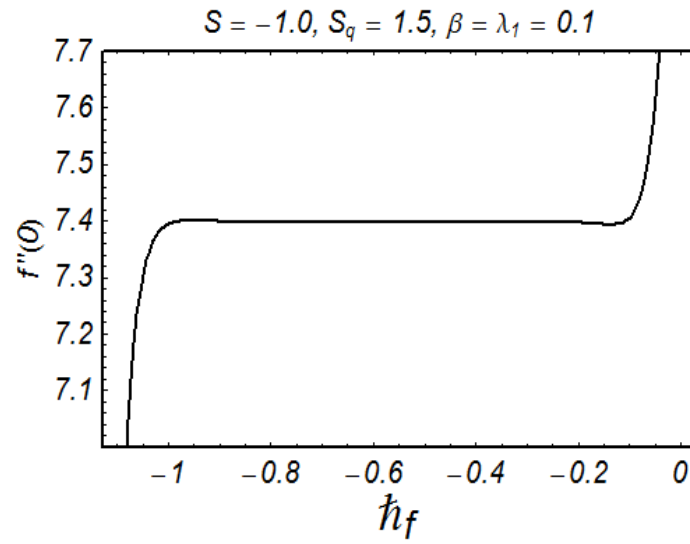the domain η $(0 < \eta < \infty)$ when $\hbar_f = -0.5$.

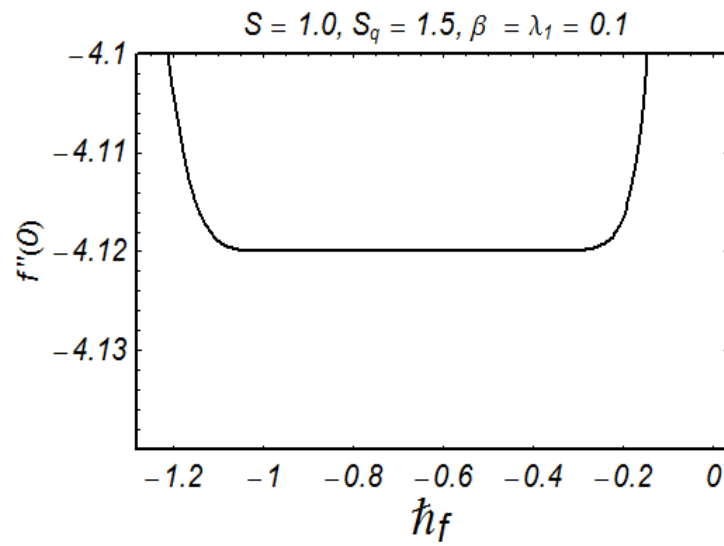Fig.2.1: Convergence region of f at $\eta = 0$ for blowing.

Fig.2.2: Convergence region of f at $\eta = 0$ for suction.
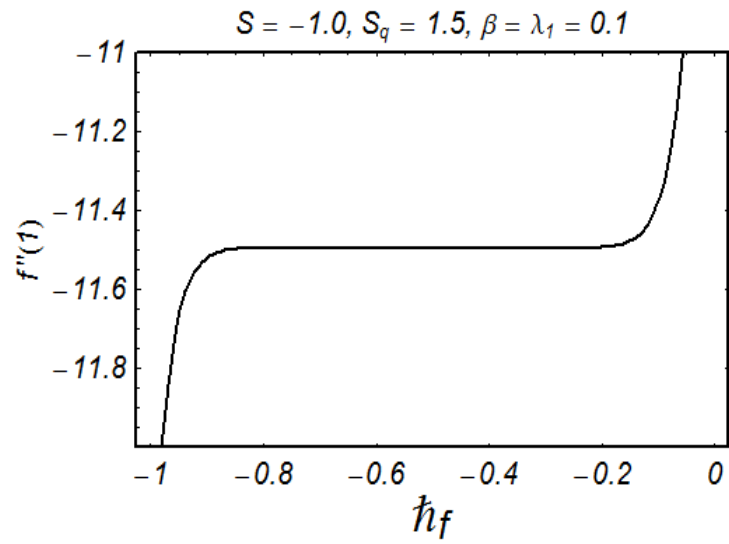
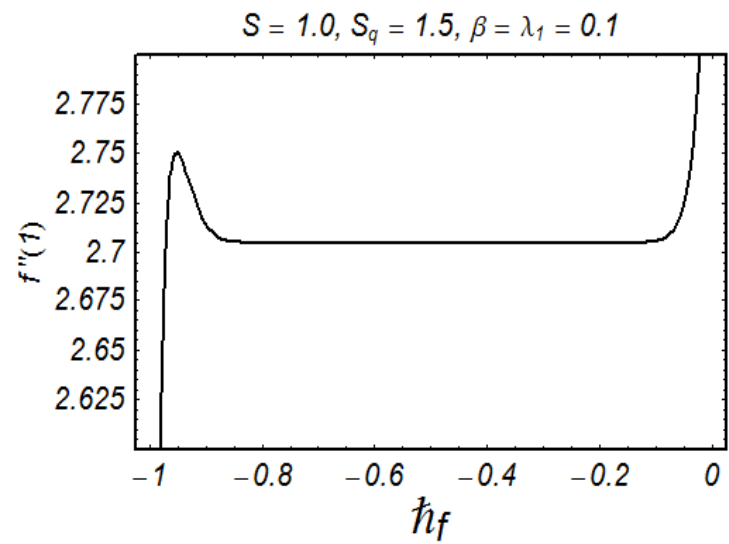Fig. 2.3: Convergence region of f at $\eta = 1$ for blowing.

Fig. 2.4: Convergence region of f at $\eta = 1$ for suction.

Table 2.1: Series solution's convergence by HAM for different order of approximations when $S_q = 1.5$, $\beta = 0.2$ and $\lambda_1 = 0.1$.

Order of approximation	(for blowing) $S = -1.0$		(for suction) $S = 1.0$	
	$f''(0)$	$f''(1)$	$f''(0)$	$f''(1)$
1	7.617214286	-10.58721429	-3.747642857	2.757642857
5	7.392289170	-11.49335115	-4.117403138	2.704699243
10	7.398693247	-11.49336023	-4.119968397	2.704914073
15	7.398569715	-11.49316106	-4.119969183	2.704914241
20	7.398573463	-11.49317065	-4.119969180	2.704914240
25	7.398573339	-11.49317027	-4.119969180	2.704914240
30	7.398573344	-11.49317029	-4.119969180	2.704914240
35	7.398573344	-11.49317029	-4.119969180	2.704914240
40	7.398573344	-11.49317029	-4.119969180	2.704914240

2.3   Graphical analysis and discussion

Our intention now is to predict the impact of the embedding parameters on the radial velocity profile $f'(\eta)$ for suction and blowing cases. Variation of S_q on the velocity field f' in suction and blowing have been displayed through the Figs. 2.5 and 2.6. It is analyzed that the velocity field f' decreases near the porous walls where suction effects are dominant which is presented in Fig. 2.5. Since the upper wall is moving towards the stationary porous wall generating a pressure which enhances the flow. Thus velocity field near the upper wall increases in order to satisfy the mass conservation. Fig. 2.6 describes that blowing at the lower wall acts as a retarding force which shows a decrease in fluid velocity. However in the upper half region of the channel, the fluid velocity increases. This is because of the reason that the squeezing effects are dominant in the upper half region of the channel. Influence of β on f' in suction case is illustrated in Fig. 2.7. It is observed that β causes a decrease in the radial velocity f' in the lower region of the channel. However f' increases in the channel's upper region by increasing β. Fig. 2.8 depicts opposite results in blowing situation. Figs. 2.9 and 2.10 plot the variation

of λ_1 on f' in suction $(S > 0)$ and blowing $(S < 0)$ respectively. It is found that effect of λ_1 on f' is quite opposite to that of β in both cases of suction and blowing respectively.

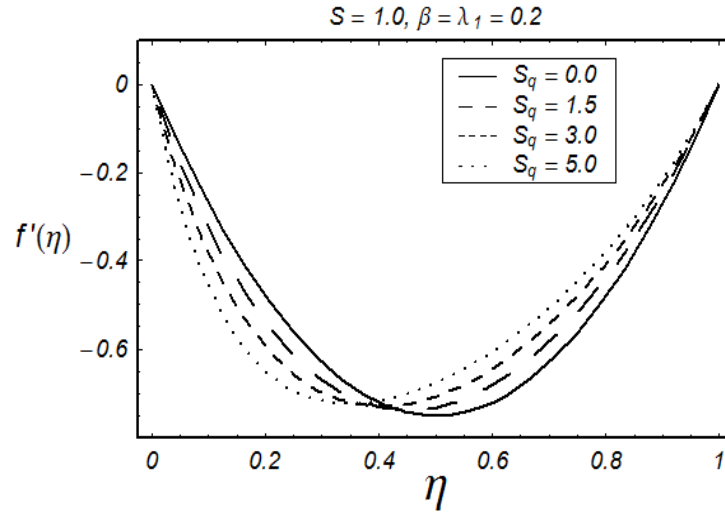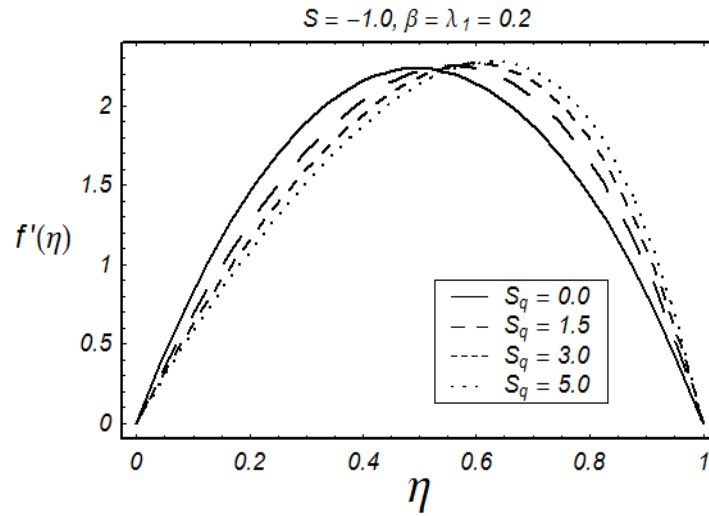Fig. 2.5: Influence of S_q on f' for suction.

Fig. 2.6: Influence of S_q on f' for injection.
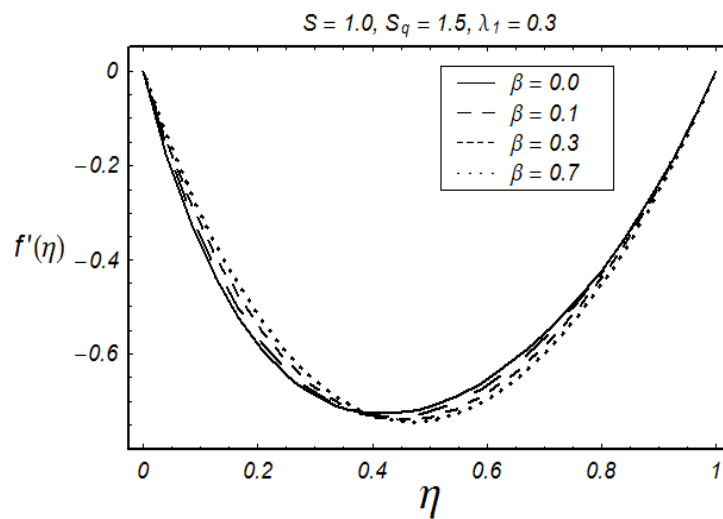
Fig. 2.7: Influence of β on f' for suction.
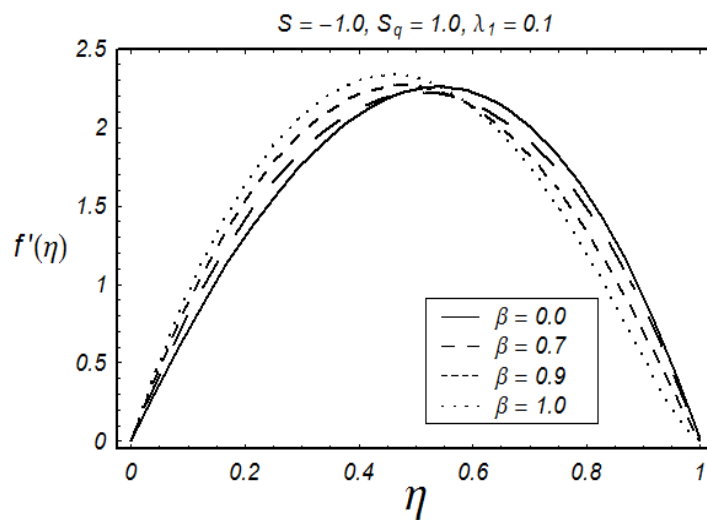
Fig. 2.8: Influence of β on f' for injection.
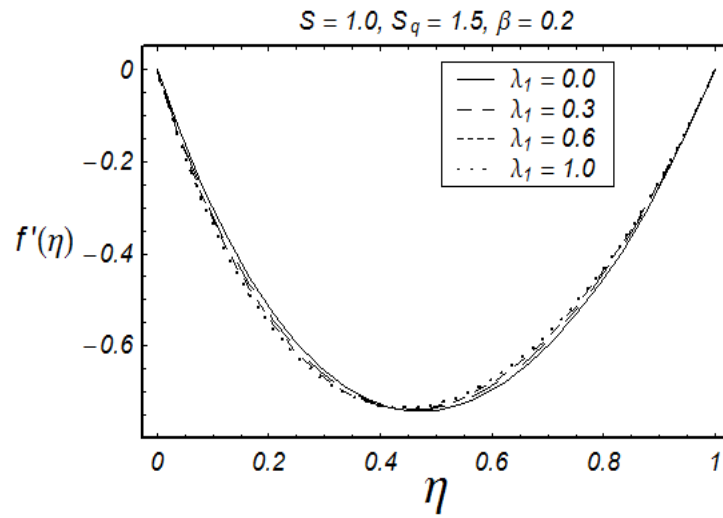
Fig. 2.9: Influence of λ_1 on f' for suction.
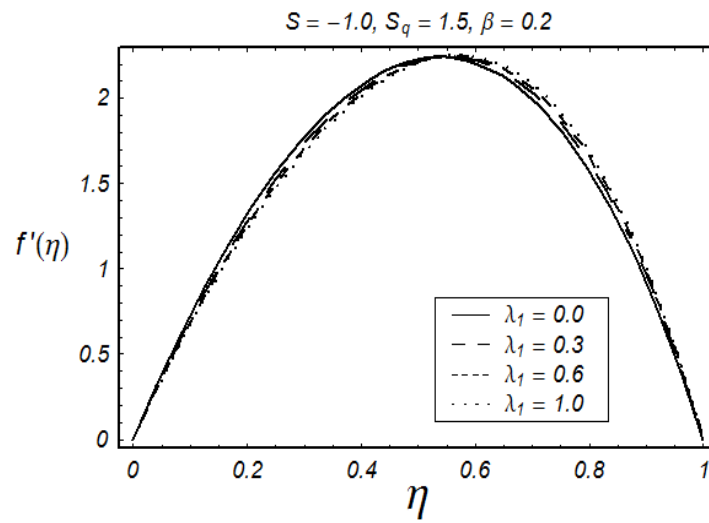
Fig. 2.10: Influence of λ_1 on f' for injection.

21

Table 2.2 provides the numerical values of skin friction coefficient $\left(\frac{H^2}{r^2}R_{er}C_{fr}\right)$ for different embedded parameters. Here the skin friction coefficient increases by increasing S whereas it decreases for positive values of S_q, λ_1 and β. Table 2.3 highlights a comparative study of present work with the previous published result. An excellent agreement with previous research in a limiting sense has been found.

Table 2.2: Values of skin friction coefficient $\frac{H^2}{r^2}R_{er}C_{fr}$ for different values of emerging parameters.

S	S_q	λ_1	β	$\frac{H^2}{r^2}R_{er}C_{fr}$
-1.5	1.5	0.1	0.1	-19.76512
-0.5				-7.94205
0.5				0.00000
1.5				5.85264
-1.0	0.5			-11.42769
	1.0			-12.34814
	1.5			-13.21714
	2.0			-14.03591
	1.5	0.0		-12.98520
		0.1		-13.21714
		0.2		-13.44533
		0.1	0	-11.37973
			0.1	-13.21714
			0.2	-15.01379

Table 2.3: Comparison between HAM and HPM solutions [69]

S	$f''(1)$	
	HPM [69]	HAM (Present results)
0.1	2.97682	2.97682
0.5	–	2.89177
1.0	–	2.80242
1.5	–	2.73094

2.4   Closing remarks

In the present analysis we discussed the flow of Jeffrey fluid between two parallel disk using the modern technique known as the homotopy analysis method (HAM). Influence of emerging physical parameters are discussed via graphs. The following points have been noted.

- Effects of squeezing parameter S_q on velocity profile $f'(\eta)$ in suction and blowing are reverse.

- Variations of Deborah number (β) on the radial velocity $f'(\eta)$ are opposite for suction and blowing cases.

- Influence of ratio parameter λ_1 on radial velocity $f'(\eta)$ is opposite in suction and blowing cases.

- The skin friction coefficient $\left(\frac{H^2}{r^2} R_{er} C_{fr}\right)$ increases by increasing S whereas it decreases for positive values of S_q, λ_1 and β.

Chapter 3

Thermal Radiation effects in squeezing flow of a Jeffery fluid

This chapter extends the flow analysis of previous chapter through heat transfer. Conservation law of energy is employed for the development of problem in addition to the conservation laws of mass and linear momentum. Radiative effects in the energy equation are retained. Attention is mainly focused to the temperature field. The relevant differential system is solved for the convergent series solution. Effects of the various physical parameters on both suction and blowing cases are analyzed. It is noted that temperature decreases for larger Prandtl number in both suction and blowing situations. There are opposite effects of thermal radiation on the temperature in suction and blowing cases.

3.1 Mathematical analysis

Axisymmetric flow of an incompressible Jeffrey fluid is considered. The flow is bounded between two parallel disks distant $H(1 - at)^{\frac{1}{2}}$ apart. The upper disk is located at $z = h(t)$; $(h(t) = H(1 - at)^{\frac{1}{2}})$. The upper disk moves with velocity $-\frac{aH}{2}(1 - at)^{-\frac{1}{2}}$ while the lower permeable disk at $z = 0$ is stationary. Heat transfer is considered in the presence of linear thermal radiation. Rosselands approximation for thermal radiation is used. The laws of conservation of

mass, linear momentum and energy yield

$$\frac{\partial u}{\partial r} + \frac{u}{r} + \frac{\partial w}{\partial z} = 0, \tag{3.1}$$

$$
\begin{aligned}
\rho\left(\frac{\partial u}{\partial t} + u\frac{\partial u}{\partial r} + w\frac{\partial u}{\partial z}\right) ={} & -\frac{\partial p}{\partial r} + \frac{\mu}{1+\lambda_1}\left(\frac{\partial^2 u}{\partial r^2} + \frac{\partial^2 u}{\partial z^2} + \frac{1}{r}\frac{\partial u}{\partial r} - \frac{u}{r^2}\right) \\
& + \frac{\mu\lambda_2}{1+\lambda_1}\left[\frac{\partial^3 u}{\partial t\partial z^2} + 2\frac{\partial^2 u}{\partial t\partial r^2} + \frac{2}{r}\frac{\partial^2 u}{\partial t\partial r} + \frac{\partial^3 w}{\partial t\partial r\partial z}\right. \\
& -\frac{2}{r^2}\frac{\partial u}{\partial t} + \frac{\partial u}{\partial r}\left(\frac{\partial^2 u}{\partial r^2} - \frac{2u}{r^2}\right) + \frac{\partial w}{\partial r}\frac{\partial^2 u}{\partial z\partial r} \\
& + u\left(\frac{\partial^3 u}{\partial r^3} + \frac{\partial^3 w}{\partial r^2\partial z} + \frac{\partial^3 u}{\partial r\partial z^2} + \frac{2u}{r^3}\right) \\
& + w\left(\frac{\partial^3 u}{\partial z\partial r^2} + \frac{2}{r}\frac{\partial^2 u}{\partial z\partial r} + \frac{\partial^3 w}{\partial z^3} + \frac{\partial^2 w}{\partial r\partial z}\right) \\
& + \frac{\partial u}{\partial z}\left(\frac{\partial^2 w}{\partial r^2} - \frac{2w}{r^2} + \frac{\partial^2 u}{\partial z\partial r}\right) \\
& \left. + \frac{\partial w}{\partial z}\left(\frac{\partial^2 u}{\partial z^2} + \frac{\partial^2 w}{\partial r\partial z}\right) + \frac{2}{r}\frac{\partial^2 u}{\partial r^2}\right], \tag{3.2}
\end{aligned}
$$

$$
\begin{aligned}
\rho\left(\frac{\partial w}{\partial t} + u\frac{\partial w}{\partial r} + w\frac{\partial w}{\partial z}\right) ={} & -\frac{\partial p}{\partial z} + \frac{\mu}{1+\lambda_1}\left(\frac{\partial^2 w}{\partial r^2} + \frac{\partial^2 w}{\partial z^2} + \frac{1}{r}\frac{\partial w}{\partial r}\right) \\
& + \frac{\mu\lambda_2}{1+\lambda_1}\left[\frac{\partial^3 w}{\partial r\partial t\partial z} + \frac{\partial^3 w}{\partial t\partial r^2} + 2\frac{\partial^3 u}{\partial r\partial z^2} + 2\frac{\partial u}{\partial z}\frac{\partial^2 w}{\partial r\partial z}\right. \\
& + \frac{\partial u}{\partial r}\left(\frac{\partial^2 u}{\partial r\partial z} + \frac{\partial^2 w}{\partial r^2}\right) + u\left(\frac{\partial^3 u}{\partial r^2\partial z} + \frac{\partial^3 v}{\partial r^3}\right) \\
& + \frac{\partial w}{\partial r}\left(\frac{\partial^2 u}{\partial z^2} + \frac{\partial^3 u}{\partial t\partial z^2}\right) \\
& + w\left(\frac{\partial^3 u}{\partial r\partial z^2} + \frac{\partial^3 w}{\partial r^2\partial z} + \frac{\partial^3 w}{\partial z^3} + \frac{1}{r}\frac{\partial^2 u}{\partial z^2} + \frac{1}{r}\frac{\partial^2 w}{\partial z\partial r}\right) \\
& \left. + \frac{u}{r}\left(\frac{\partial^2 u}{\partial r\partial z} + \frac{\partial^2 w}{\partial r^2}\right) + \frac{1}{r}\left(\frac{\partial^2 u}{\partial t\partial z} + \frac{\partial^2 w}{\partial t\partial r}\right)\right], \tag{3.3}
\end{aligned}
$$

$$\rho c_p\left(\frac{\partial T}{\partial t} + u\frac{\partial T}{\partial r} + w\frac{\partial T}{\partial z}\right) = K_c\left(\frac{\partial^2 T}{\partial r^2} + \frac{\partial^2 T}{\partial z^2} + \frac{1}{r}\frac{\partial T}{\partial r}\right) + \frac{16\sigma^* T_0^3}{3k^*}\frac{\partial^2 T}{\partial z^2}, \tag{3.4}$$

where u denotes the radial velocity, the axial velocity (v), (T) the fluid temperature, (ρ) the fluid density, (c_p) the specific heat at constant temperature, (p) the pressure, (μ) the dynamic

viscosity, (λ_1) relaxation and retardation times ratio, (λ_2) the retardation time, (K_c) the thermal conductivity, (σ^*) the Stefan-Boltzmann constant, (k^*) the mean absorption coefficient and (T_0) temperature of the wall.

The relevant boundary conditions are presented in the following forms:

$$
\begin{aligned}
u &= 0, & w &= \frac{\partial h}{\partial t},\, T = T_0 + \frac{T_0}{1-at} & \text{at} & \quad z = h(t), \\
u &= 0, & w &= -w_0,\, T = T_0 & \text{at} & \quad z = 0.
\end{aligned}
\tag{3.5}
$$

Defining the transformations

$$
u = \frac{ar}{2\,(1-at)} f'\,(\eta)\,, \qquad w = -\frac{aH}{\sqrt{1-at}} f\,(\eta)\,, \qquad \eta = \frac{z}{H\sqrt{1-at}}, \qquad T = T_0 + \frac{T_0}{1-at}\theta\,(\eta)\,,
\tag{3.6}
$$

equation (3.1) is automatically satisfied and eliminating pressure from Eqs. $(3.2) - (3.5)$ give

$$
\begin{aligned}
& f^{(iv)} - S_q\,(1+\lambda_1)\left(\eta f''' + 3f'' - 2ff'''\right) \\
& +\frac{\beta}{2}\left(\eta f^{(v)} + 5f^{(iv)} + f'' f''' - 3f' f^{(iv)}\right) = 0,
\end{aligned}
\tag{3.7}
$$

$$
\theta''\left(1+\frac{4}{3}Rd\right) - RePr\left(\eta\theta' + 2\theta - 2f\theta'\right) = 0,
\tag{3.8}
$$

$$
f\,(0) = S,\; f'\,(0) = 0,\; f\,(1) = \frac{1}{2},\; f'\,(1) = 0,\; \theta\,(0) = 0,\; \theta\,(1) = 1,
\tag{3.9}
$$

where $S > 0$ and $S < 0$ respectively denote the suction and injection (or blowing) at the lower permeable static disk. The squeezing parameter S_q, the Deborah number (β), the Reynolds number (Re), the Prandtl number (Pr) and the radiation parameter (Rd) are introduced in the following expressions

$$
S_q = \frac{aH^2}{2\nu}, \quad \beta = \frac{\lambda_2 a}{(1-at)}, \quad Re = \frac{\rho aH^2}{2\mu}, \quad Pr = \frac{c_p\mu}{K_c}, \quad Rd = \frac{4\sigma^* T_0^3}{k^* K_c}.
\tag{3.10}
$$

3.2 Solution for $\theta(\eta)$

The dimensionless temperature $\theta(\eta)$ in terms of base functions

$$\left\{ \eta^k \mid k \geq 0 \right\}, \tag{3.11}$$

is expressed in the following series

$$\theta(\eta) = \sum_{k=0}^{\infty} a_k \eta^k,$$

where a_k are the coefficients. The initial approximation $\theta_0(\eta)$ and linear operator $\mathcal{L}_\theta$ are chosen as follows:

$$\theta_0(\eta) = \eta, \tag{3.12}$$

$$\mathcal{L}_\theta = \theta'', \tag{3.13}$$

where

$$\mathcal{L}_\theta [C_1 + C_2 \eta] = 0, \tag{3.14}$$

and C_i $(i = 1, 2)$ denote the arbitrary constants.

3.2.1 Zeroth order deformation problem

The zeroth order deformation equation can be written as

$$(1 - q) \mathcal{L}_\theta \left[\bar{\theta}(\eta; q) - \theta_0(\eta) \right] = q \hbar_\theta \mathcal{N}_\theta \left[\bar{\theta}(\eta; q) \right], \tag{3.15}$$

with

$$\bar{\theta}(0; q) = S, \ \bar{\theta}(1, q) = 1, \tag{3.16}$$

where $\hbar_\theta \neq 0$ denotes the auxiliary parameter and $0 \leq q \leq 1$ indicates embedding parameter. It is ensured that when q changes from 0 to 1 then $\bar{\theta}(\eta, q)$ vary from $\theta_0(\eta)$ to $\theta(\eta)$. When $q = 0$ and $q = 1$, one obtains

$$\bar{\theta}(\eta, 0) = \theta_0(\eta), \ \bar{\theta}(\eta, 1) = \theta(\eta). \tag{3.17}$$

28

The nonlinear operator is by

$$\mathcal{N}_\theta \left[\bar{\theta}\left(\eta; q\right)\right] = \left(1 + \frac{4}{3} Rd\right) \frac{\partial^2 \bar{\theta}\left(\eta; q\right)}{\partial \eta^2} - RePr \left(\eta \frac{\partial \bar{\theta}\left(\eta; q\right)}{\partial \eta} + 2\bar{\theta}\left(\eta; q\right) - 2\bar{f}\left(\eta; q\right) \frac{\partial \bar{\theta}\left(\eta; q\right)}{\partial \eta}\right).$$

(3.18)

By applying Taylor series on $\theta(\eta)$ one can write

$$\theta(\eta) = \theta_0(\eta) + \sum_{m=1}^{\infty} \theta_m(\eta) q^m,$$

(3.19)

$$\theta_m(\eta) = \frac{1}{m!} \frac{\partial^m \bar{\theta}(\eta, q)}{\partial q^m}\bigg|_{q=0}.$$

(3.20)

3.2.2 mth-order deformation problems

We differentiate Eq. (3.15) with respect to q ($m - $ times) then divide by $m!$ and putting $q = 0$ we get

$$\mathcal{L}_\theta \left[\theta_m\left(\eta\right) - \chi_m \theta_{m-1}\left(\eta\right)\right] = \hbar_\theta \mathfrak{R}_m^\theta \left(\theta_{m-1}\left(\eta\right)\right),$$

(3.21)

$$\theta_m\left(0\right) = 0, \ \theta_m\left(1\right) = 0,$$

(3.22)

in which

$$\chi_m = \begin{cases} 0, & m \leq 1, \\ 1, & m > 1, \end{cases}$$

$$\mathfrak{R}_m^\theta \left(\theta_{m-1}\left(\eta\right)\right) = \left(1 + \frac{4}{3} Rd\right) \theta_{m-1}''\left(\eta\right) - RePr \left[\eta \theta_{m-1}'\left(\eta\right) + 2\theta_{m-1}\left(\eta\right)\right]$$

$$+ RePr \sum_{n=0}^{m-1} \left[f_n\left(\eta\right) \theta_{m-1-n}'\left(\eta\right)\right]$$

(3.23)

The general solution is given by

$$\theta_m(\eta) = \theta_m^*(\eta) + C_1 + C_2 \eta,$$

(3.24)

where $\theta_m^*(\eta)$ is the particular solution of the problem given in Eq. (3.15). The coefficients C_i ($i = 1 - 2$) can be found through the boundary conditions (3.16).
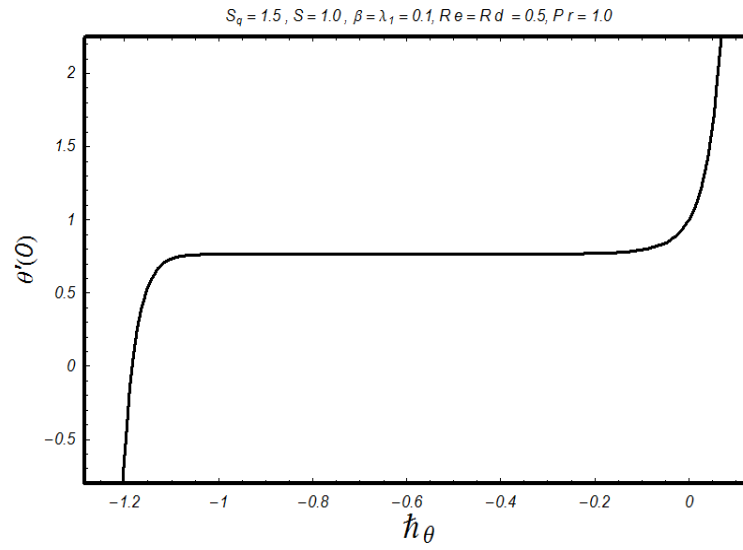
3.2.3   Convergence analysis

Fig. 3.1: Convergence region for θ at $\eta = 0$ in suction case.
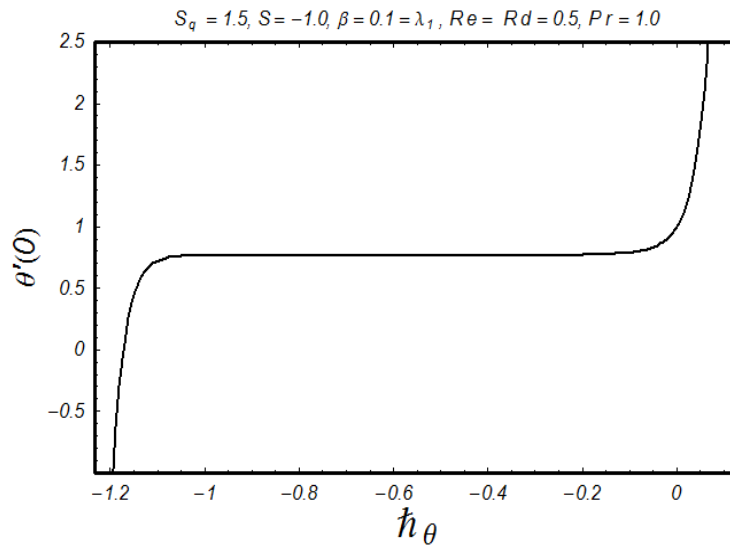
Fig. 3.2: Convergence region for θ at $\eta = 0$ in blowing case.
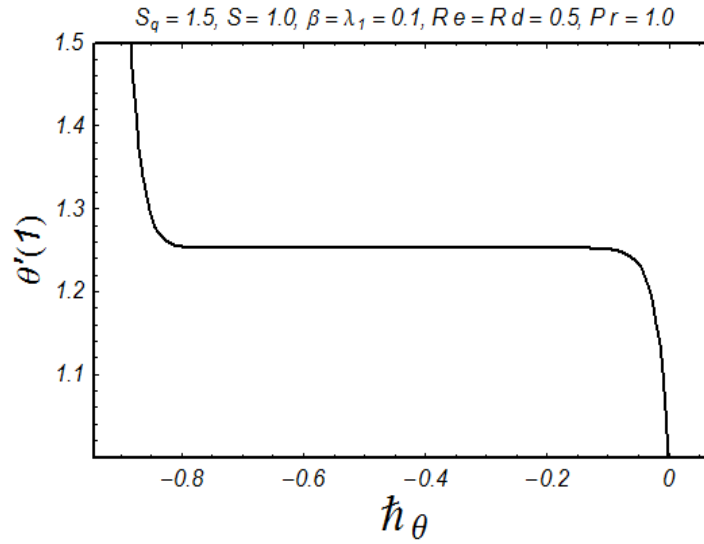
Fig. 3.3: Convergence region for θ at $\eta = 1$ in suction case.
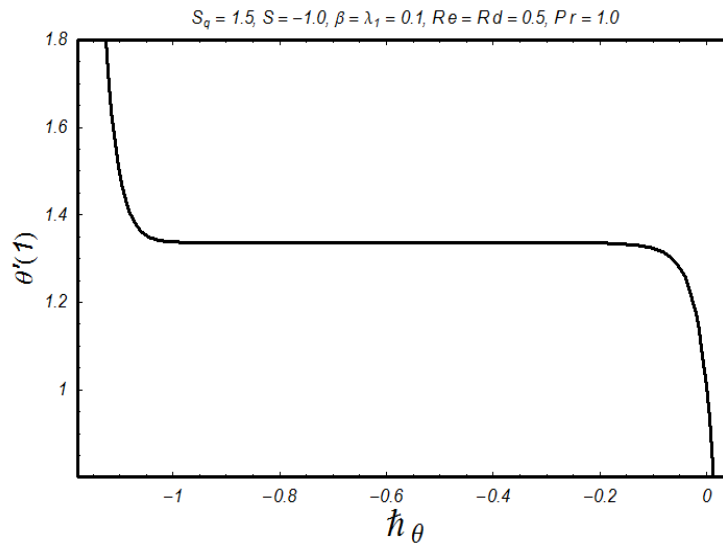
Fig. 3.4: Convergence region for θ at $\eta = 1$ in blowing case.

We know that the convergence of the series solution (by HAM) highly depends upon the auxiliary parameter. For that we choose $\hbar_\theta$ as the auxiliary parameter for the function θ. This parameter is useful in controlling and adjusting the convergence of the obtained solution. To obtain the admissible values of auxiliary parameter, we have plotted Figs. $(3.1 - 3.4)$ at $\eta = 0$

31

and $\eta = 1$ respectively. It is established that range for suitable values of $\hbar_\theta$ is $-0.7 \leq \hbar_\theta \leq -0.1$ for $\eta = 0$ and $\eta = 1$ respectively for $S = 1$ and it is $-1.0 \leq \hbar_\theta \leq -0.2$ for $\eta = 0$ and $\eta = 1$ when $S = -1$. As mentioned earlier that we here extended the work of chapter 2 for the case when heat transport phenomenon in the presence of thermal radiation effect is taken into account. Therefore we have just plotted the graphs for temperature field in this study since the results of velocity field have been already reported in chapter 2.

Table 3.1:. Series solution's convergence by HAM for different order of approximations when $S_q = 1.5$, $\lambda_1 = 0.1 = \beta$, $Rd = 0.5$, $Pr = 1.0$ and $Re = 0.5$.

Order of approximation	(for blowing)		(for suction)	
	$\theta'(0)$	$\theta'(1)$	$\theta'(0)$	$\theta'(1)$
1	0.8500000000	1.300000000	0.8500000000	1.300000000
5	0.7765901549	1.330436766	0.8878770710	1.252678964
10	0.7666196235	1.336478432	0.8890118171	1.252236295
15	0.7653444817	1.336716279	0.8889946572	1.252241035
20	0.7651313344	1.336747677	0.8889949365	1.252240969
25	0.7650916868	1.336752519	0.8889949318	1.252240970
30	0.7650838167	1.336753354	0.8889949319	1.252240970
35	0.7650821876	1.336753508	0.8889949319	1.252240970
40	0.7650818402	1.336753538	0.8889949319	1.252240970

3.3 Discussion

Our aim now is to present the impact of the embedding parameters on the temperature profile $\theta(\eta)$ for suction and blowing cases. Variations of Prandtl number (Pr) on the temperature field $\theta(\eta)$ for suction and blowing have been sketched in the Figs. 3.5 and 3.6. It is observed from Figs. 3.5 and 3.6 that temperature field decreases when we increase (Pr) for both suction and injection cases. It is due to the fact that higher Prandtl number relates to weaker thermal diffusivity and smaller Prandtl number has stronger thermal diffusivity. Smaller Prandtl fluid has larger temperature in comparison to the higher Prandtl fluid. In Figs. 3.7 and 3.8, we discussed the influence of radiation parameter (Rd) for both suction and injection cases. It is noticed from Fig. 3.7 that when we increase (Rd) the temperature profile decreases for suction case and it increases for injection case. Physically an increase in radiation parameter provides more heat to the working fluid for the injection case that causes an increase in temperature for the injection case. Table 3.2 highlights a comparative study of present work with the previous published result. It is observed that present analysis is in good agreement with existing research in a limiting sense.
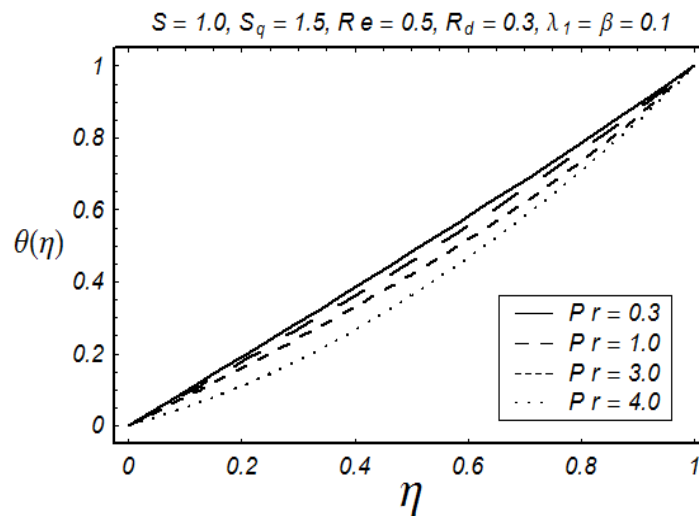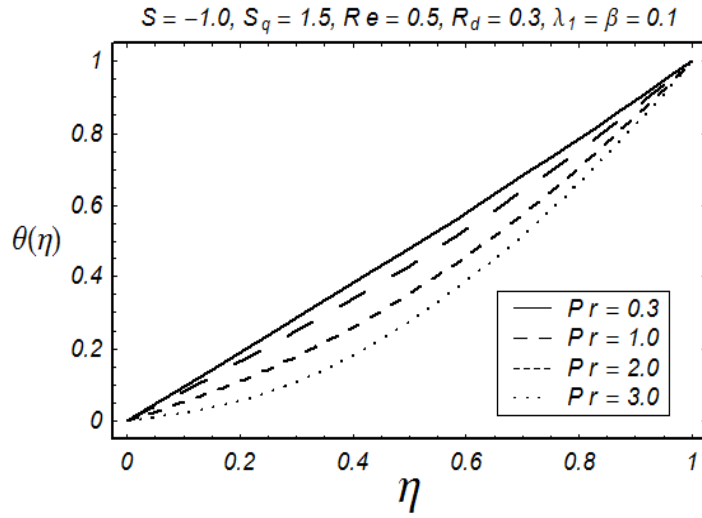

Fig. 3.5: Influence of Pr on θ for suction.
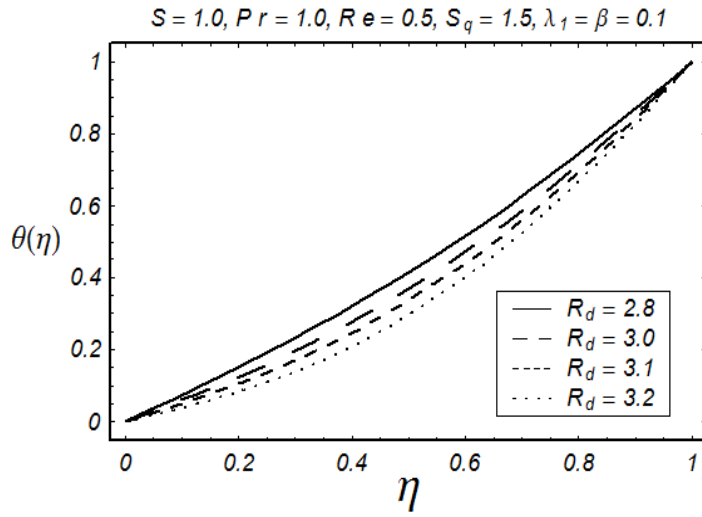
Fig. 3.6: Influence of Pr on θ for blowing.

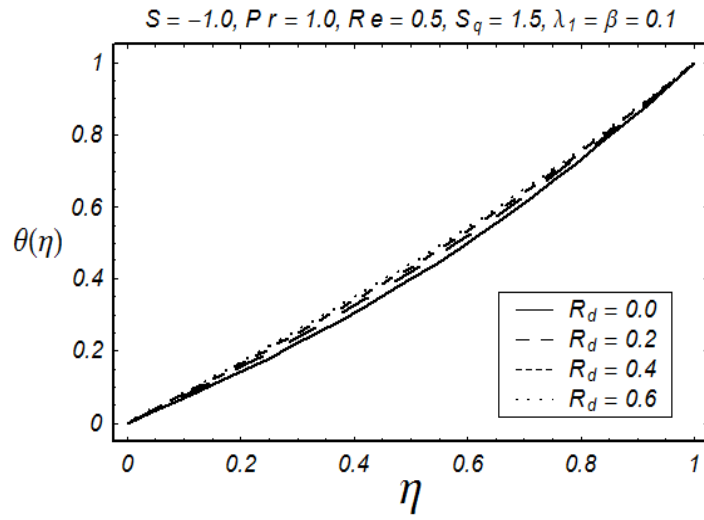Fig. 3.7: Influence of Rd on θ for suction.

34

Fig. 3.8: Influence of Rd on θ for blowing.

Chapter 4

Soret-Dufour effects in MHD squeezing flow of a Jeffrey fluid with Joule heating

This chapter is concerned with the unsteady squeezing flow of Jeffrey fluid between two parallel plates. Soret-Dufour and Joule heating effects are also considered. The fluid is electrically conducting in the presence of magnetic field. Transformation procedure reduces the partial differential equations into the ordinary differential equations. Convergent series solutions are developed. The solution expressions for velocity, temperature and concentration fields are computed and discussed. In addition the skin friction coefficient, Nusselt number and Sherwood number are tabulated and analyzed.

4.1   Mathematical analysis

We examine heat and mass transfer effects in axisymmetric squeezing flow of an electrically conducting Jeffrey fluid. The flow is bounded between two parallel disks distant $H\sqrt{1-at}$ apart. The flow is considered symmetric about $z = 0$. A constant magnetic field $\mathbf{B}_0$ is applied along the radial direction. The induced magnetic and electric fields are neglected. Joule heating is also taken into account. The temperature and concentration of the lower disk are T_0 and C_0 respectively. The upper disk at $z = h(t) = H\sqrt{1-at}$ is moving with velocity

$\frac{dz}{dt} = -\frac{aH}{2\sqrt{1-at}}$ while lower porous disk at $z = 0$ is stationary. The governing equations for magnetohydrodynamic (MHD) axisymmetric flow of Jeffrey fluid are given by

$$\frac{\partial u}{\partial r} + \frac{u}{r} + \frac{\partial w}{\partial z} = 0, \tag{4.1}$$

$$
\begin{aligned}
\rho\left(\frac{\partial u}{\partial t} + u\frac{\partial u}{\partial r} + w\frac{\partial u}{\partial z}\right) = {} & -\frac{\partial p}{\partial r} + \frac{\mu}{1+\lambda_1}\left(\frac{\partial^2 u}{\partial r^2} + \frac{\partial^2 u}{\partial z^2} + \frac{1}{r}\frac{\partial u}{\partial r} - \frac{u}{r^2}\right) \\
& + \frac{\mu\lambda_2}{1+\lambda_1}\left[\frac{\partial^3 u}{\partial t\partial z^2} + 2\frac{\partial^2 u}{\partial t\partial r^2} + \frac{2}{r}\frac{\partial^2 u}{\partial t\partial r} + \frac{\partial^3 w}{\partial t\partial r\partial z}\right. \\
& - \frac{2}{r^2}\frac{\partial u}{\partial t} + \frac{\partial u}{\partial r}\left(\frac{\partial^2 u}{\partial r^2} - \frac{2u}{r^2}\right) + \frac{\partial w}{\partial r}\frac{\partial^2 u}{\partial z\partial r} \\
& + u\left(\frac{\partial^3 u}{\partial r^3} + \frac{\partial^3 w}{\partial r^2\partial z} + \frac{\partial^3 u}{\partial r\partial z^2} + \frac{2u}{r^3}\right) \\
& + w\left(\frac{\partial^3 u}{\partial z\partial r^2} + \frac{2}{r}\frac{\partial^2 u}{\partial z\partial r} + \frac{\partial^3 w}{\partial z^3} + \frac{\partial^2 w}{\partial r\partial z}\right) \\
& + \frac{\partial u}{\partial z}\left(\frac{\partial^2 w}{\partial r^2} - \frac{2w}{r^2} + \frac{\partial^2 u}{\partial z\partial r}\right) \\
& + \left.\frac{\partial w}{\partial z}\left(\frac{\partial^2 u}{\partial z^2} + \frac{\partial^2 w}{\partial r\partial z}\right) + \frac{2}{r}\frac{\partial^2 u}{\partial r^2}\right] - \sigma B_0^2 u, \tag{4.2}
\end{aligned}
$$

$$
\begin{aligned}
\rho\left(\frac{\partial w}{\partial t} + u\frac{\partial w}{\partial r} + w\frac{\partial w}{\partial z}\right) = {} & -\frac{\partial p}{\partial z} + \frac{\mu}{1+\lambda_1}\left(\frac{\partial^2 w}{\partial r^2} + \frac{1}{r}\frac{\partial w}{\partial r} + \frac{\partial^2 w}{\partial z^2}\right) \\
& + \frac{\mu\lambda_2}{1+\lambda_1}\left[\frac{\partial^3 w}{\partial r\partial t\partial z} + \frac{\partial^3 w}{\partial t\partial r^2} + 2\frac{\partial^3 u}{\partial r\partial z^2} + 2\frac{\partial u}{\partial z}\frac{\partial^2 w}{\partial r\partial z}\right. \\
& + \frac{\partial u}{\partial r}\left(\frac{\partial^2 u}{\partial r\partial z} + \frac{\partial^2 w}{\partial r^2}\right) + u\left(\frac{\partial^3 u}{\partial r^2\partial z} + \frac{\partial^3 v}{\partial r^3}\right) \\
& + \frac{\partial w}{\partial r}\left(\frac{\partial^2 u}{\partial z^2} + \frac{\partial^3 u}{\partial t\partial z^2}\right) \\
& + w\left(\frac{\partial^3 u}{\partial r\partial z^2} + \frac{\partial^3 w}{\partial r^2\partial z} + \frac{\partial^3 w}{\partial z^3} + \frac{1}{r}\frac{\partial^2 u}{\partial z^2} + \frac{1}{r}\frac{\partial^2 w}{\partial z\partial r}\right) \\
& + \left.\frac{u}{r}\left(\frac{\partial^2 u}{\partial r\partial z} + \frac{\partial^2 w}{\partial r^2}\right) + \frac{1}{r}\left(\frac{\partial^2 u}{\partial t\partial z} + \frac{\partial^2 w}{\partial t\partial r}\right)\right], \tag{4.3}
\end{aligned}
$$

37

$$\rho c_p \left(\frac{\partial T}{\partial t} + u\frac{\partial T}{\partial r} + w\frac{\partial T}{\partial z} \right) = K_c \left(\frac{\partial^2 T}{\partial r^2} + \frac{\partial^2 T}{\partial z^2} + \frac{1}{r}\frac{\partial T}{\partial r} \right) + \sigma B_0^2 u^2$$

$$+ \frac{\rho D K_T}{C_s} \left[\frac{\partial^2 C}{\partial r^2} + \frac{\partial^2 C}{\partial z^2} + \frac{1}{r}\frac{\partial C}{\partial r} \right], \tag{4.4}$$

$$\frac{\partial C}{\partial t} + u\frac{\partial C}{\partial r} + w\frac{\partial C}{\partial z} = D \left(\frac{\partial^2 C}{\partial r^2} + \frac{\partial^2 C}{\partial z^2} + \frac{1}{r}\frac{\partial C}{\partial r} \right)$$

$$+ \frac{D K_T}{T_m} \left(\frac{\partial^2 T}{\partial r^2} + \frac{\partial^2 T}{\partial z^2} + \frac{1}{r}\frac{\partial T}{\partial r} \right). \tag{4.5}$$

In above equations u the radial velocity, w the axial velocity, T the fluid temperature, ρ the fluid density, c_p the specific heat, p the pressure, μ the dynamic viscosity, σ the electrical conductivity of fluid, λ_1 the ratio of relaxation to retardation times, λ_2 the retardation time, T the fluid temperature, C the concentration field, D the thermal diffusivity, K_c the thermal conductivity, C_s the concentration susceptibility, T_m the mean fluid temperature and K_T the thermal-diffusion ratio.

The subjected boundary conditions are:

$$u = 0, \quad w = \frac{\partial h}{\partial t}, T = T_0 + \frac{T_0}{1-at}, \ C = C_0 + \frac{C_0}{1-at} \quad \text{at} \quad z = h(t),$$

$$u = 0, \quad w = -w_0, T = T_0, \ C = C_0 \text{ at } z = 0. \tag{4.6}$$

Defining the transformations

$$u = \frac{ar}{2(1-at)} f'(\eta), \ w = -\frac{aH}{\sqrt{1-at}} f(\eta), \ \eta = \frac{z}{H\sqrt{1-at}},$$

$$T = T_0 + \frac{T_0}{1-at} \theta(\eta), \ C = C_0 + \frac{C_0}{1-at} \phi(\eta), \tag{4.7}$$

equation (4.1) is automatically satisfied and eliminating pressure from Eqs. $(4.2) - (4.5)$ we have

$$f^{(iv)} - S_q (1+\lambda_1) \left(\eta f''' + 3f'' - 2ff''' \right)$$

$$+ \frac{\beta}{2} \left(\eta f^{(v)} + 5f^{(iv)} + f''f''' - 3f'f^{(iv)} \right) - M^2 (1+\lambda_1) f'' = 0, \tag{4.8}$$

$$\theta'' - RePr \left(\eta\theta' + 2\theta - 2f\theta' \right) + M^2 RePrEcf'^2 + PrDu\phi'' = 0, \tag{4.9}$$

$$\phi'' - ReSc \left(\eta\phi' + 2\phi - 2f\phi' \right) + SrSc\theta'' = 0, \tag{4.10}$$

$$f\left(0\right) = S, \ f'\left(0\right) = 0, \ f\left(1\right) = \frac{1}{2}, \ f'\left(1\right) = 0, \ \theta\left(0\right) = 0, \ \theta\left(1\right) = 1, \ \phi\left(0\right) = 0, \ \phi\left(1\right) = 1, \quad (4.11)$$

where $S > 0$ and $S < 0$ respectively denote the suction and injection at the lower static disk. S_q the squeezing parameter, β the Deborah number, Re the Reynolds number, Pr the Prandtl number, M denotes the Hartman number, Ec the Eckert number, Sc the Schmidt number Sc, Du the Dufour number and Sr the Soret number. These quantities are defined as

$$
\begin{aligned}
S_q &= \frac{aH^2}{2\nu}, \quad \beta = \frac{\lambda_2 a}{1 - at}, \quad M^2 = \frac{\sigma B_0^2}{\rho a}, \quad Re = \frac{\rho a H^2}{2\mu}, \quad Pr = \frac{\mu c_p}{K_C}, \\
Ec &= \frac{a^2 r^2}{2c_p T_0}, \quad Sc = \frac{\nu}{D}, \quad Du = \frac{DK_T C_0}{\nu C_s c_p T_0}, \quad Sr = \frac{DK_T T_0}{\nu T_m C_0}.
\end{aligned}
\quad (4.12)
$$

The skin friction coefficient, local Nusselt number and Sherwood number are

$$C_f = \frac{\tau_{rz} \mid_{z=h(t)}}{\rho \left(\frac{aH}{2(1-at)^{1/2}}\right)^2}, \ N_u = -\frac{H}{T_0}\left(\frac{\partial T}{\partial z}\right)_{z=h(t)}, \ Sh = -\frac{H}{C_0}\left(\frac{\partial C}{\partial z}\right)_{z=h(t)}. \quad (4.13)$$

The dimensionless form of above quantities are

$$\frac{H^2}{r^2} Re_r C_f = \left(1 + \frac{3}{2}\beta\right) f''(1), \quad (4.14)$$

$$(1 - at)^{3/2} Nu = -\theta'(1), \quad (4.15)$$

$$(1 - at)^{3/2} Sh = -\phi'(1). \quad (4.16)$$

4.2 Solution expressions

We write $f(\eta)$, $\theta(\eta)$ and $\phi(\eta)$ in term of base functions

$$\left\{\eta^k \mid k \geq 0\right\}, \quad (4.17)$$

through the following definitions

$$f\left(\eta\right) = \sum_{k=0}^{\infty} a_k \eta^k, \ \theta\left(\eta\right) = \sum_{k=0}^{\infty} b_k \eta^k, \ \phi\left(\eta\right) = \sum_{k=0}^{\infty} c_k \eta^k,$$

where a_k, b_k and c_k are the coefficients. The initial approximations $f_0(\eta)$, $\theta_0(\eta)$, $\phi_0(\eta)$ and linear operators $\mathcal{L}_f$, $\mathcal{L}_\theta$, $\mathcal{L}_\phi$ are chosen as follows:

$$f_0(\eta) = S + \left(\frac{3}{2} - 2S\right)\eta^2 + (2S - 1)\eta^3, \ \theta_0(\eta) = \eta, \ \phi_0(\eta) = \eta, \tag{4.18}$$

$$\mathcal{L}_f = f^{(iv)}, \ \mathcal{L}_\theta = \theta'', \ \mathcal{L}_\phi = \phi'', \tag{4.19}$$

where

$$\mathcal{L}_f\left(C_1 + C_2\eta + C_3\eta^2 + C_4\eta^3\right) = 0, \ \mathcal{L}_\theta\left[C_5 + C_6\eta\right] = 0, \ \mathcal{L}_\phi\left[C_7 + C_8\eta\right] = 0, \tag{4.20}$$

and C_i $(i = 1 - 8)$ are the arbitrary constants.

4.2.1 Zeroth order deformation problems

The zeroth order problems ensures the following statements:

$$(1 - q)\mathcal{L}_f\left[\bar{f}(\eta; q) - f_0(\eta)\right] = q\hbar_f\mathcal{N}_f\left[\bar{f}(\eta; q)\right],$$
$$\bar{f}(0; q) = S, \ \bar{f}'(0, q) = 1, \ \bar{f}(1, q) = \frac{S_q}{2}, \ \bar{f}'(1, q) = 0, \tag{4.21}$$

$$(1 - q)\mathcal{L}_\theta\left[\bar{\theta}(\eta; q) - \theta_0(\eta)\right] = q\hbar_\theta\mathcal{N}_\theta\left[\bar{\theta}(\eta; q)\right],$$
$$\bar{\theta}(0; q) = 0, \ \bar{\theta}(1, q) = 1, \tag{4.22}$$

$$(1 - q)\mathcal{L}_\phi\left[\bar{\phi}(\eta; q) - \phi_0(\eta)\right] = q\hbar_\phi\mathcal{N}_\phi\left[\bar{\phi}(\eta; q)\right],$$
$$\bar{\phi}(0; q) = 0, \ \bar{\phi}(1, q) = 1, \tag{4.23}$$

In expressions (4.21), (4.22) and (4.23), $\hbar_f \neq 0$, $\hbar_\theta \neq 0$ and $\hbar_\phi \neq 0$ denote the auxiliary parameters and $0 \leq q \leq 1$ denotes an embedding parameter. It is observed that when q changes from 0 to 1, then $\bar{f}(\eta, q)$, $\bar{\theta}(\eta, q)$ and $\bar{\phi}(\eta; q)$ vary from $f_0(\eta)$ to $f(\eta)$, $\theta_0(\eta)$ to $\theta(\eta)$

and $\phi_0(\eta)$ to $\phi(\eta)$ respectively. When $q = 0$ and $q = 1$, one obtains

$$\bar{f}(\eta; 0) = f_0(\eta), \ \bar{f}(\eta; 1) = f(\eta), \tag{4.24}$$

$$\bar{\theta}(\eta, 0) = \theta_0(\eta), \ \bar{\theta}(\eta, 1) = \theta(\eta), \tag{4.25}$$

$$\bar{\phi}(\eta, 0) = \phi_0(\eta), \ \bar{\phi}(\eta, 1) = \phi(\eta). \tag{4.26}$$

The nonlinear operator is defined as follows

$$\mathcal{N}_f\left[\bar{f}(\eta; q)\right] = \frac{\partial^4 \bar{f}(\eta; q)}{\partial \eta^4} - M^2(1 + \lambda_1)\frac{\partial^2 \bar{f}(\eta; q)}{\partial \eta^2}$$

$$-S_q(1 + \lambda_1)\left(\eta\frac{\partial^3 \bar{f}(\eta; q)}{\partial \eta^3} + 3\frac{\partial^2 \bar{f}(\eta; q)}{\partial \eta^2} - 2\bar{f}(\eta; q)\frac{\partial^3 \bar{f}(\eta; q)}{\partial \eta^3}\right)$$

$$+\frac{\beta}{2}\left(\eta\frac{\partial^5 \bar{f}(\eta; q)}{\partial \eta^5} + 5\frac{\partial^4 \bar{f}(\eta; q)}{\partial \eta^4} + \frac{\partial^2 \bar{f}(\eta; q)}{\partial \eta^2}\frac{\partial^3 \bar{f}(\eta; q)}{\partial \eta^3} - 3\frac{\partial \bar{f}(\eta; q)}{\partial \eta}\frac{\partial^4 \bar{f}(\eta; q)}{\partial \eta^4}\right) \tag{4.27}$$

$$\mathcal{N}_\theta\left[\bar{\theta}(\eta; q)\right] = \frac{\partial^2 \bar{\theta}(\eta; q)}{\partial \eta^2} - RePr\left(\eta\frac{\partial \bar{\theta}(\eta; q)}{\partial \eta} + 2\bar{\theta}(\eta; q) - 2\bar{f}(\eta; q)\frac{\partial \bar{\theta}(\eta; q)}{\partial \eta}\right)$$

$$+M^2 ReEc\left(\frac{\partial \bar{f}(\eta; q)}{\partial \eta}\right)^2 + PrDu\frac{\partial^2 \bar{\phi}(\eta; q)}{\partial \eta^2}, \tag{4.28}$$

$$\mathcal{N}_\phi\left[\bar{\phi}(\eta; q)\right] = \frac{\partial^2 \bar{\theta}(\eta; q)}{\partial \eta^2} - ReSc\left(\eta\frac{\partial \bar{\phi}(\eta; q)}{\partial \eta} + 2\bar{\phi}(\eta; q) - 2\bar{f}(\eta; q)\frac{\partial \bar{\phi}(\eta; q)}{\partial \eta}\right)$$

$$+SrSc\frac{\partial^2 \bar{\theta}(\eta; q)}{\partial \eta^2}. \tag{4.29}$$

By applying the Taylor series on $f(\eta)$, $\theta(\eta)$ and $\phi(\eta)$ one can write

$$f(\eta) = f_0(\eta) + \sum_{m=1}^{\infty} f_m(\eta)q^m, \tag{4.30}$$

$$\theta(\eta) = \theta_0(\eta) + \sum_{m=1}^{\infty} \theta_m(\eta)q^m, \tag{4.31}$$

$$\phi(\eta) = \phi_0(\eta) + \sum_{m=1}^{\infty} \phi_m(\eta)q^m, \tag{4.32}$$

$$f_m(\eta) = \frac{1}{m!}\frac{\partial^m \bar{f}(\eta, q)}{\partial q^m}\bigg|_{q=0}, \ \theta_m(\eta) = \frac{1}{m!}\frac{\partial^m \bar{\theta}(\eta, q)}{\partial q^m}\bigg|_{q=0}, \ \phi_m(\eta) = \frac{1}{m!}\frac{\partial^m \bar{\phi}(\eta, q)}{\partial q^m}\bigg|_{q=0}. \tag{4.33}$$

41

We select the auxiliary parameter in such a way that the series $(4.30 - 4.32)$ converge at $q = 1$ and we have

$$f(\eta) \;=\; f_0(\eta) + \sum_{m=1}^{\infty} f_m(\eta), \tag{4.34}$$

$$\theta(\eta) \;=\; \theta_0(\eta) + \sum_{m=1}^{\infty} \theta_m(\eta), \tag{4.35}$$

$$\phi(\eta) \;=\; \phi_0(\eta) + \sum_{m=1}^{\infty} \phi_m(\eta), \tag{4.36}$$

4.2.2 Higher order deformation problems

The mth order deformation problems are

$$\mathcal{L}_f \left[f_m\left(\eta\right) - \chi_m f_{m-1}\left(\eta\right) \right] = \hbar_f \Re_m^f \left(f_{m-1}\left(\eta\right)\right),$$
$$f_m\left(0\right) = 0, \;\; f_m'\left(0\right) = 0, \;\; f_m\left(1\right) = 0, \;\; f_m'\left(1\right) = 0, \tag{4.37}$$

$$\mathcal{L}_\theta \left[\theta_m\left(\eta\right) - \chi_m \theta_{m-1}\left(\eta\right) \right] = \hbar_\theta \Re_m^\theta \left(\theta_{m-1}\left(\eta\right)\right),$$
$$\theta_m\left(0\right) = 0, \;\; \theta_m\left(1\right) = 0, \tag{4.38}$$

$$\mathcal{L}_\phi \left[\phi_m\left(\eta\right) - \chi_m \phi_{m-1}\left(\eta\right) \right] = \hbar_\phi \Re_m^\phi \left(\phi_{m-1}\left(\eta\right)\right),$$
$$\phi_m\left(0\right) = 0, \;\; \phi_m\left(1\right) = 0, \tag{4.39}$$

where

$$\chi_m = \begin{cases} 0, & m \leq 1, \\ 1, & m > 1, \end{cases}$$

$$\Re_m^f (f_{m-1}(\eta)) = f_{m-1}^{(iv)}(\eta) - S_q(1+\lambda_1)\left[\eta f_{m-1}'''(\eta) + 3f_{m-1}''(\eta)\right]$$

$$+\frac{\beta}{2}\left[\eta f_{m-1}^{(v)}(\eta) + 5f_{m-1}^{(iv)}(\eta)\right] - M^2(1+\lambda_1)f_{m-1}''(\eta)$$

$$+\sum_{n=0}^{m-1}\left[2S_q(1+\lambda_1)f_n(\eta)f_{m-1-n}'''(\eta) + \frac{\beta}{2}\left(f_n''(\eta)f_{m-1-n}'''(\eta)\right)\right.$$

$$\left.-3f_n'(\eta)f_{m-1-n}^{(iv)}(\eta)\right)\right], \tag{4.40}$$

$$\Re_m^\theta(\theta_{m-1}(\eta)) = \theta_{m-1}''(\eta) - RePr\left[\eta\theta_{m-1}'(\eta) + 2\theta_{m-1}(\eta)\right] + PrDu\phi_{m-1}''(\eta)$$

$$+RePr\sum_{n=0}^{m-1}\left[2f_n(\eta)\theta_{m-1-n}'(\eta) + M^2Ecf_n'(\eta)f_{m-1-n}'(\eta)\right], \tag{4.41}$$

$$\Re_m^\phi(\theta_{m-1}(\eta)) = \phi_{m-1}''(\eta) - ReSc\left[\eta\phi_{m-1}'(\eta) + 2\phi_{m-1}(\eta)\right] + SrSc\theta_{m-1}''(\eta)$$

$$+2ReSc\sum_{n=0}^{m-1}f_n(\eta)\phi_{m-1-n}'(\eta). \tag{4.42}$$

The general solutions of boundary value problems given in Eqs. $(4.37 - 4.39)$ are

$$f_m(\eta) = f_m^*(\eta) + C_1 + C_2\eta + C_3\eta^2 + C_4\eta^3 \tag{4.43}$$

$$\theta_m(\eta) = \theta_m^*(\eta) + C_5 + C_6\eta \tag{4.44}$$

$$\phi_m(\eta) = \phi_m^*(\eta) + C_7 + C_8\eta \tag{4.45}$$

in which $f_m^*(\eta)$, $\theta_m^*(\eta)$ and $\phi_m^*(\eta)$ are the special solutions of the problem given in Eqs. $(4.37 - 4.39)$. The coefficients C_i $(i = 1 - 8)$ can be found through the boundary conditions Eqs. $(4.37 - 4.39)$.

4.2.3 Convergence of solutions

We know that the convergence of the series solution (by HAM) highly depends upon the auxiliary parameters. For that we choose $\hbar_f$, $\hbar_\theta$ and $\hbar_\phi$ for the functions f, θ and ϕ as the auxiliary parameters. These parameters are useful in controlling and adjusting the convergence of the obtained solutions. To obtain the admissible values of auxiliary parameters, we have sketched Figs. $(4.1 - 4.4)$ at $\eta = 0$ for both suction and injection. It is noticed that ranges for suitable

43

values of $\hbar_f$, $\hbar_\theta$ and $\hbar_\phi$ are $-1.0 \le \hbar_f \le -0.35$ (for suction), $-0.9 \le \hbar_f \le -0.3$ (for injection), $-1.9 \le \hbar_\theta, \hbar_\phi \le -0.5$ (for suction) and $-1.0 \le \hbar_\theta, \hbar_\phi \le -0.4$ (for injection) at $\eta = 0$. Table 4.1 is constructed to show that the orders of approximation up to six decimal places are achieved at 16th, 32th and 35th order of approximations at $\eta = 0$, 16th, 30th and 32th order of approximations at $\eta = 1$ for blowing and 15th, 30th and 30th order of approximations at $\eta = 0$, 10th, 27th and 27th order of approximations at $\eta = 1$ for suction.
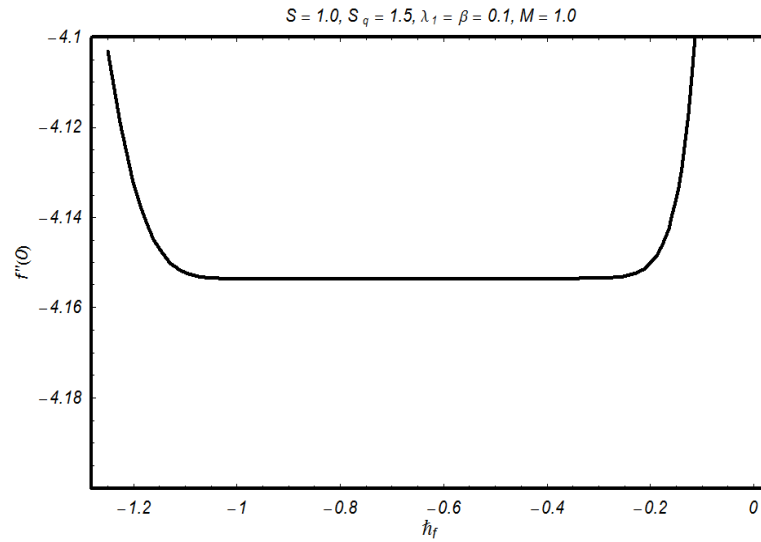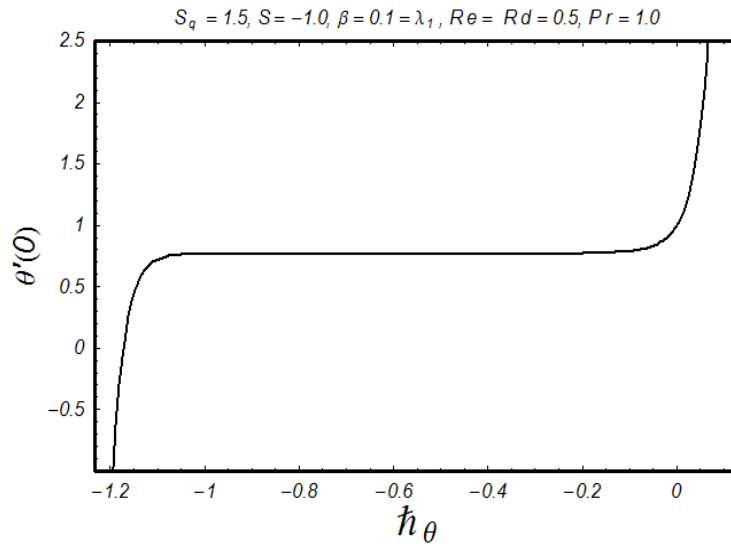

Fig. 4.1: Convergence region for f at $\eta = 0$ in suction.

Fig. 4.2: Convergence region for f at $\eta = 0$ in blowing.

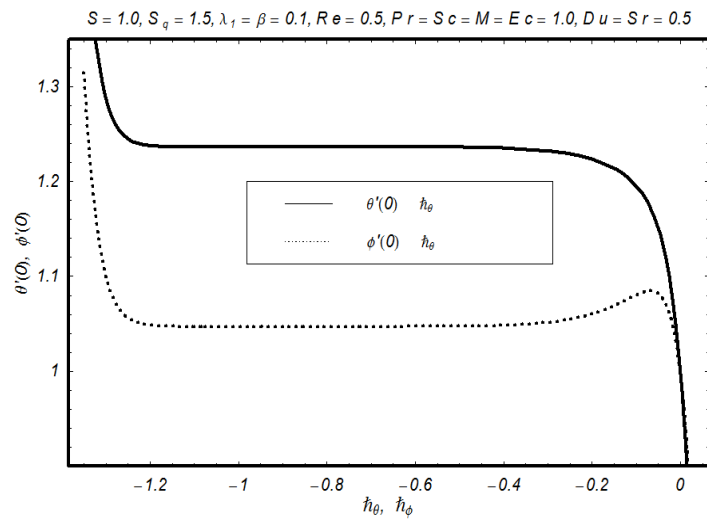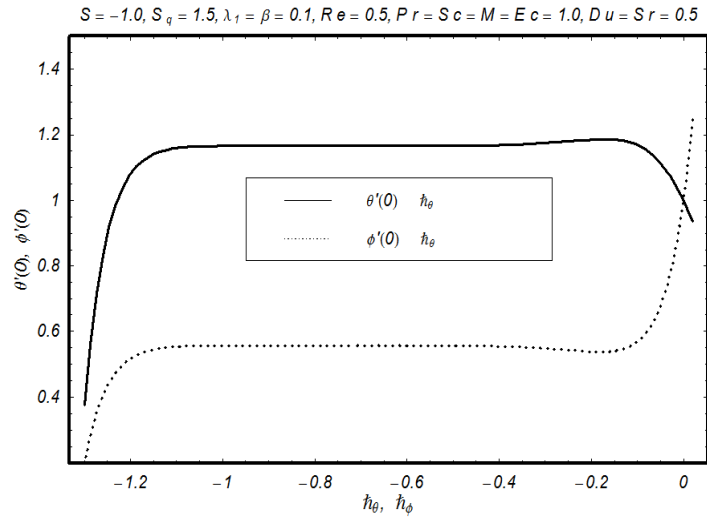Fig. 4.3: Convergence region for θ and ϕ at $\eta = 0$ in suction.

$S = -1.0,\ S_q = 1.5,\ \lambda_1 = \beta = 0.1,\ Re = 0.5,\ Pr = Sc = M = Ec = 1.0,\ Du = Sr = 0.5$

Fig. 4.4: Convergence region for θ and ϕ at $\eta = 0$ in blowing.

Table 4.1:. Series solution's convergence by HAM for different order of approximations when $S_q = 1.5$, $\lambda_1 = \beta = 0.1$, $Pr = Sc = M = Ec = 1.0$, $Re = Du = Sr = 0.5$ and $\hbar_f = -0.4$.

Order of approximation	(for blowing)					
	$f''(0)$	$f''(1)$	$\theta'(0)$	$\theta'(1)$	$\phi'(0)$	$\phi'(1)$
1	7.716214	-10.68621	1.090000	0.880000	0.685000	1.285000
5	7.565773	-11.54585	1.194840	0.579025	0.527470	1.595504
10	7.569565	-11.54259	1.172617	0.529937	0.550204	1.644717
15	7.569505	-11.54250	1.166880	0.525442	0.555935	1.649210
16	7.569507	-11.54251	1.166617	0.525265	0.556198	1.649387
20	7.569507	-11.54251	1.166288	0.525006	0.556527	1.649646
25	7.569507	-11.54251	1.166277	0.524958	0.556538	1.649695
30	7.569507	-11.54251	1.166287	0.524951	0.556529	1.649701
32	7.569507	-11.54251	1.166288	0.524951	0.556527	1.649702
35	7.569507	-11.54251	1.166288	0.524951	0.556526	1.649702
40	7.569507	-11.54251	1.166288	0.524951	0.556526	1.649702
45	7.569507	-11.54251	1.166288	0.524951	0.556526	1.649702

Order of approximation	(for suction)					
	$f''(0)$	$f''(1)$	$\theta'(0)$	$\theta'(1)$	$\phi'(0)$	$\phi'(1)$
1	-3.780643	2.790643	1.150000	1.060000	1.105000	1.105000
5	-4.154397	2.746023	1.214939	1.047257	1.068955	1.150789
10	-4.156797	2.746224	1.232270	1.042944	1.051616	1.155099
15	-4.156798	2.746224	1.235803	1.042745	1.048083	1.155298
20	-4.156798	2.746224	1.236467	1.042774	1.047418	1.155269
25	-4.156798	2.746224	1.236585	1.042785	1.047301	1.155258
27	-4.156798	2.746224	1.236605	1.042786	1.047281	1.155256
30	-4.156798	2.746224	1.236608	1.042786	1.047278	1.155256
35	-4.156798	2.746224	1.236608	1.042786	1.047278	1.155256
40	-4.156798	2.746224	1.236608	1.042786	1.047278	1.155256

4.3   Analysis

The purpose of this section is to analyze the influence of the emerging parameters on the radial velocity $f'(\eta)$, temperature $\theta(\eta)$ and concentration $\phi(\eta)$ fields in the suction and blowing (or injection) cases. Effects of Hartman number M on radial velocity are discussed in the Figs. 4.5 and 4.6 for both suction and injection cases. In Fig. 4.5, the velocity field f' decreases near the porous $(0 \leq \eta \leq 0.21)$ and squeezing $(0.61 \leq \eta \leq 1)$ walls but it increases at the centre $(0.21 \leq \eta \leq 0.61)$ of the channel when we increase Hartman number M for the suction case. In fact the magnetic field slows down the fluid particles and retards the motion of the fluid particles in the region of both walls but obviously to satisfy law of conservation of mass an increase in fluid velocity occurs at the central region. Fig. 4.6 shows opposite trend in case of blowing when compared to the case of suction. Combined effects of Dufour and Soret numbers on the temperature field $\theta(\eta)$ are discussed in the Figs. 4.7 and 4.8. Both cases of suction and injection are taken. Fig. 4.7 shows that with the increase of Dufour number Du and decrease of Soret number Sr, the temperature field decreases in the vicinity of lower porous disk $(0 \leq \eta \leq 0.41)$ and it increases in the vicinity of upper squeezing disk $(0.41 \leq \eta \leq 1.0)$. Fig. 4.8 shows that with the increase of Dufour number (Du) and decrease of Soret number (Sr), the temperature field increases for blowing case. Physically we can observe that Dufour effect describes the heat flux created when a chemical system is under concentration gradient. Such effect depends upon thermal diffusion which is generally very small but can be sometimes significant when the participating species are of widely differing molecular weights. Mass diffusion occurs if the species are initially distributed unevenly i.e., when a concentration gradient exists. A temperature gradient can also work as a driving force for mass diffusion called thermo-diffusion or Soret effects. Therefore the higher the temperature gradient, the larger the Soret effects. Effect of Hartman number M on temperature profile $\theta(\eta)$ is illustrated in Fig. 4.9 for the suction case. The temperature increases when M is increased. Figs. 4.10 and 4.11 illustrate the effects of Eckert number Ec on temperature profile $\theta(\eta)$ for both suction and blowing cases. Temperature profile increases with an increase of Eckert number Ec in both suction and injection cases. Since the Eckert number is the ratio of kinetic energy to the enthalpy. An increase in the Eckert number indicates an increase in kinetic energy. Since temperature is the average kinetic energy of fluid particles. Therefore $\theta(\eta)$ increases with an increase in

the Eckert number. When the electrical current passes through a medium then some of the electrical energy is converted into heat energy which is called Joule heating. Hence an increase in Hartman number corresponds to an increase in the intensity of the magnetic field. Thus more heat dissipates and adds to the system. As a consequence the $\theta(\eta)$ increases. Effects of Schmidt number Sc on concentration profile $\phi(\eta)$ are illustrated in the Figs. 4.12 and 4.13 for suction and injection respectively. With an increase of Schmidt number Sc, the concentration field decreases when $0 \leq \eta \leq 0.41$ while it increases when $0.41 \leq \eta \leq 1.0$ for the suction case. For blowing case, the concentration field decreases with the increase of Schmidt number Sc. Combined effects of Dufour and Soret numbers on the concentration field are drawn in the Figs. 4.14 and 4.15 for suction and injection cases respectively. Fig. 4.14 indicates that with increase of Dufour number Du and decrease of Soret number Sr, the concentration field decreases for $0 \leq \eta \leq 0.54$ and it increases for $0.54 \leq \eta \leq 1.0$ in the suction case. Fig. 4.15 illustrates that concentration field decreases with the increase of Dufour number Du and it decreases with Soret number Sr.

Tables 4.2 and 4.3 provide the numerical values of skin friction coefficient, local Nusselt number and Sherwood number for different embedded parameters. The skin friction coefficient increases by increasing S whereas it decreases for positive values of S_q, λ_1, M and β. With the increase of S, S_q, λ_1 and β, the local Nusselt number decreases while it increases with the increase of M, Du and Sr. Through increase of S, S_q, λ_1, M, Du and Sr, the Sherwood number decreases while it increases with the increase of β. Table 4.4 highlights a comparison of present work with the previous published attempts. It is found that present results are in an excellent

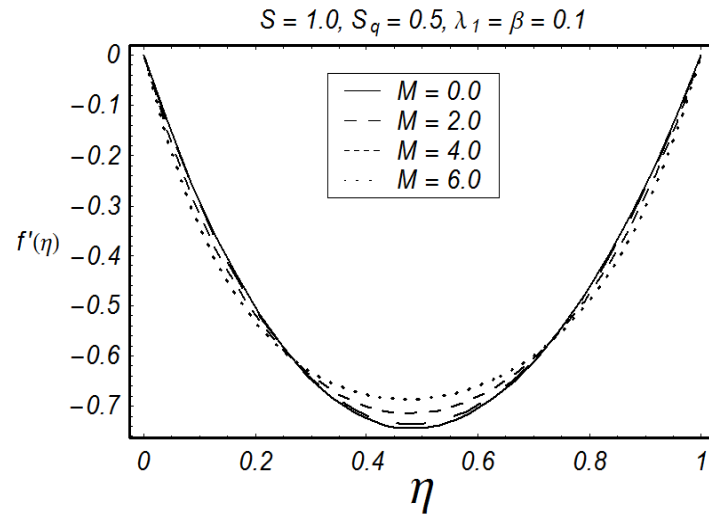agreement with previous research in the limiting cases.
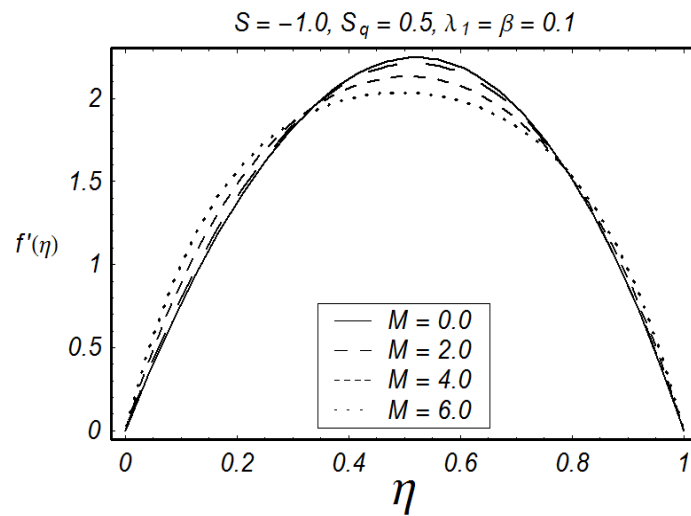

Fig. 4.5: Influence of M on f' for suction.
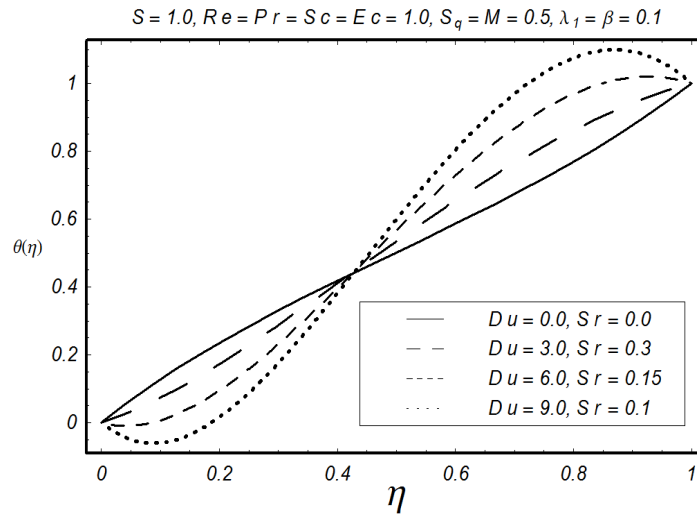

Fig. 4.6: Influence of M on f' for blowing.

Fig. 4.7: Influence of Du and Sr on θ for suction.
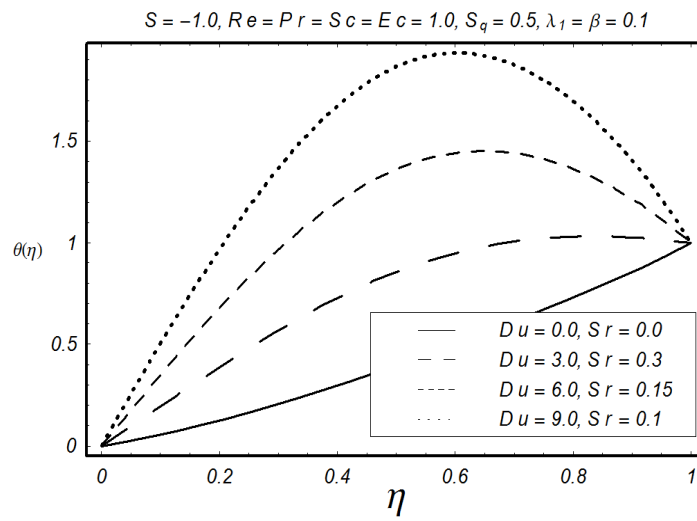

Fig. 4.8: Influence of Du and Sr on θ for blowing.
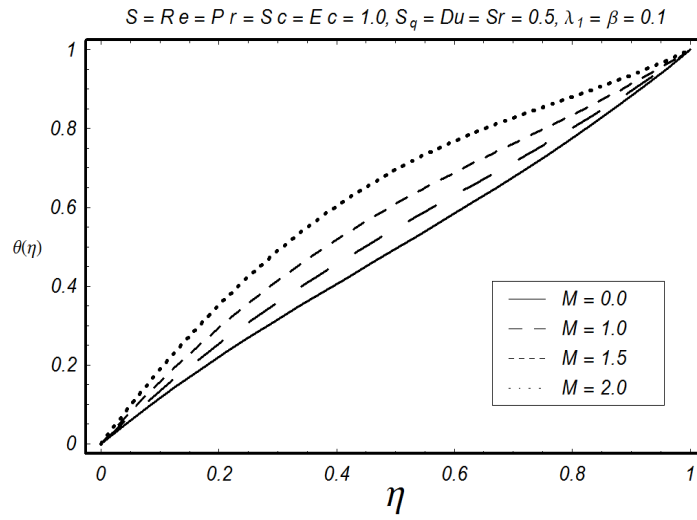
Fig. 4.9: Influence of M on θ for suction.
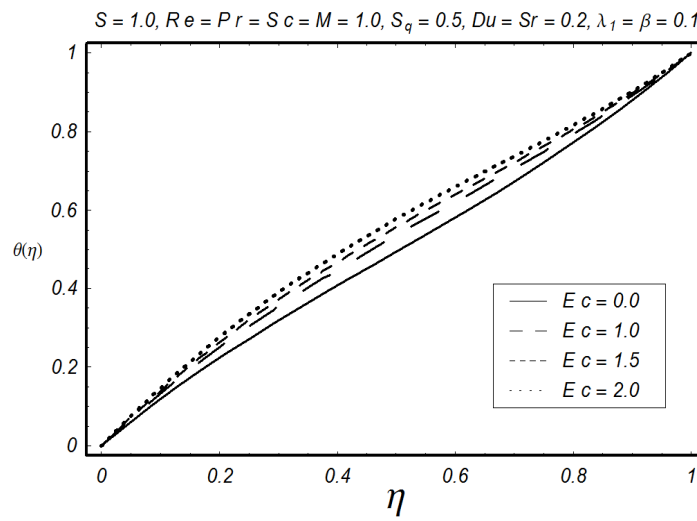
Fig. 4.10: Influence of Ec on θ for suction.

$S = -1.0,\, Re = Pr = Sc = M = 1.0,\, S_q = 0.5,\, Du = Sr = 0.2,\, \lambda_1 = \beta = 0.1$

Fig. 4.11: Influence of Ec on θ for blowing.

$S = 1.0,\, Re = Pr = Ec = 1.0,\, S_q = M = 0.5,\, \lambda_1 = \beta = 0.1,\, Du = Sr = 0.2$
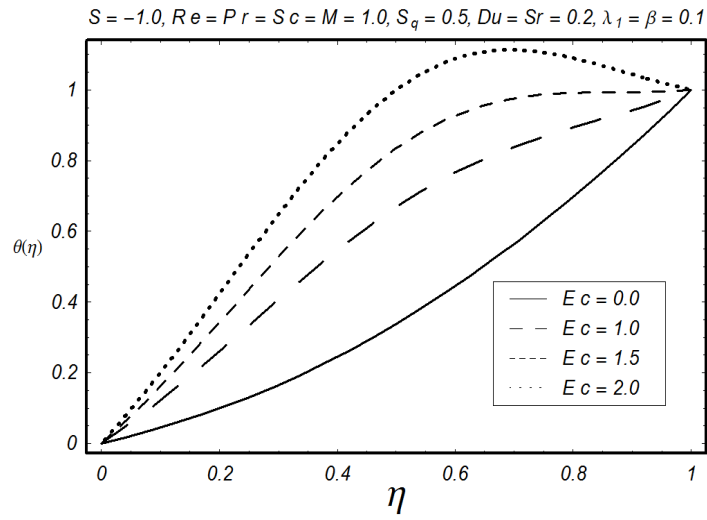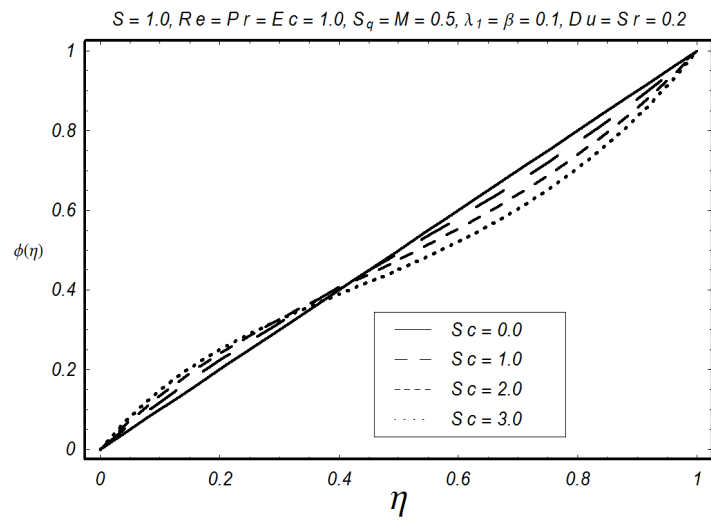
Fig. 4.12: Influence of Sc on ϕ for suction.
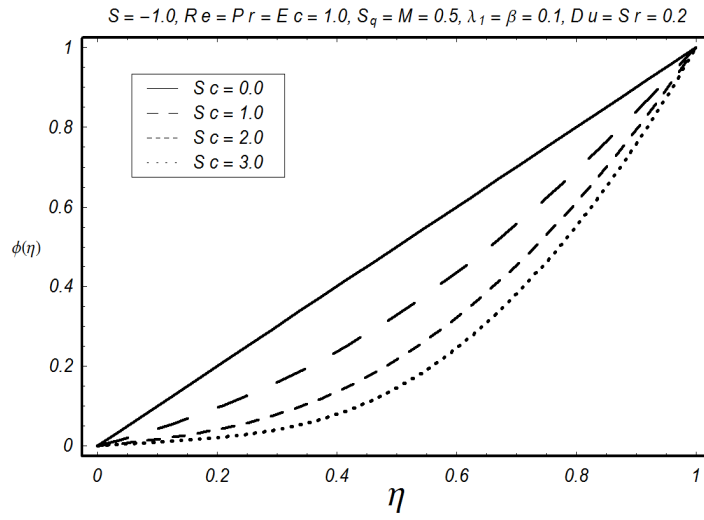
Fig. 4.13: Influence of Sc on ϕ for blowing.
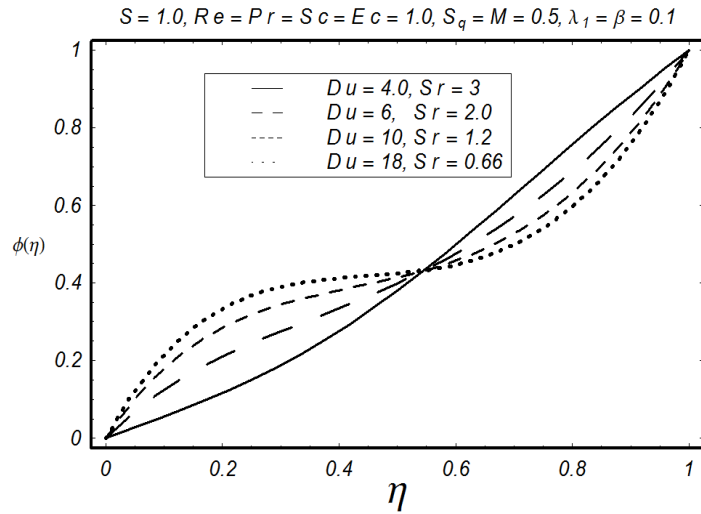
Fig. 4.14: Influence of Du and Sr on ϕ for suction.

$S = -1.0, Re = Pr = Sc = Ec = 1.0, S_q = M = 0.5, \lambda_1 = \beta = 0.1$

Legend:
- $Du = 4.0, Sr = 3$
- $Du = 6, \quad Sr = 2.0$
- $Du = 10, Sr = 1.2$
- $Du = 18, Sr = 0.66$

$\phi(\eta)$

Fig. 4.15: Influence of Du and Sr on ϕ for blowing.

Table 4.2: Values of skin friction coefficient, local Nusselt number and Sherwood number for different emerging parameters when $Pr = Sc = Ec = 1.0$, $\text{Re} = Du = Sr = 0.5$.
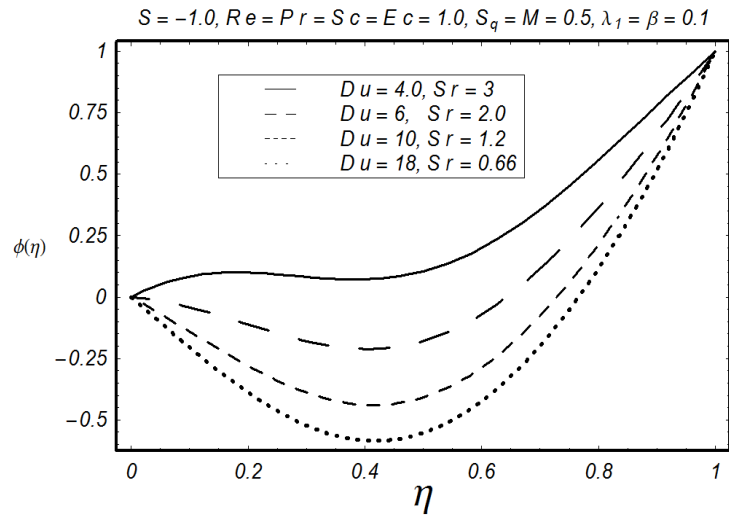
S	S_q	λ_1	β	M	$\frac{H^2}{r^2} Re_{r} C_f$	$(1-at)^{3/2} Nu$	$(1-at)^{3/2} Sh$
-2.0	1.0	0.1	0.1	0.5	-24.84606	-0.8655236	-1.647918
-1.0					-12.36713	-1.111552	-1.387342
0.5					0.000000	-1.162187	-1.162187
1.0					3.214864	-1.099825	-1.128748
-0.5	0.5	0.1	0.1	0.5	-7.312816	-1.169153	-1.289044
	1.5				-7.957332	-1.169678	-1.292141
	2.0				-8.258052	-1.169909	-1.293497
	2.5				-8.545881	-1.170122	-1.294742
-0.5	1.0	0.0	0.1	0.5	-7.582271	-1.169375	-1.290382
		0.2			-7.702460	-1.169479	-1.290935
		0.3			-7.761728	-1.169530	-1.291204
		0.4			-7.820456	-1.169580	-1.291469
-0.5	1.0	0.1	0.0	0.5	-6.701664	-1.169409	-1.291181
			0.2		-8.567625	-1.169438	-1.290135
			0.3		-9.477623	-1.169439	-1.289611
-0.5	1.0	0.1	0.1	0.0	-7.625739	-1.253467	-1.253467
				0.4	-7.636556	-1.199665	-1.277278
				1.0	-7.693446	-0.9181438	-1.401899

Table **4.3**. Values of local Nusselt number for different emerging parameters when $S = -1.0$, $\mathrm{Re} = 0.5$, $S_q = Pr = Ec = Sc = M = 1.0$, and $\beta = \lambda_1 = 0.1$.

Du	Sr	$(1-at)^{3/2}\,Nu$	$(1-at)^{3/2}\,Sh$
0.0	0.5	-0.8226191	-1.511866
0.2		-0.7237254	-1.555881
0.4		-0.6061634	-1.608229
0.6		-0.4640282	-1.671562
0.5	0.0	-0.6234136	-1.440144
	0.2	-0.5934533	-1.510079
	0.4	-0.5584374	-1.591943
	0.6	-0.5170207	-1.688961
	0.8	-0.4673695	-1.805563

Table **4.4**: Comparison between HAM and HPM solutions [69]

S	$f''(1)$		
	HPM [69]	HPM [69]	Present results
0.1	2.97682	2.97682	2.97682
0.5	–	2.89177	2.89177
1.0	–	2.80242	2.80242
1.5	–	2.73094	2.73094

4.4   Concluding remarks

Squeezing flow of Jeffrey fluid with Soret and Dufour effects is analyzed in the presence of Joule heating. The main observations are listed below.

- Effects of Hartman number on velocity profile $f'(\eta)$ are opposite for suction and blowing.

- Temperature profile $\theta(\eta)$ in suction case decreases near the lower disk and it increases near the upper disk when Soret and Dufour numbers increase.

- Temperature profile $\theta(\eta)$ in injection case increases through out the domain with the increase of Soret and Dufour number.

- Temperature profile $\theta(\eta)$ is higher for larger values of Hartman number M.

- Temperature profile $\theta(\eta)$ is higher for larger values of Eckert number Ec for both suction and injection.

- Concentration field $\phi(\eta)$ is an increasing function of Schmidt number Sc near the lower disk while it is decreasing function of Sc near the upper wall for suction case but concentration field $\phi(\eta)$ decreases through out the domain for injection.

- Behavior of concentration profile $\phi(\eta)$ in suction is opposite near the lower and upper walls with the increase of Soret and Dufour numbers.

- Behavior of concentration profile $\phi(\eta)$ in injection is opposite for Soret and Dufour numbers.

- Skin friction coefficient increases by increasing S whereas it decreases for positive values of S_q, λ_1, M and β.

- With the increase of S, S_q, λ_1 and β, the local Nusselt number decreases while it increases with the increase of M, Du and Sr.

- Through increase of S, S_q, λ_1, M, Du and Sr, the Sherwood number decreases while it increases with the increase of β.

Chapter 5

Squeezing flow of Jeffrey fluid with chemical reaction

This chapter explores the simultaneous effects of heat and mass transfer in squeezing flow of Jeffrey fluid between parallel plates. Viscous dissipation and chemical reaction effects are present. Series solution to the involved system is computed. A parametric study of pertinent variables is conducted. The skin friction coefficient, local Nusselt and Sherwood numbers are computed and examined.

5.1 Mathematical analysis

We examine the time-dependent squeezing flow of Jeffrey fluid with heat and mass transfer. The flow is bounded by two parallel plates situated at $z = \pm H (1 - at)^{\frac{1}{2}} = \pm h(t)$. For $a > 0$ the plates are squeezed and the squeezing plates touch each other for $t = 1/a$ while separation between the plates occurs for $a < 0$. The flow analysis has been investigated by considering viscous dissipation and heat generation due to friction produced by shear forces in Jeffrey fluid. This effect is relatively significant in the case when the fluid is mainly viscous or flowing at a high speed. This situation occurs when Eckert number ($Ec >> 1$) is very high. Mass transfer is considered in the presence of chemical reaction and flow is taken symmetric. Fundamental laws of mass, momentum, energy and concentration for time-dependent two-dimensional flow

of Jeffrey fluid give

$$\frac{\partial u}{\partial x} + \frac{\partial v}{\partial y} = 0, \tag{5.1}$$

$$\rho \left[\frac{\partial u}{\partial t} + u\frac{\partial u}{\partial x} + v\frac{\partial u}{\partial y} \right] = -\frac{\partial p}{\partial x} + \frac{\mu}{1+\lambda_1} \left[\frac{\partial^2 u}{\partial x^2} + \frac{\partial^2 u}{\partial y^2} \right.$$
$$+ \lambda_2 \left(\frac{\partial^3 u}{\partial t \partial x^2} + \frac{\partial^3 u}{\partial t \partial y^2} + 2\frac{\partial u}{\partial x}\frac{\partial^2 u}{\partial x^2} + 2\frac{\partial v}{\partial x}\frac{\partial^2 u}{\partial x \partial y} + u\left(\frac{\partial^3 u}{\partial x^3} + \frac{\partial^3 u}{\partial x \partial y^2} \right) \right.$$
$$\left. \left. + v\left(\frac{\partial^3 u}{\partial x^2 \partial y} + \frac{\partial^3 u}{\partial y^3} \right) + \frac{\partial u}{\partial y}\left(\frac{\partial^2 u}{\partial x \partial y} + \frac{\partial^2 v}{\partial x^2} \right) + \frac{\partial v}{\partial y}\left(\frac{\partial^2 u}{\partial y^2} + \frac{\partial^2 v}{\partial x \partial y} \right) \right) \right], \tag{5.2}$$

$$\rho \left[\frac{\partial v}{\partial t} + u\frac{\partial v}{\partial x} + v\frac{\partial v}{\partial y} \right] = -\frac{\partial p}{\partial y} + \frac{\mu}{1+\lambda_1} \left[\frac{\partial^2 v}{\partial x^2} + \frac{\partial^2 v}{\partial y^2} \right.$$
$$+ \lambda_2 \frac{\partial^3 v}{\partial t \partial x^2} + \frac{\partial^3 v}{\partial t \partial y^2} + 2\frac{\partial u}{\partial y}\frac{\partial^2 v}{\partial x \partial y} + 2\frac{\partial v}{\partial y}\frac{\partial^2 v}{\partial y^2} + u\left(\frac{\partial^3 v}{\partial x^3} + \frac{\partial^3 v}{\partial x \partial y^2} \right)$$
$$\left. \left. + v\left(\frac{\partial^3 v}{\partial y^3} + \frac{\partial^3 v}{\partial x^2 \partial y} \right) + \frac{\partial u}{\partial x}\left(\frac{\partial^2 v}{\partial x^2} + \frac{\partial^2 u}{\partial x \partial y} \right) + \frac{\partial v}{\partial x}\left(\frac{\partial^2 u}{\partial y^2} + \frac{\partial^2 v}{\partial x \partial y} \right) \right) \right], \tag{5.3}$$

$$\rho C_p \left[\frac{\partial T}{\partial t} + u\frac{\partial T}{\partial x} + v\frac{\partial T}{\partial y} \right] = K_c \left(\frac{\partial^2 T}{\partial x^2} + \frac{\partial^2 T}{\partial y^2} \right) + \frac{\mu}{1+\lambda_1} \left[2\left(\frac{\partial u}{\partial x} \right)^2 + 2\left(\frac{\partial v}{\partial y} \right)^2 + \left(\frac{\partial u}{\partial y} + \frac{\partial v}{\partial x} \right)^2 \right.$$
$$+ \lambda_2 \left\{ 2\frac{\partial u}{\partial x}\left(\frac{\partial^2 u}{\partial t \partial x} + u\frac{\partial^2 u}{\partial x^2} + v\frac{\partial^2 u}{\partial x \partial y} \right) + \left(\frac{\partial u}{\partial y} + \frac{\partial v}{\partial x} \right)\left(\frac{\partial^2 u}{\partial t \partial y} + \frac{\partial^2 v}{\partial t \partial x} \right. \right.$$
$$\left. \left. \left. + u\left(\frac{\partial^2 u}{\partial x \partial y} + \frac{\partial^2 v}{\partial x^2} \right) + v\left(\frac{\partial^2 u}{\partial y^2} + \frac{\partial^2 v}{\partial x \partial y} \right) \right) + 2\frac{\partial v}{\partial y}\left(\frac{\partial^2 v}{\partial t \partial y} + u\frac{\partial^2 v}{\partial x \partial y} + v\frac{\partial^2 v}{\partial y^2} \right) \right\} \right], \tag{5.4}$$

$$\frac{\partial C}{\partial t} + u\frac{\partial C}{\partial x} + v\frac{\partial C}{\partial y} = D\left(\frac{\partial^2 C}{\partial x^2} + \frac{\partial^2 C}{\partial y^2} \right) - K_1(t)C. \tag{5.5}$$

Here u denotes velocity along the $x-$direction, v the velocity along the $y-$direction, T, C, p, ρ, ν, K_c, C_p, D and $K_1(t) = \frac{k_1}{1-\alpha t}$ represent the temperature, the concentration, the pressure, the fluid density, the kinematic viscosity, the thermal conductivity, the specific heat, the diffusion species and the reaction rate respectively.

The boundary conditions are prescribed as follows:

$$u = 0, \quad v = v_w = \frac{dh}{dt}, \quad T = T_H, \quad C = C_H \quad \text{at} \quad y = h(t),$$

$$v = \frac{\partial u}{\partial y} = \frac{\partial T}{\partial y} = \frac{\partial C}{\partial y} = 0 \quad \text{at} \quad y = 0. \tag{5.6}$$

Eliminating pressure gradient from Eqs. $(5.2 - 5.3)$ and using the transformations

$$\eta = \frac{y}{H\sqrt{1-at}}, \quad u = \frac{ax}{2(1-at)}f'(\eta), \quad v = \frac{-aH}{2\sqrt{1-at}}f(\eta),$$

$$\theta = \frac{T}{T_H}, \quad \phi = \frac{C}{C_H}. \tag{5.7}$$

we arrive at

$$f^{(iv)} - S_q(1+\lambda_1)\left(\eta f''' + 3f'' + f'f'' - ff'''\right)$$
$$+\frac{\beta}{2}\left(\eta f^{(v)} + 5f^{(iv)} + 2f''f''' - ff^{(iv)} - f'f^{(iv)}\right) = 0, \tag{5.8}$$

$$(1+\lambda_1)\left[\theta'' + PrS_q\left(f\theta' - \eta\theta'\right)\right]$$
$$+PrEc\left[f''^2 + 4\delta^2 f'^2 + \frac{\beta}{2}\left\{3f''^2 + f'^2 f''^2 + \eta f''f''' - ff''f'''\right.\right.$$
$$\left.\left.+4\delta^2\left(2f'^2 + \eta f'f'' - ff'f''\right)\right\}\right] = 0, \tag{5.9}$$

$$\phi'' + ScS_q\left(f\phi' - \eta\phi'\right) - Sc\gamma\phi = 0. \tag{5.10}$$

$$f(0) = 0, \; f(1) = 1, \; f'(1) = 0, \; f''(0) = 0,$$

$$\theta(1) = 1 = \phi(1), \; \theta'(0) = 0 = \phi'(0). \tag{5.11}$$

where squeezing parameter S_q, the Deborah number β, the Prandtl number (Pr), the Eckert number (Ec), the Schmidt number (Sc) and the chemical reaction parameter γ are given by

$$S_q = \frac{aH^2}{2\nu}, \quad \beta = \frac{\lambda_2 a}{1-at}, \quad Pr = \frac{\mu C_p}{K_c},$$

$$Ec = \frac{1}{T_H C_p}\left(\frac{ax}{2(1-at)}\right)^2, \quad Sc = \frac{\nu}{D}, \quad \gamma = \frac{k_1 H^2}{\nu}, \quad \delta^2 = \frac{H^2(1-at)}{x^2}. \tag{5.12}$$

Note that the plate movement is described by the squeezing parameter S_q. When $S_q > 0$,

61

the plates moving away from each other and when $S_q < 0$, the plates are moving together. For $Ec = 0$ the viscous dissipation effect is not present. Further $\gamma > 0$ shows the destructive chemical reaction and $\gamma < 0$ illustrates the generative chemical reaction. The case of $\beta = 0$, $\lambda_1 = 0$ corresponds to the viscous fluid. The skin friction coefficient, Nusselt number and Sherwood number are as follows

$$
C_f = \frac{(\tau_{xy})_{y=h(t)}}{\rho v_w^2}, \ \ Nu = \frac{-HK_c\left(\frac{\partial T}{\partial y}\right)_{y=h(t)}}{K_c T_H}, \ \ Sh = \frac{-HD\left(\frac{\partial C}{\partial y}\right)_{y=h(t)}}{DC_H} \tag{5.13}
$$

Using (5.7) in (5.13), we get

$$
\begin{aligned}
\frac{H^2}{x^2}(1-\alpha t)\,\mathrm{Re}_x\,C_f &= \frac{1}{1+\lambda_1}\left[f''(1) + \frac{\beta}{2}(f'''(1) + 3f''(1) + f'(1)f''(1) - f(1)f'''(1))\right], \\
\sqrt{1-\alpha t}Nu &= -\theta'(1), \quad \sqrt{1-\alpha t}Sh = -\phi'(1).
\end{aligned} \tag{5.14}
$$

5.2 Solution of the problem

Here $f(\eta)$, $\theta(\eta)$ and $\phi(\eta)$ are expressed by the set of base functions

$$
\left\{\eta^{2k+1} \mid k \geq 0\right\}, \tag{5.15}
$$

in the form of the following series

$$
f(\eta) = \sum_{k=0}^{\infty} a_k \eta^{2k+1}, \ \ \theta(\eta) = \sum_{k=0}^{\infty} b_k \eta^{2k+1}, \ \ \phi(\eta) = \sum_{k=0}^{\infty} c_k \eta^{2k+1},
$$

where (a_k), (b_k) and (c_k) are the coefficients. The initial approximations $f_0(\eta)$, $\theta_0(\eta)$, $\phi_0(\eta)$ and linear operators $\mathcal{L}_f$, $\mathcal{L}_\theta$, $\mathcal{L}_\phi$ are chosen as follows:

$$
\begin{aligned}
f_0(\eta) &= \frac{1}{2}\left(3\eta - \eta^3\right), \ \theta_0(\eta) = 1, \ \phi_0(\eta) = 1, \tag{5.16} \\
\mathcal{L}_f &= f^{(iv)}, \ \mathcal{L}_\theta = \theta'', \ \mathcal{L}_\phi = \phi'', \tag{5.17}
\end{aligned}
$$

where

$$\mathcal{L}_f \left(C_1 + C_2 \eta + C_3 \eta^2 + C_4 \eta^3 \right) = 0, \ \mathcal{L}_\theta \left[C_5 + C_6 \eta \right] = 0, \ \mathcal{L}_\phi \left[C_7 + C_8 \eta \right] = 0, \tag{5.18}$$

and $C_i \ (i = 1 - 8)$ are the arbitrary constants.

5.2.1 Zeroth order deformation problems

The zeroth order problems ensures the following statements:

$$(1 - q) \mathcal{L}_f \left[\bar{f} (\eta; q) - f_0 (\eta) \right] = q \hbar_f \mathcal{N}_f \left[\bar{f} (\eta; q) \right],$$
$$\bar{f} (0; q) = 0, \ \bar{f}'' (0, q) = 0, \ \bar{f} (1, q) = 1, \ \bar{f}' (1, q) = 0, \tag{5.19}$$

$$(1 - q) \mathcal{L}_\theta \left[\bar{\theta} (\eta; q) - \theta_0 (\eta) \right] = q \hbar_\theta \mathcal{N}_\theta \left[\bar{\theta} (\eta; q) \right],$$
$$\bar{\theta}' (0; q) = 0, \ \bar{\theta} (1, q) = 1, \tag{5.20}$$

$$(1 - q) \mathcal{L}_\phi \left[\bar{\phi} (\eta; q) - \phi_0 (\eta) \right] = q \hbar_\phi \mathcal{N}_\phi \left[\bar{\phi} (\eta; q) \right],$$
$$\bar{\phi}' (0; q) = 0, \ \bar{\phi} (1, q) = 1, \tag{5.21}$$

In expressions (5.20), (5.21) and (5.22), $\hbar_f$, $\hbar_\theta$, $\hbar_\phi$ denotes the auxiliary parameters and $0 \leq q \leq 1$ denotes the embedding parameter. It is observed that, when q varies from 0 to 1, then $\bar{f}(\eta, q)$, $\bar{\theta}(\eta, q)$ and $\bar{\phi} (\eta; q)$ vary from $f_0 (\eta)$ to $f(\eta)$, $\theta_0 (\eta)$ to $\theta (\eta)$ and $\phi_0 (\eta)$ to $\phi (\eta)$ respectively. When $q = 0$ and $q = 1$, one obtains

$$\bar{f} (\eta; 0) = f_0 (\eta), \ \bar{f} (\eta; 1) = f (\eta), \tag{5.22}$$
$$\bar{\theta}(\eta, 0) = \theta_0(\eta), \ \bar{\theta}(\eta, 1) = \theta(\eta), \tag{5.23}$$
$$\bar{\phi}(\eta, 0) = \phi_0(\eta), \ \bar{\phi}(\eta, 1) = \phi(\eta). \tag{5.24}$$

The nonlinear operator is defined as follows:

$$
\mathcal{N}_f\left[\bar{f}\left(\eta;q\right)\right] = \frac{\partial^4 \bar{f}\left(\eta;q\right)}{\partial \eta^4} - S_q\left(1+\lambda_1\right)\left(\eta\frac{\partial^3 \bar{f}\left(\eta;q\right)}{\partial \eta^3} + 3\frac{\partial^2 \bar{f}\left(\eta;q\right)}{\partial \eta^2}\right.
$$

$$
\left.+\frac{\partial \bar{f}\left(\eta;q\right)}{\partial \eta}\frac{\partial^2 \bar{f}\left(\eta;q\right)}{\partial \eta^2} - \bar{f}\left(\eta;q\right)\frac{\partial^3 \bar{f}\left(\eta;q\right)}{\partial \eta^3}\right) + \frac{\beta}{2}\left(\eta\frac{\partial^5 \bar{f}\left(\eta;q\right)}{\partial \eta^5} + 5\frac{\partial^4 \bar{f}\left(\eta;q\right)}{\partial \eta^4}\right.
$$

$$
\left.+2\frac{\partial^2 \bar{f}\left(\eta;q\right)}{\partial \eta^2}\frac{\partial^3 \bar{f}\left(\eta;q\right)}{\partial \eta^3} - \bar{f}\left(\eta;q\right)\frac{\partial^5 \bar{f}\left(\eta;q\right)}{\partial \eta^5} - \frac{\partial \bar{f}\left(\eta;q\right)}{\partial \eta}\frac{\partial^4 \bar{f}\left(\eta;q\right)}{\partial \eta^4}\right), \tag{5.25}
$$

$$
\mathcal{N}_\theta\left[\bar{\theta}\left(\eta;q\right)\right] = \left(1+\lambda_1\right)\left[\frac{\partial^2 \bar{\theta}\left(\eta;q\right)}{\partial \eta^2} + PrS_q\left(\bar{f}\left(\eta;q\right)\frac{\partial \bar{\theta}\left(\eta;q\right)}{\partial \eta} - \eta\frac{\partial \bar{\theta}\left(\eta;q\right)}{\partial \eta}\right)\right]
$$

$$
+PrEc\left[\left(\frac{\partial^2 \bar{f}\left(\eta;q\right)}{\partial \eta^2}\right)^2 + 4\delta^2\left(\frac{\partial \bar{f}\left(\eta;q\right)}{\partial \eta}\right)^2 + \frac{\beta}{2}\left\{3\left(\frac{\partial^2 \bar{f}\left(\eta;q\right)}{\partial \eta^2}\right)^2 + \left(\frac{\partial \bar{f}\left(\eta;q\right)}{\partial \eta}\right)^2\right.\right.
$$

$$
+\eta\frac{\partial^2 \bar{f}\left(\eta;q\right)}{\partial \eta^2}\frac{\partial^3 \bar{f}\left(\eta;q\right)}{\partial \eta^3} - \bar{f}\left(\eta;q\right)\frac{\partial^2 \bar{f}\left(\eta;q\right)}{\partial \eta^2}\frac{\partial^3 \bar{f}\left(\eta;q\right)}{\partial \eta^3}
$$

$$
\left.\left.+4\delta^2\left(2\left(\frac{\partial \bar{f}\left(\eta;q\right)}{\partial \eta}\right)^2 + \eta\frac{\partial \bar{f}\left(\eta;q\right)}{\partial \eta}\frac{\partial^2 \bar{f}\left(\eta;q\right)}{\partial \eta^2} - \bar{f}\left(\eta;q\right)\frac{\partial \bar{f}\left(\eta;q\right)}{\partial \eta}\frac{\partial^2 \bar{f}\left(\eta;q\right)}{\partial \eta^2}\right)\right\}\right], \tag{5.26}
$$

$$
\mathcal{N}_\phi\left[\bar{\phi}\left(\eta;q\right)\right] = \frac{\partial^2 \bar{\phi}\left(\eta;q\right)}{\partial \eta^2} + S_q Sc\left(\bar{f}\left(\eta;q\right)\frac{\partial \bar{\phi}\left(\eta;q\right)}{\partial \eta} - \eta\frac{\partial \bar{\phi}\left(\eta;q\right)}{\partial \eta}\right) - Sr\gamma\bar{\phi}. \tag{5.27}
$$

Employing Taylor series for $f(\eta)$, $\theta(\eta)$ and $\phi(\eta)$ one can write

$$
f(\eta) = f_0(\eta) + \sum_{m=1}^{\infty} f_m(\eta)q^m, \tag{5.28}
$$

$$
\theta(\eta) = \theta_0(\eta) + \sum_{m=1}^{\infty} \theta_m(\eta)q^m, \tag{5.29}
$$

$$
\phi(\eta) = \phi_0(\eta) + \sum_{m=1}^{\infty} \phi_m(\eta)q^m, \tag{5.30}
$$

$$
f_m(\eta) = \frac{1}{m!}\frac{\partial^m \bar{f}(\eta,q)}{\partial q^m}\bigg|_{q=0}, \quad \theta_m(\eta) = \frac{1}{m!}\frac{\partial^m \bar{\theta}(\eta,q)}{\partial q^m}\bigg|_{q=0}, \quad \phi_m(\eta) = \frac{1}{m!}\frac{\partial^m \bar{\phi}(\eta,q)}{\partial q^m}\bigg|_{q=0}. \tag{5.31}
$$

5.2.2 Higher order deformation problems

The corresponding problems here are

$$\mathcal{L}_f \left[f_m \left(\eta \right) - \chi_m f_{m-1} \left(\eta \right) \right] = \hbar_f \Re_m^f \left(f_{m-1} \left(\eta \right) \right),$$

$$f_m \left(0 \right) = 0, \; f_m'' \left(0 \right) = 0, \; f_m \left(1 \right) = 0, \; f_m' \left(1 \right) = 0, \tag{5.32}$$

$$\mathcal{L}_\theta \left[\theta_m \left(\eta \right) - \chi_m \theta_{m-1} \left(\eta \right) \right] = \hbar_\theta \Re_m^\theta \left(\theta_{m-1} \left(\eta \right) \right),$$

$$\theta_m' \left(0 \right) = 0, \; \theta_m \left(1 \right) = 0, \tag{5.33}$$

$$\mathcal{L}_\phi \left[\phi_m \left(\eta \right) - \chi_m \phi_{m-1} \left(\eta \right) \right] = \hbar_\phi \Re_m^\phi \left(\phi_{m-1} \left(\eta \right) \right),$$

$$\phi_m' \left(0 \right) = 0, \; \phi_m \left(1 \right) = 0, \tag{5.34}$$

in which

$$\chi_m = \begin{cases} 0, & m \leq 1, \\ 1, & m > 1, \end{cases}$$

$$
\begin{aligned}
\Re_m^f \left(f_{m-1} \left(\eta \right) \right) = \; & f_{m-1}^{(iv)} \left(\eta \right) - S_q \left(1 + \lambda_1 \right) \left[\eta f_{m-1}''' \left(\eta \right) + 3 f_{m-1}'' \left(\eta \right) \right] + \frac{\beta}{2} \left[\eta f_{m-1}^{(v)} \left(\eta \right) + 5 f_{m-1}^{(iv)} \left(\eta \right) \right] \\
& + \sum_{n=0}^{m-1} \left[-S_q \left(1 + \lambda_1 \right) \left(f_n' \left(\eta \right) f_{m-1-n}'' \left(\eta \right) - f_n \left(\eta \right) f_{m-1-n}''' \left(\eta \right) \right) + \frac{\beta}{2} \left(2 f_n'' \left(\eta \right) f_{m-1-n}''' \left(\eta \right) \right. \right. \\
& \left. \left. - f_n \left(\eta \right) f_{m-1-n}^{(v)} \left(\eta \right) - f_n' \left(\eta \right) f_{m-1-n}^{(iv)} \left(\eta \right) \right) \right], \tag{5.35}
\end{aligned}
$$

$$\Re_m^\theta \left(\theta_{m-1} \left(\eta \right) \right) \quad = \quad \left(1 + \lambda_1 \right) \left[\theta_{m-1}'' \left(\eta \right) - PrS_q \theta_{m-1}' \left(\eta \right) \right] + PrS_q \sum_{n=0}^{m-1} f_n \left(\eta \right) \theta_{m-1-n}' \left(\eta \right)$$

$$+ PrEc \sum_{n=0}^{m-1} \left[f_n'' \left(\eta \right) f_{m-1-n}'' \left(\eta \right) + 4\delta^2 f_n' \left(\eta \right) f_{m-1-n}' \left(\eta \right) + \frac{\beta}{2} \left\{ 3 f_n'' \left(\eta \right) f_{m-1-n}'' \left(\eta \right) \right. \right.$$

$$+ \eta f_n'' \left(\eta \right) f_{m-1-n}''' \left(\eta \right) + 4\delta^2 \left(2 f' \left(\eta \right) f_{m-1-n}' \left(\eta \right) + \eta f' \left(\eta \right) f_{m-1-n}'' \left(\eta \right) \right)$$

$$- f_{m-1-n}(\eta) \sum_{k=0}^{n} f_{n-k}'' \left(\eta \right) \left(f_k''' \left(\eta \right) + 4\delta^2 f_k' \left(\eta \right) \right)$$

$$\left. \left. + f_{m-1-n}'(\eta) \sum_{k=0}^{n} f_{n-k}' \left(\eta \right) \sum_{l=0}^{n} f_{k-l}'' \left(\eta \right) f_l'' \left(\eta \right) \right\} \right], \tag{5.36}$$

$$\Re_m^\phi \left(\phi_{m-1} \left(\eta \right) \right) = \phi_{m-1}'' \left(\eta \right) - ScS_q \eta \phi_{m-1}' \left(\eta \right) - Sc\gamma \phi_{m-1} \left(\eta \right) + ScS_q \sum_{n=0}^{m-1} f_n \left(\eta \right) \phi_{m-1-n}' \left(\eta \right) . \tag{5.37}$$

The general solution of the problems given in Eq. $(5.33 - 5.35)$ are

$$f_m(\eta) \quad = \quad f_m^*(\eta) + C_1 + C_2 \eta + C_3 \eta^2 + C_4 \eta^3 \tag{5.38}$$

$$\theta_m(\eta) \quad = \quad \theta_m^*(\eta) + C_5 + C_6 \eta \tag{5.39}$$

$$\phi_m(\eta) \quad = \quad \phi_m^*(\eta) + C_7 + C_8 \eta \tag{5.40}$$

where $f_m^*(\eta)$, $\theta_m^*(\eta)$ and $\phi_m^*(\eta)$ are the special solutions of the problems given in Eqs. (5.33), (5.34) and (5.35). The coefficients C_i $(i = 1 - 8)$ can be found by the Eqs. (5.33), (5.34) and (5.35).

5.2.3   Convergence of solutions

The convergence of series solutions totally depend upon the auxiliary parameters. We select these parameters $\hbar_f$, $\hbar_\theta$ and $\hbar_\phi$ corresponding to the functions f, θ and ϕ respectively. These parameters adjust and control the convergence of the obtained series solutions. Figs. $(5.1 - 5.2)$ show the $h-$curves of the functions f, θ and ϕ for $S_q = \lambda_1 = 1.0$, $\beta = 0.5$, $Pr = Ec = 1.0$ and $\delta = 0.1$. The permissible values of these auxiliary parameters $\hbar_f$, $\hbar_\theta$ and $\hbar_\phi$ are $-0.75 \le (\hbar_f, \hbar_\theta) \le -0.15$ and $-0.80 \le \hbar_\phi \le -0.18$ respectively. Table 5.1 is useful in making a guess that how much order of approximations are required for a convergent solution. This table shows that the $20th$ order of approximations are sufficient for the convergent solution. Figs. $(5.3 - 5.5)$ are

drawn for the residual errors. These Figs. illustrate that the residual error is negligible. It is observed that the lowest possible error of f, θ and ϕ for $\hbar_f \in [-0.55, -0.3]$, $\hbar_\theta \in [-0.4, -0.3]$ and $\hbar_\phi \in [-0.65, -0.4]$ respectively. Residual errors increase as we move away from the line parallel to the $\hbar-$axis. Therefore it shows oscillatory/divergent behavior.
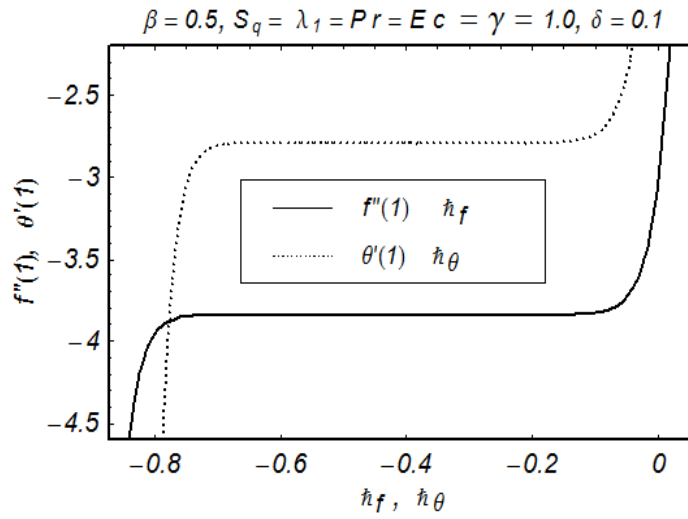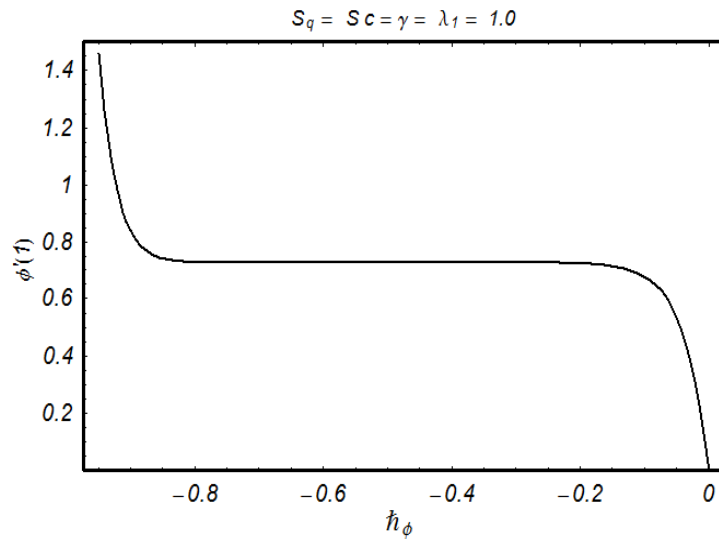

Fig. 5.1: Convergence region for f and θ at $\eta = 1$.

Fig. 5.2: Convergence region for ϕ and θ at $\eta = 1$.
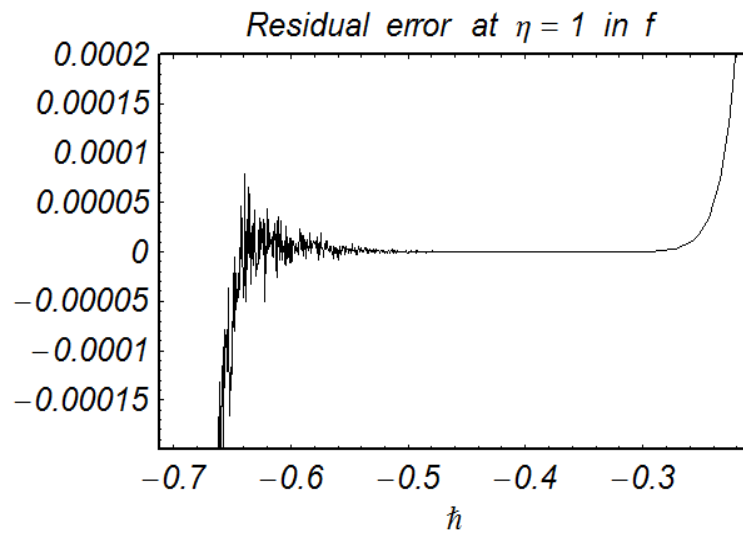
Fig. 5.3: Convergence region for residual error in $f(\eta)$.
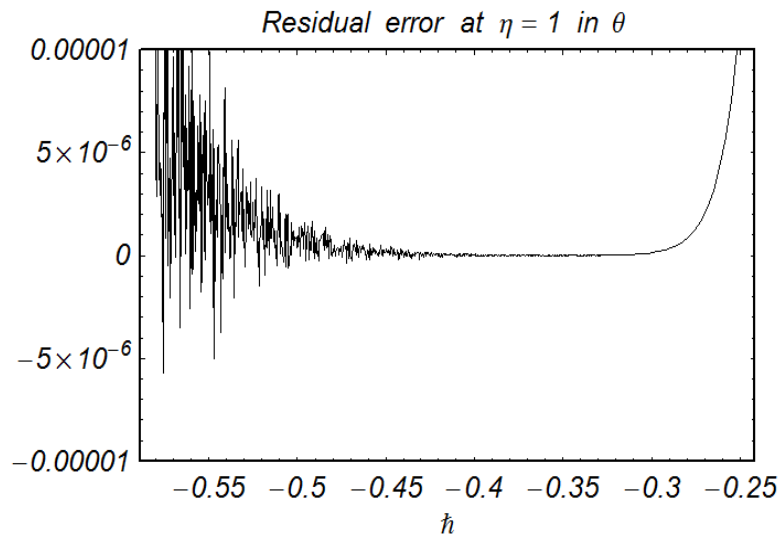
Fig. 5.4: Convergence region for residual error in $\theta(\eta)$.
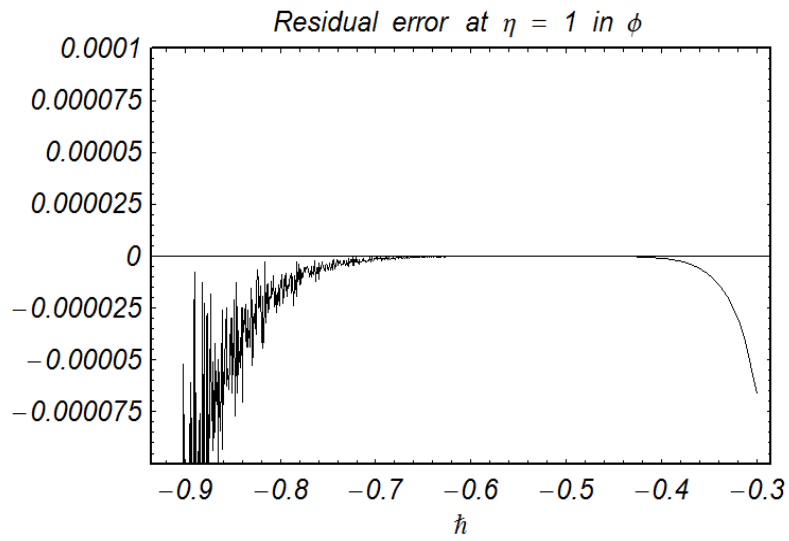
Fig. 5.5: Convergence region for residual error in $\phi(\eta)$.

Table 5.1. Series solution's convergence by HAM for different order of approximations when $\beta = 0.5$, $S_q = Pr = Ec = Sc = \gamma = \lambda_1 = 1.0$ and $\delta = 0.1$.

Order of approximations	$-f''(1)$	$-\theta'(1)$	$\phi'(1)$
1	3.691428	2.249485	0.400000
5	3.841897	2.789644	0.711241
10	3.842650	2.793175	0.728652
15	3.842652	2.793181	0.729459
20	3.842652	2.793181	0.729512
25	3.842652	2.793181	0.729515
30	3.842652	2.793181	0.729516
35	3.842652	2.793181	0.729516
40	3.842652	2.793181	0.729516

5.3 Discussion

This section concerns with the analysis of involved parameters for the velocity, temperature and concentration fields. Hence we have plotted the Figs. $(5.6 - 5.17)$. Figs. $(5.6, 5.7)$ depict the effects of squeezing parameter on velocity profile. Here the effects of positive and negative squeezing parameter on velocity profile are opposite. The effects of squeezing parameter S_q on f' is discussed in the Figs. $(5.8 - 5.9)$. Fig. 5.8 shows that f' decreases when $0 \leq \eta \leq$ 0.4 and it increases when $0.4 \leq \eta \leq 1$ with the increase of $S_q > 0$. Reverse behavior has seen for $S_q < 0$. Figs. 5.10 and 5.11 indicate the effects of relaxation to retardation times ratio λ_1 on f' for positive and negative squeezing parameter S_q. These Figs. depict that the effect of λ_1 is similar to that of S_q on f'. In Fig. 5.12 we have discussed the combined effects of squeezing parameter on the temperature field. This Fig. indicates that when we increase S_q, the temperature decreases. Here the temperature is comparatively higher when the plates are moving to each other. The kinematic viscosity decreases upon increasing S_q. Effects of Prandtl number (Pr) on the temperature profile θ is displayed in Fig. 5.13. This Fig. shows that an increase in Prandtl number enhances the temperature profile. Note that the temperature increases from the walls to the middle of the channel. Effects of Eckert number

on fluid temperature is displayed in Fig. 5.14. There is an increase in temperature when Eckert number increases. This is because of the fact that presence of viscous dissipation effects significantly increases the temperature θ. Fig. 5.15 shows the combined effects of positive and negative squeezing parameter on the concentration field. The concentration decreases for fixed values of parameters. Significant decrease in the concentration field is observed for larger values of S_q. This is expected because the concentration is quite higher when the plates are moving towards each other. An increase in S_q can be related with the reduction in the kinematic viscosity which consequently depends upon the velocity and the distance between the plates. Effect of Schmidt number Sc on concentration field is displayed in Fig. 5.16. Note that with the increase of Schmidt number Sc, the concentration profile ϕ increases. This is due to the decrease in process of diffusion of species. Effects of chemical reaction parameter (γ) on the concentration field is discussed in Fig. 5.17. A reduction occurred in the concentration for larger values of chemical reaction parameter $(\gamma > 0)$. Further enhancement is noted in the concentration field for higher values of generative chemical reaction parameter $(\gamma < 0)$. Larger values of γ result in the enhancement of concentration at the lower wall.
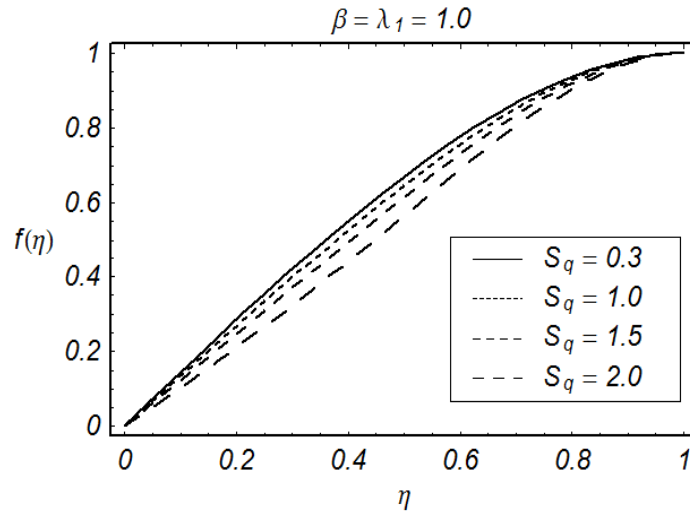
Fig. 5.6: Influence of $S_q > 0$ on f.
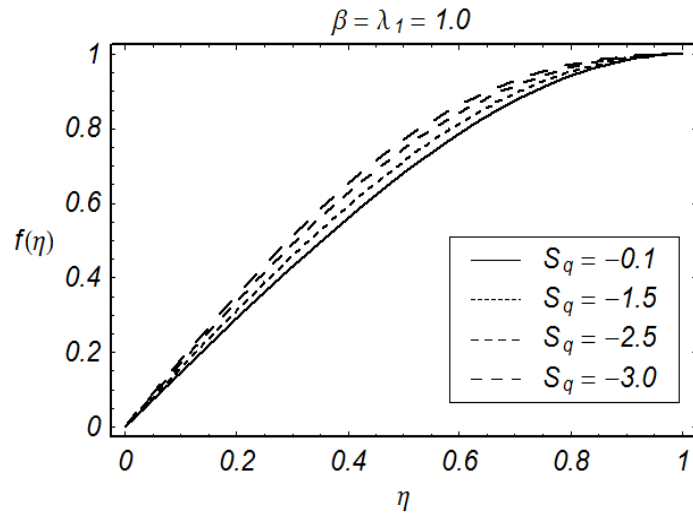
Fig. 5.7: Influence of $S_q < 0$ on f.
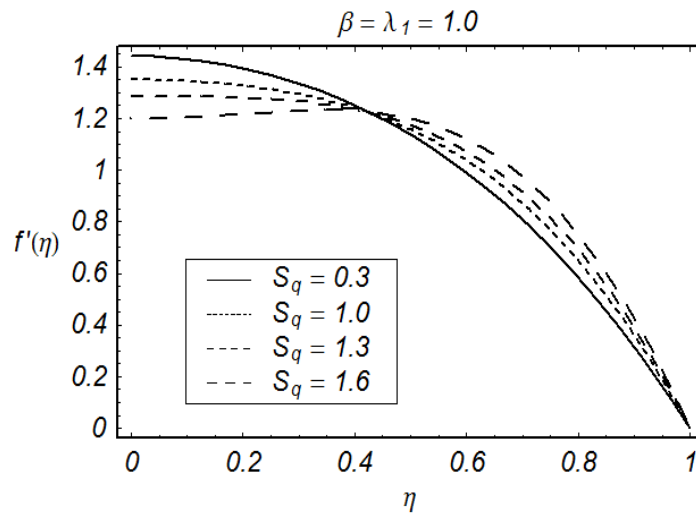
Fig. 5.8: Influence of $S_q > 0$ on f'.

Fig. 5.9: Influence of $S_q < 0$ on f'.

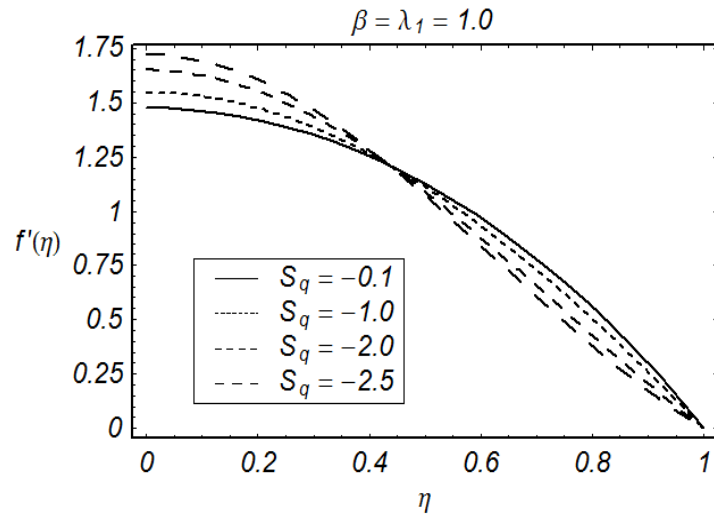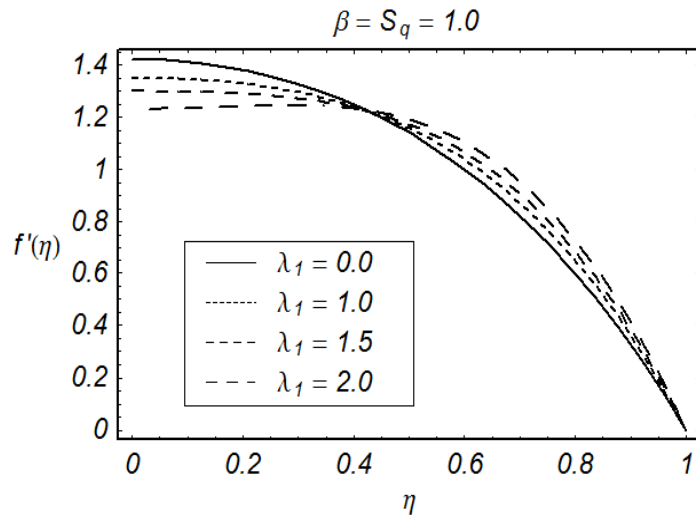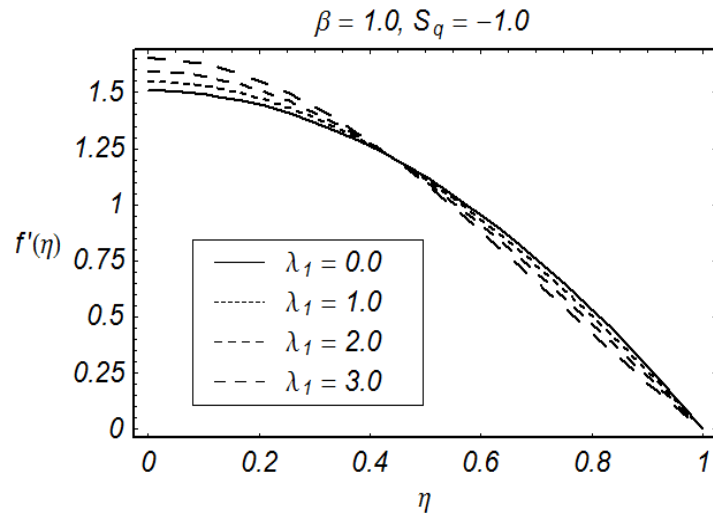Fig. 5.10: Influence of λ_1 on f' when $S_q > 0$.

Fig. 5.11: Influence of λ_1 on f' when $S_q < 0$.
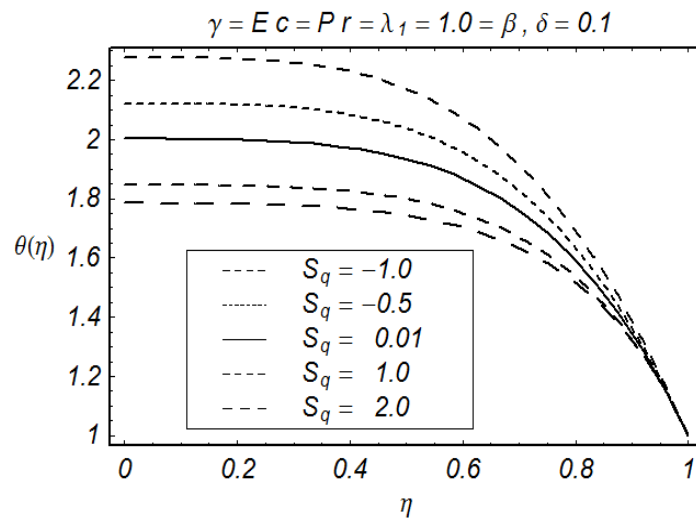
Fig. 5.12: Influence of S_q on θ.
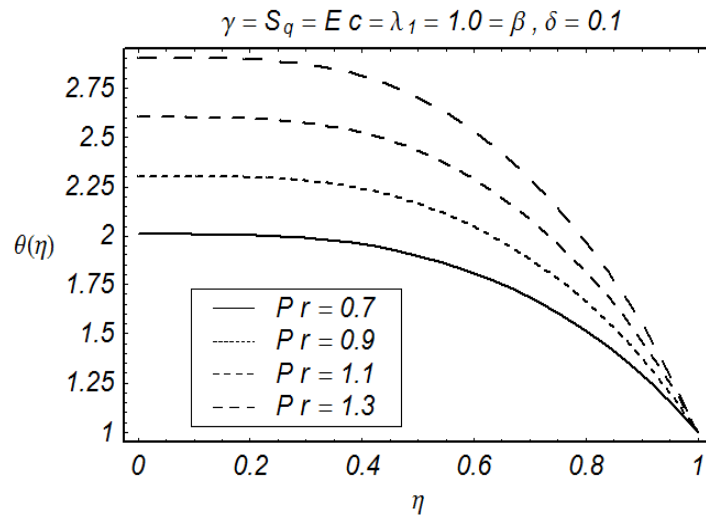
Fig. 5.13: Influence of Pr on θ.
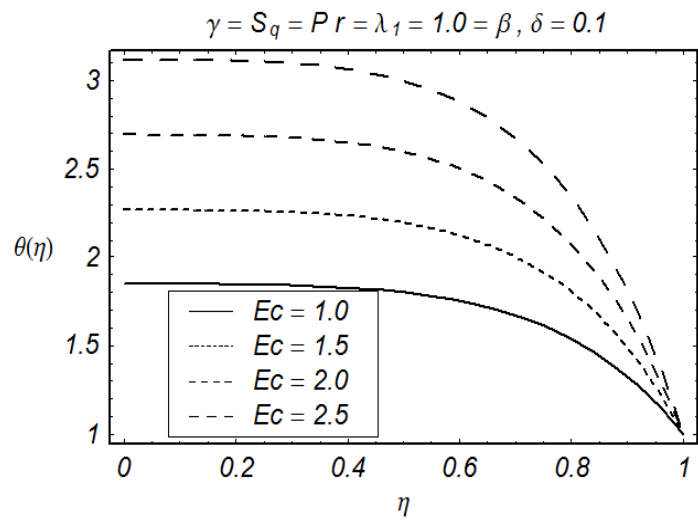
Fig. 5.14: Influence of Ec on θ.
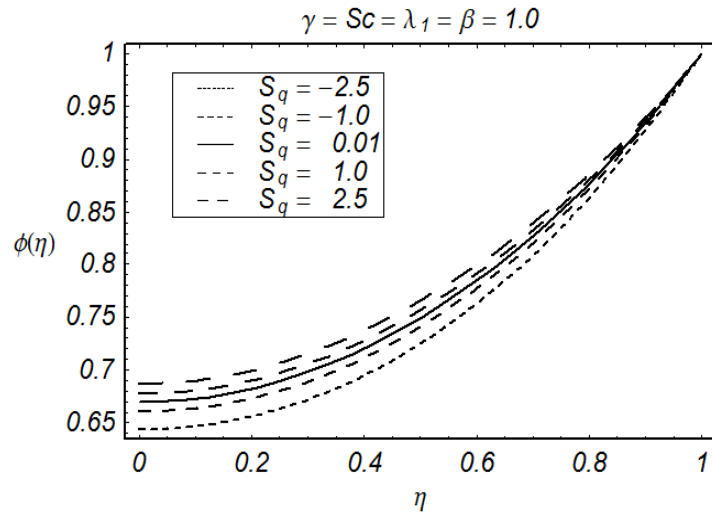
Fig. 5.15: Influence of S_q on ϕ.
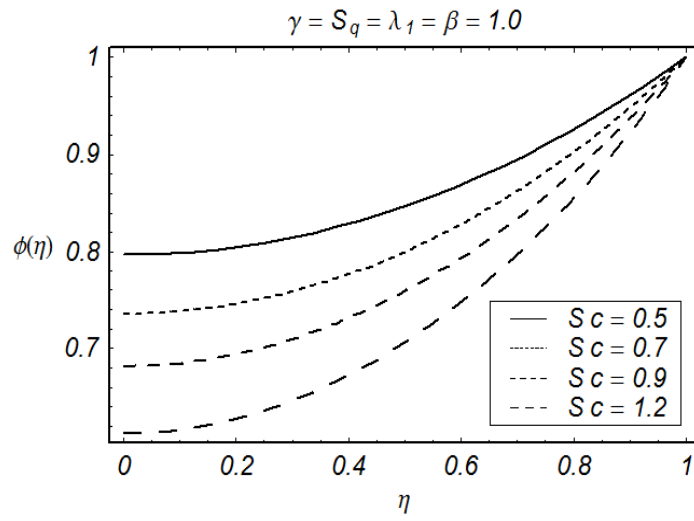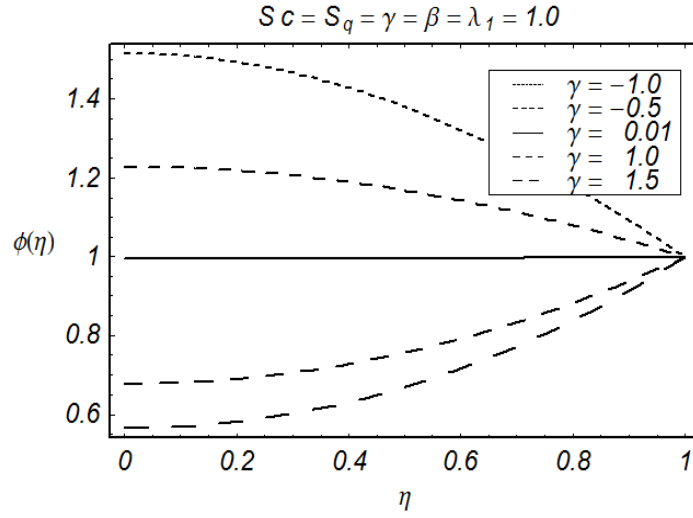

Fig. 5.16: Influence of Sc on ϕ.

Fig. 5.17: Influence of γ on ϕ.

Table 5.2. Values of skin friction coefficient, local Nusselt number and local Sherwood number for different values of S_q, β and λ_1 when $Pr = Ec = Sc = \gamma = 1.0$.

S_q	β	λ_1	$-k(1)$	$-\theta(1)$	$-\phi(1)$
-1.0	1.0	1.0	3.3226037	4.3341184	0.80164969
-0.5			3.6940223	4.1729478	0.78049337
0.01			4.0382409	4.0795752	0.76123593
0.5			4.3423886	4.0346438	0.74451077
1.0	0.3	1.0	2.8529501	2.3060473	0.72991231
	0.5		3.3623203	2.7931806	0.72951620
	0.8		4.1239018	3.5279497	0.72911225
	1.0		4.6306425	4.0195272	0.72891934
1.0	0.5	0.2	5.2327614	4.5967155	0.72844349
		0.5	4.3002619	3.6934855	0.72886089
		1.0	3.3623203	2.7931806	0.72951620
		2.0	2.4125553	1.8982217	0.73069644

77

Table 5.3. Values of local Nusselt number for different values of Pr and Ec when $S_q = \lambda_1 = \beta = 1.0$ and $\delta = 0.1$

Pr	Ec	$-\theta'(1)$
0.5	1.0	2.030517
1.0		4.019537
2.0		7.879131
5.0		18.60918
1.0	0.5	2.009763
	1.2	4.823432
	2.0	8.039054
	5.0	20.09768

Table 5.4. Values of local Sherwood number for different values of Sc and γ when $S_q = \lambda_1 = \beta = 1.0$

Sc	γ	$\phi'(1)$
0.5	1.0	0.419756
1.0		0.728919
1.5		0.971904
2.0		1.171940
1.0	-0.5	-0.561622
	-0.1	-0.097266
	0.5	0.409349
	1.0	0.728919

Table 5.5: Comparison between HAM and HPM solutions [69]

S	$f''(1)$	
	HPM [69]	HAM (Present results)
0.1	2.97682	2.97682
0.5	–	2.89177
1.0	–	2.80242
1.5	–	2.73094

5.4 Conclusions

Here we have discussed the heat and mass transfer effects in squeezing flow of Jeffrey fluid between two parallel plates. The main outcomes are as follows:

- Effects of positive and negative squeezing parameter on velocity profile are quite opposite.

- Variations of the ratio of relaxation to retardation times λ_1 on f' for positive and negative squeezing parameter S_q are opposite.

- Effects of Prandtl number (Pr) and Eckert number Ec have increasing behavior for the temperature θ.

- Increase in squeezing parameter S_q decreases the temperature θ.

- Concentration field ϕ increases when squeezing parameter is increased.

- Schmidt number (Sc) results in the reduction of concentration profile and enhancement in Sherwood number.

- Destructive and generative chemical reaction parameters ($\gamma > 0, \gamma < 0$) have opposite effects on concentration field ϕ.

- Larger the relaxation to retardation times ratio λ_1 decreases the magnitude of skin friction coefficient. However the local Nusselt number and local Sherwood number are increased for larger λ_1.

- Increase of Pr and Ec leads to enhancement in Nusselt number.

Chapter 6

Axisymmetric flow of couple stress fluid due to squeezing disks

The purpose of this chapter is to revisit the flow analysis of chapter two for couple stress fluid. The considered fluid model here has distinct features through polar effects when compared with the other non-Newtonian fluid models. Specifically the present fluid model allows polar effects such as the presence of couple stress, body couple and non-symmetric tensors. The modeled nonlinear flow problem is reduced into the ordinary differential system. Computations have been carried out by homotopy analysis method (HAM). Effects of the squeezing and couple stress parameters on the velocity profile are discussed.

6.1   Mathematical analysis

Let us consider an incompressible axisymmetric flow of a couple stress fluid between two parallel disks distant $H \left(1 - at\right)^{\frac{1}{2}}$ apart. The upper disk at $z = h\left(t\right) = H\left(1 - at\right)^{\frac{1}{2}}$ is moving with velocity $\frac{-aH(1-at)^{-\frac{1}{2}}}{2}$ while lower porous disk at $z = 0$ is fixed. The fundamental equations governing the motion of an incompressible couple stress fluid are:

$$\nabla \cdot \mathbf{V} = \mathbf{0}, \tag{6.1}$$

$$\rho \frac{D\mathbf{V}}{Dt} = -\nabla p + \mu \nabla^2 \mathbf{V} - \xi \nabla^4 \mathbf{V} \tag{6.2}$$

where $\mathbf{V}$ denotes the velocity vector, ρ the density, p denotes the pressure, μ the Newtonian viscosity and ξ the material constant characterizing the couple stresses. The ratio μ/ξ has the dimension of length square and, hence, characterizes the material length of the fluid.

Equations (6.1) and (6.2) for the flow under consideration give

$$\frac{\partial u}{\partial r} + \frac{u}{r} + \frac{\partial w}{\partial z} = 0, \tag{6.3}$$

$$\rho \left(\frac{\partial u}{\partial t} + u\frac{\partial u}{\partial r} + w\frac{\partial u}{\partial z} \right) = -\frac{\partial p}{\partial r} + \mu \left(\frac{\partial^2 w}{\partial z\partial r} - \frac{\partial^2 u}{\partial z^2} \right)$$
$$-\xi \left[\frac{\partial^4 u}{\partial z^4} + \frac{\partial^4 u}{\partial r^2\partial z^2} - \frac{\partial^4 w}{\partial z^3\partial r} - \frac{\partial^4 w}{\partial z\partial r^3} \right], \tag{6.4}$$

$$\rho \left(\frac{\partial w}{\partial t} + u\frac{\partial w}{\partial r} + w\frac{\partial w}{\partial z} \right) = -\frac{\partial p}{\partial z} + \mu \left(\frac{\partial^2 u}{\partial z\partial r} - \frac{\partial^2 w}{\partial r^2} \right)$$
$$-\xi \left[\frac{\partial^4 w}{\partial r^4} + \frac{\partial^4 w}{\partial z^2\partial r^2} - \frac{\partial^4 u}{\partial z\partial r^3} - \frac{\partial^4 u}{\partial r\partial z^3} \right], \tag{6.5}$$

where u denotes the velocity component along radial direction and w the velocity component along the axial (z) direction.

The boundary conditions are prescribed in the forms

$$u = 0, \quad w = \frac{\partial h}{\partial t} \quad \text{at } z = h(t),$$
$$u = 0, \quad w = -w_0 \quad \text{at } z = 0. \tag{6.6}$$

Substituting the transformations

$$u = \frac{ar}{2(1-at)} f'(\eta), \quad w = -\frac{aH}{\sqrt{1-at}} f(\eta), \quad \eta = \frac{z}{H\sqrt{1-at}}, \tag{6.7}$$

equation (6.3) is readily satisfied and Eqs. (6.4) and (6.5) are reduced as

$$f^{(iv)} + Kf^{(vi)} - S_q \left(\eta f''' + 3f'' - 2ff''' \right) = 0, \tag{6.8}$$

81

$$f(0) = S, \ f'(0) = 0, \ f(1) = \frac{1}{2}, \ f'(1) = 0, \tag{6.9}$$

where $S > 0$ and $S < 0$ respectively denote the suction and injection at the lower disk. The squeezing parameter S_q and couple stress parameter K are introduced through the following definitions

$$S_q = \frac{aH^2}{2\nu}, \quad K = \frac{\xi}{\mu H^2 (1 - at)}. \tag{6.10}$$

6.2 Homotopy analysis solution

For homotopy solution, we define $f(\eta)$ by a set of base function

$$\eta^k \mid k \geq 0 \tag{6.11}$$

in the form of the following series

$$f(\eta) = \sum_{k=0}^{\infty} a_k \eta^k, \tag{6.12}$$

where a_k are the coefficients. The initial approximation and linear operator are selected as follows:

$$f_0(\eta) = S + \left(\frac{3}{2} - 2S\right)\eta^2 + (2S - 1)\eta^3, \tag{6.13}$$

$$\mathcal{L}_f = f^{(iv)}, \tag{6.14}$$

with

$$\mathcal{L}_f \left(C_1 + C_2\eta + C_3\eta^2 + C_4\eta^3\right) = 0, \tag{6.15}$$

and $C_i \ (i = 1 - 4)$ are the arbitrary constants.

6.2.1 Zeroth order deformation problem

The zeroth order problem satisfies

$$(1 - q)\mathcal{L}_f \left[\bar{f}(\eta; q) - f_0(\eta)\right] = q\hbar_f \mathcal{N}_f \left[\bar{f}(\eta; q)\right], \tag{6.16}$$

$$\bar{f}(0;q) = S, \ \bar{f}'(0,q) = 1, \ \bar{f}(1,q) = \frac{S_q}{2}, \ \bar{f}'(1,q) = 0, \tag{6.17}$$

where $\hbar_f$ is an auxiliary parameter and $0 \le q \le 1$ is embedding parameter. It is observed that, when q changes from 0 to 1, then $\bar{f}(\eta, q)$ varies from $f_0(\eta)$ to $f(\eta)$. For $q = 0$ and $q = 1$, we have

$$\bar{f}(\eta, 0) = f_0(\eta), \ \bar{f}(\eta, 1) = f(\eta). \tag{6.18}$$

The nonlinear operator is defined as follows:

$$\mathcal{N}_f\left[\bar{f}(\eta;q)\right] = \frac{\partial^4 \bar{f}(\eta;q)}{\partial \eta^4} + K\frac{\partial^6 \bar{f}(\eta;q)}{\partial \eta^6} - S_q\left(\eta\frac{\partial^3 \bar{f}(\eta;q)}{\partial \eta^3} + 3\frac{\partial^2 \bar{f}(\eta;q)}{\partial \eta^2} - 2\bar{f}(\eta;q)\frac{\partial^3 \bar{f}(\eta;q)}{\partial \eta^3}\right). \tag{6.19}$$

Taylor series for $f(\eta)$ yields

$$f(\eta) = f_0(\eta) + \sum_{m=1}^{\infty} f_m(\eta)q^m, \tag{6.20}$$

$$f_m(\eta) = \frac{1}{m!}\frac{\partial^m \bar{f}(\eta, q)}{\partial q^m}\bigg|_{q=0}. \tag{6.21}$$

6.2.2 mth-order deformation problems

We differentiate Eq. (6.16) with respect to q ($m-$times) then divide by $m!$ and setting $q = 0$ we get

$$\mathcal{L}_f\left[f_m(\eta) - \chi_m f_{m-1}(\eta)\right] = \hbar_f \mathfrak{R}_m^f(f_{m-1}(\eta)), \tag{6.22}$$

$$f_m(0) = 0, \quad f_m'(0) = 0, \quad f_m(1) = 0, \quad f_m'(1) = 0, \tag{6.23}$$

in which

$$\chi_m = \begin{cases} 0, & m \le 1, \\ 1, & m > 1, \end{cases}$$

$$\mathfrak{R}_m^f(f_{m-1}(\eta)) = f_{m-1}^{(iv)}(\eta) + Kf_{m-1}^{(vi)}(\eta) - S_q\left[\eta f_{m-1}'''(\eta) + 3f_{m-1}''(\eta)\right] + 2S_q\sum_{n=0}^{m-1}\left[f_n(\eta) f_{m-1-n}'''(\eta)\right]. \tag{6.24}$$

83

The general solution for mth order problems is

$$f_m(\eta) = f_m^*(\eta) + C_1 + C_2\eta + C_3\eta^2 + C_4\eta^3, \tag{6.25}$$

where $f_m^*(\eta)$ is the particular solution of problem given in Eq. (6.15). The coefficients C_i ($i = 1 - 4$) can be found through the boundary conditions (6.16).

6.2.3 Convergence analysis

We know that convergence of series solution highly depends upon the auxiliary parameter. For that we choose $\hbar_f$ as the auxiliary parameter for the function f. This parameter is useful in controlling and adjusting the convergence of the obtained solution. In order to obtain the admissible values of auxiliary parameter, we have plotted the Figs. $(6.1 - 6.4)$ at $\eta = 0$ and $\eta = 1$ respectively. It is found that range for suitable values of $\hbar_f$ are $-0.5 \le \hbar_f \le -0.2$ and $-0.45 \le \hbar_f \le -0.1$ when $\eta = 0$ for suction and injection respectively. From Figs. $(6.3, 6.4)$ the ranges of suitable values of $\hbar_f$ are $-0.5 \le \hbar_f \le -0.15$ and $-0.5 \le \hbar_f \le -0.1$ when $\eta = 1$ for suction and injection respectively. Table 6.1 is useful in making a guess that how much order of approximations are necessary for a convergent series solution.
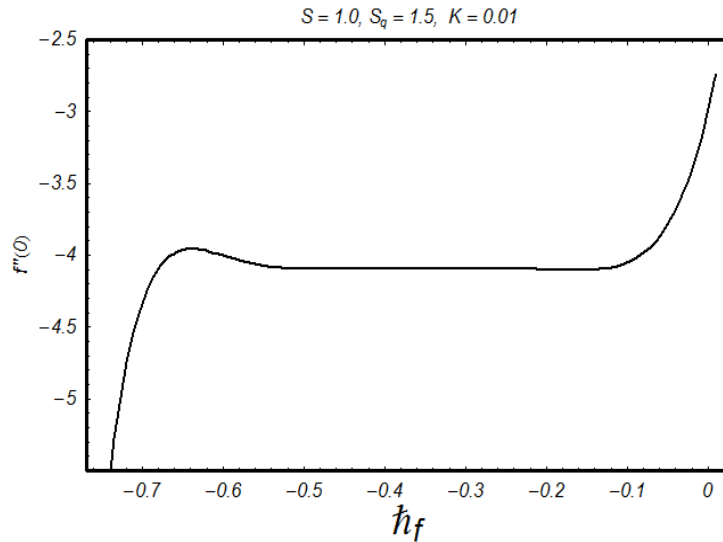
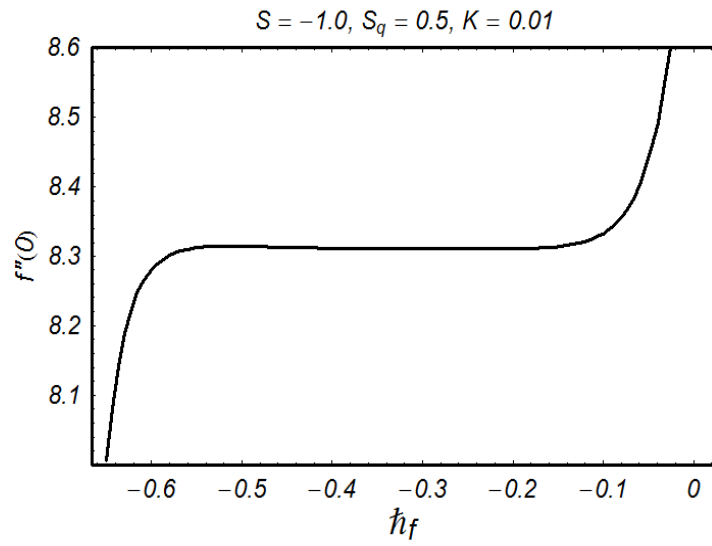Fig. 6.1: Convergence region of f at $\eta = 0$ for suction.

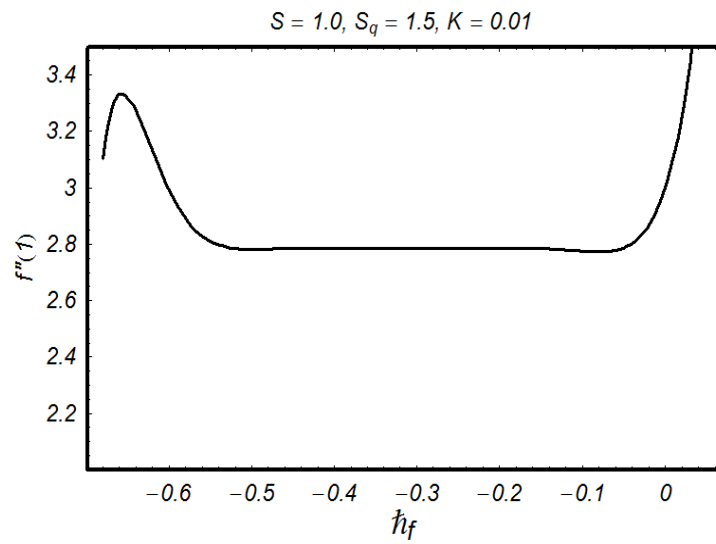Fig. 6.2: Convergence region of f at $\eta = 0$ for blowing.

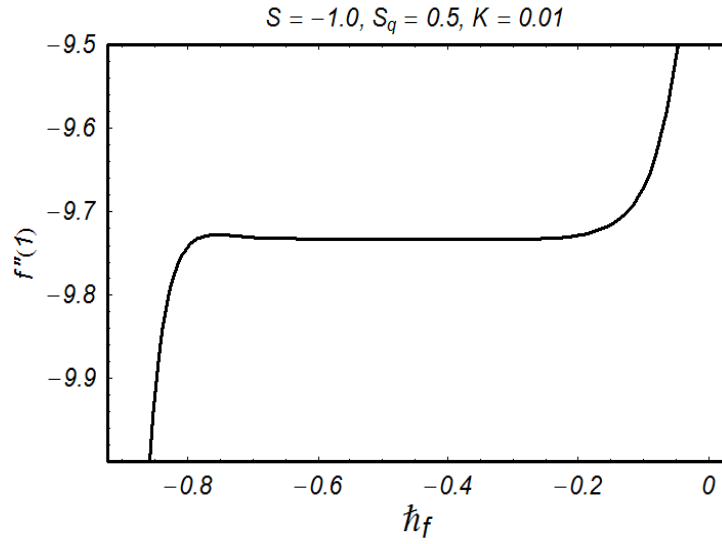Fig. 6.3: Convergence region of f at $\eta = 1$ for suction.

Fig. 6.4: Convergence region of f at $\eta = 1$ for blowing.

Table 6.1:. Convergence of series solution by HAM for different order of approximations when $S_q = 1.5$ and $K = 0.01$.

Order of	(for blowing)		(for suction)	
approximation	$f(0)$	$-f(1)$	$-f(0)$	$f(1)$
1	8.5564	9.1521	3.2293	2.9764
5	7.7012	9.5079	3.8176	2.9234
10	7.4518	9.6707	4.1278	2.9013
15	7.4136	9.7228	4.2374	2.8951
20	7.4112	9.7395	4.2733	2.8935
25	7.4125	9.7448	4.2839	2.8931
30	7.4133	9.7465	4.2866	2.8931
32	7.4135	9.7468	4.2869	2.8931
34	7.4135	9.7470	4.2871	2.8931
35	7.4135	9.7470	4.2871	2.8931
40	7.4135	9.7470	4.2871	2.8931

6.3   Discussion

In the Figs. $(6.5, 6.6)$ it is noted that the velocity profile f' in the lower half of the channel increases when the couple stress parameter K is increased. However it decreases at the center of the channel and again increases in the upper half of the channel for both suction and injection cases. The effects of squeezing parameter S_q are discussed in the Figs. $(6.7, 6.8)$ for suction and injection respectively. It is noted that for suction case the velocity profile f' decreases near porous wall. It is obvious because suction effects are foremost. As we know that the upper disk is moving towards the fixed porous lower disk creating pressure which increases the flow. Hence law of conservation of mass is satisfied at the upper half of the disk. Fig. 6.8 depicts that injection at the lower wall acts as a retarding force which shows a decrease in fluid velocity when we increase the squeezing parameter. Notice that in the upper half of the channel, the fluid velocity increases because the squeezing effects are dominant in the upper half of the channel. It is also noticed that the squeezing and couple stress parameters have opposite effects in the suction and blowing cases.
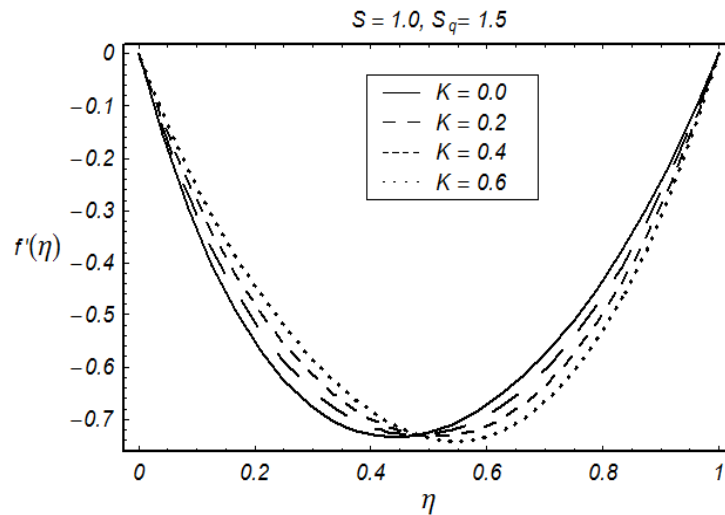

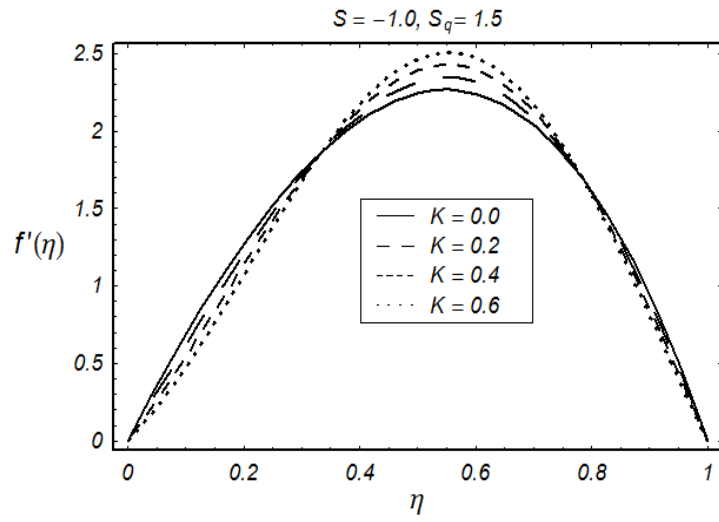
Fig. 6.5: Influence of K on f' for suction.

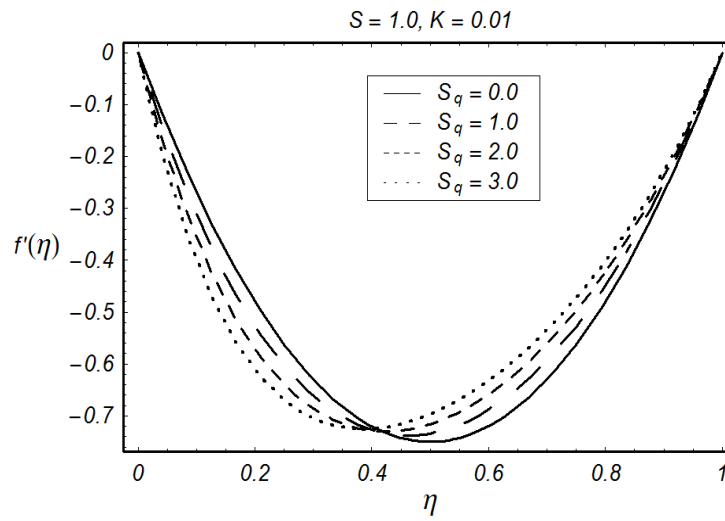Fig. 6.6: Influence of K on f' for blowing.

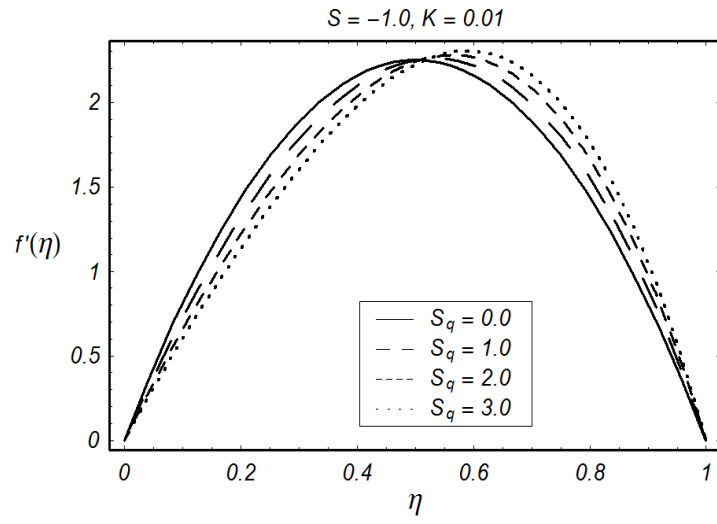Fig. 6.7: Influence of S_q on f' for suction.

Fig. 6.8: Influence of S_q on f' for blowing.

Chapter 7

Squeezing flow of couple stress fluid with heat transfer and chemical reaction

This chapter examines the unsteady two-dimensional squeezing flow of couple stress fluid between parallel plates. Mathematical analysis is presented in the presence of heat and mass transfer. Effects of viscous dissipation and chemical reaction are taken into account. Transformation procedure is adopted in obtaining the ordinary differential systems. The governing problems are computed by homotopy analysis method (HAM). Quantities of interest are illustrated graphically. The skin friction coefficient, Nusselt and Sherwood numbers are computed and analyzed.

7.1   Mathematical analysis

We examine the time-dependent squeezing flow of couple stress fluid with heat and mass transfer. The flow is bounded between two infinite parallel plates located at $z = \pm \frac{H}{2}(1 - at) = h(t)$. For $a > 0$ the plates are squeezed and the squeezing plates touch each other for $t = \frac{1}{a}$ while separation between the plates occurs for $a < 0$. The flow analysis has been investigated by considering viscous dissipation and heat generation due to friction produced by shear forces. This effect is relatively significant in the case when the fluid is mainly viscous or flowing at a

high speed. This situation occurs when Eckert number $(Ec \gg 1)$ is very high. Mass transfer is considered in the presence of chemical reaction and flow is taken symmetric. The governing equations of mass, momentum, energy and mass in time-dependent two-dimensional flow of couple stress fluid become

$$\frac{\partial u}{\partial x} + \frac{\partial v}{\partial y} = 0, \tag{7.1}$$

$$\rho \left(\frac{\partial u}{\partial t} + u\frac{\partial u}{\partial x} + v\frac{\partial u}{\partial y} \right) = -\frac{\partial p}{\partial x} - \mu \left(\frac{\partial^2 v}{\partial x \partial y} - \frac{\partial^2 u}{\partial y^2} \right) - \xi \left(\frac{\partial^4 u}{\partial x^2 \partial y^2} - \frac{\partial^4 v}{\partial x^3 \partial y} \right.$$
$$\left. -\frac{\partial^4 v}{\partial x \partial y^3} + \frac{\partial^4 u}{\partial y^4} \right), \tag{7.2}$$

$$\rho \left(\frac{\partial v}{\partial t} + u\frac{\partial v}{\partial x} + v\frac{\partial v}{\partial y} \right) = -\frac{\partial p}{\partial y} - \mu \left(\frac{\partial^2 u}{\partial x \partial y} - \frac{\partial^2 v}{\partial x^2} \right) - \xi \left(\frac{\partial^4 u}{\partial x^3 \partial y} - \frac{\partial^4 v}{\partial x^4} \right.$$
$$\left. -\frac{\partial^4 v}{\partial x^2 \partial y^2} + \frac{\partial^4 u}{\partial x \partial y^3} \right), \tag{7.3}$$

$$\frac{\partial T}{\partial t} + u\frac{\partial T}{\partial x} + v\frac{\partial T}{\partial y} = \frac{K_c}{\rho C_p} \left(\frac{\partial^2 T}{\partial x^2} + \frac{\partial^2 T}{\partial y^2} \right) + \mu \left[2 \left\{ \left(\frac{\partial u}{\partial x} \right)^2 + \left(\frac{\partial v}{\partial y} \right)^2 \right\} + \left(\frac{\partial u}{\partial y} + \frac{\partial v}{\partial x} \right)^2 \right]$$
$$+\xi \left[\left(\frac{\partial^2 v}{\partial x^2} + \frac{\partial^2 v}{\partial y^2} \right)^2 + \left(\frac{\partial^2 u}{\partial x^2} + \frac{\partial^2 u}{\partial y^2} \right)^2 \right], \tag{7.4}$$

$$\frac{\partial C}{\partial t} + u\frac{\partial C}{\partial x} + v\frac{\partial C}{\partial y} = D \left(\frac{\partial^2 C}{\partial x^2} + \frac{\partial^2 C}{\partial y^2} \right) - K_1(t)\,C. \tag{7.5}$$

Here u denotes the velocity component in the $x-$direction and v the velocity component in the y direction, T, C, p, ρ, ν, K_c, C_p, D, k_1 and $K_1(t) = \frac{k_1}{1-at}$ are the temperature, the concentration, the pressure, the fluid density, the kinematic viscosity, the thermal conductivity, the specific heat, the diffusion species, chemical reaction parameter and the time dependent reaction rate respectively. Also (μ) is the Newtonian viscosity and (ξ) is the material constant characterizing the couple stresses. The dimension of μ/ξ is of length square and hence describes the material length of the fluid.

The boundary conditions are given by

$$u = 0, \quad v = v_w = \frac{dh}{dt}, \quad T = T_H, \quad C = C_H \quad \text{at} \quad y = h(t),$$
$$v = \frac{\partial u}{\partial y} = \frac{\partial T}{\partial y} = \frac{\partial C}{\partial y} = 0 \quad \text{at} \quad y = 0. \tag{7.6}$$

We define the following transformations

$$\eta = \frac{y}{H\sqrt{1-at}}, \ u = \frac{ax}{2(1-at)}f'(\eta), \ v = \frac{-aH}{2\sqrt{1-at}}f(\eta),$$

$$\theta = \frac{T}{T_H}, \ \phi = \frac{C}{C_H}. \tag{7.7}$$

Substituting the above transformations into Eqs. $(7.2) - (7.5)$, we get the following differential equations

$$f^{(iv)} - S_q(\eta f''' + 3f'' + f'f'' - ff''') - Kf^{(vi)} = 0, \tag{7.8}$$

$$\theta'' + PrS_q\left(f\theta' - \eta\theta'\right) + PrEc\left[\left(f''^2 + 4\delta^2 f'^2\right) + K\left(\delta^2 f''^2 + f'''^2\right)\right] = 0, \tag{7.9}$$

$$\phi'' + ScS_q\left(f\phi' - \eta\phi'\right) - Sc\gamma\phi = 0, \tag{7.10}$$

and the boundary conditions are

$$f(0) = 0, \ f(1) = 1, \ f'(1) = 0, \ f''(0) = 0,$$

$$\theta(1) = 1 = \phi(1), \ \theta'(0) = 0 = \phi'(0), \tag{7.11}$$

where squeezing parameter S_q, the couple stress parameter (K), the Prandtl number (Pr), the Eckert number (Ec), the Schmidt number (Sc) and the chemical reaction parameter (γ) are defined as follows:

$$S_q = \frac{aH^2}{2\nu}, \quad K = \frac{\xi}{\mu H^2(1-at)}, \quad Pr = \frac{\mu C_p}{K_c},$$

$$Ec = \frac{1}{T_H C_p}\left(\frac{ax}{2(1-at)}\right)^2, \ Sc = \frac{\nu}{D}, \ \gamma = \frac{k_1 H^2}{\nu}, \ \delta^2 = \frac{H^2(1-at)}{x^2}. \tag{7.12}$$

Here the squeeze parameter S_q represents relative distance between the plates $(S_q > 0$ shows that plates are moving apart and $S_q < 0$ represents that plates move together (which is called squeezing flow)). Note that $Ec = 0$ represents the absence of viscous dissipation effect, $\gamma > 0$ corresponds the destructive chemical reaction and $\gamma < 0$ describes the generative chemical

reaction. Skin friction coefficient, Nusselt number and Sherwood number are defined as follows:

$$C_f = \frac{(\tau_{xy})_{y=h(t)}}{\rho v_w^2}, \quad Nu = \frac{-HK_c\left(\frac{\partial T}{\partial y}\right)_{y=h(t)}}{K_c T_H}, \quad Sh = \frac{-HD\left(\frac{\partial C}{\partial y}\right)_{y=h(t)}}{DC_H} \tag{13}$$

By Eqs. (7.7) and (7.13), we have

$$\frac{H^2}{x^2}(1-at)\operatorname{Re}_x C_f = f''(1) - Kf^{(iv)}(1),$$

$$\sqrt{1-at}Nu = -\theta'(1), \quad \sqrt{1-at}Sh = -\phi'(1). \tag{7.13}$$

7.2   Homotopy analysis solutions

The initial approximations f_0, θ_0, ϕ_0 and auxiliary linear operators $\mathcal{L}_f$, $\mathcal{L}_\theta$, $\mathcal{L}_\phi$ for $f(\eta)$, $\theta(\eta)$ and $\phi(\eta)$ are

$$f_0(\eta) = \frac{1}{2}\left(3\eta - \eta^3\right), \quad \theta_0(\eta) = \phi_0(\eta) = 1, \tag{7.14}$$

$$\mathcal{L}_f = \frac{d^4}{d\eta^4}, \quad \mathcal{L}_\theta = \frac{d^2}{d\eta^2}, \quad \mathcal{L}_\phi = \frac{d^2}{d\eta^2}, \tag{7.15}$$

with

$$\mathcal{L}_f\left[C_1 + C_2\eta + C_3\eta^2 + C_4\eta^3\right] = 0, \tag{7.16}$$

$$\mathcal{L}_\theta\left[C_5 + C_6\eta\right] = 0, \tag{7.17}$$

$$\mathcal{L}_\phi\left[C_7 + C_8\eta\right] = 0, \tag{7.18}$$

where $C_i(i = 1 - 8)$ are the arbitrary constants and the zeroth order problems are

$$(1-p)\mathcal{L}_f[\bar{f}(\eta,p) - f_0(\eta)] = p\hbar_f\mathcal{N}_f\left[\bar{f}(\eta,p)\right], \tag{7.19}$$

$$(1-p)\mathcal{L}_\theta[\bar{\theta}(\eta,p) - \theta_0(\eta)] = p\hbar_\theta\mathcal{N}_\theta\left[\bar{f}(\eta,p), \bar{\theta}(\eta,p)\right], \tag{7.20}$$

$$(1-p)\mathcal{L}_\phi\left[\bar{\phi}(\eta,p) - \phi_0(\eta)\right] = p\hbar_\phi\mathcal{N}_\phi\left[\bar{f}(\eta,p), \bar{\phi}(\eta,p)\right], \tag{7.21}$$

$$\bar{f}(0;p) = 0, \ \bar{f}(1;p) = 1, \ \frac{\partial \bar{f}(1;p)}{\partial \eta} = 0, \ \frac{\partial^2 \bar{f}(1;p)}{\partial \eta^2} = 0,$$

$$\bar{\theta}(1;p) = 1, \ \bar{\phi}(1;p) = 1, \ \frac{\partial \bar{\theta}(0;p)}{\partial \eta} = 0, \ \frac{\partial \bar{\phi}(0;p)}{\partial \eta} = 0, \tag{7.22}$$

with the non-linear operators $\mathcal{N}_f$, $\mathcal{N}_\theta$ and $\mathcal{N}_\phi$ are

$$\mathcal{N}_f\left[\bar{f}(\eta;q)\right] = \frac{\partial^4 \bar{f}(\eta,q)}{\partial \eta^4} - S_q\left(\eta \frac{\partial^3 \bar{f}(\eta,q)}{\partial \eta^3} + 3\frac{\partial^2 \bar{f}(\eta,q)}{\partial \eta^2} + \frac{\partial \bar{f}(\eta,q)}{\partial \eta}\frac{\partial^2 \bar{f}(\eta,q)}{\partial \eta^2} - \hat{f}(\eta,p)\frac{\partial^3 \bar{f}(\eta,q)}{\partial \eta^3}\right)$$

$$-K\frac{\partial^6 \bar{f}(\eta,q)}{\partial \eta^6}, \tag{7.23}$$

$$\mathcal{N}_\theta\left[\bar{f}(\eta;q),\bar{\theta}(\eta;q)\right] = \frac{\partial^2 \bar{\theta}(\eta;q)}{\partial \eta^2} + PrS_q\left(\bar{f}(\eta,q)\frac{\partial \bar{\theta}(\eta;q)}{\partial \eta} - \eta\frac{\partial \bar{\theta}(\eta;q)}{\partial \eta}\right)$$

$$+PrEc\left[\left(\frac{\partial^2 \bar{f}(\eta,p)}{\partial \eta^2}\right)^2 + 4\delta^2\left(\frac{\partial \bar{f}(\eta,q)}{\partial \eta}\right)^2 + K\left\{\delta^2\left(\frac{\partial^2 \bar{f}(\eta,q)}{\partial \eta^2}\right)^2 + \left(\frac{\partial^3 \bar{f}(\eta,q)}{\partial \eta^3}\right)^2\right\}\right], \tag{7.24}$$

$$\mathcal{N}_\phi\left[\bar{f}(\eta;q),\bar{\phi}(\eta;q)\right] = \frac{\partial^2 \bar{\phi}(\eta;q)}{\partial \eta^2} + ScS_q\left(\bar{f}(\eta,q)\frac{\partial \bar{\phi}(\eta;q)}{\partial \eta} - \eta\frac{\partial \bar{\phi}(\eta;q)}{\partial \eta}\right)$$

$$-Sc\gamma\bar{\phi}(\eta;q). \tag{7.25}$$

Here $0 \leq q \leq 1$ denotes the embedding parameter and $\hbar_f \neq 0$, $\hbar_\theta \neq 0$ and $\hbar_\phi \neq 0$ indicate auxiliary parameters. When $q = 0$ and $q = 1$, one can write

$$\bar{f}(\eta;0) = f_0(\eta), \qquad \bar{f}(\eta;1) = f(\eta), \tag{7.26}$$

$$\bar{\theta}(\eta;0) = \theta_0(\eta), \qquad \bar{\theta}(\eta;1) = \theta(\eta), \tag{7.27}$$

$$\bar{\phi}(\eta;0) = \phi_0(\eta), \qquad \bar{\phi}(\eta;1) = \phi(\eta), \tag{7.28}$$

and when q changes from 0 to 1 then $\bar{f}(\eta;p)$, $\bar{\theta}(\eta;p)$ and $\bar{\phi}(\eta;p)$ vary from $f_0(\eta)$, $\theta_0(\eta)$, $\phi_0(\eta)$ to $f(\eta)$, $\theta(\eta)$, $\phi(\eta)$ respectively. Expanding $\bar{f}$, $\bar{\theta}$ and $\bar{\phi}$ using Taylor series about q we get

$$\bar{f}(\eta;q) = f_0(\eta) + \sum_{m=1}^{\infty} f_m(\eta)q^m, \qquad f_m(\eta) = \frac{1}{m!}\frac{\partial^m f(\eta;q)}{\partial q^m}\bigg|_{q=0}, \tag{7.29}$$

$$\bar{\theta}(\eta;q) = \theta_0(\eta) + \sum_{m=1}^{\infty} \theta_m(\eta)q^m, \qquad \theta_m(\eta) = \frac{1}{m!}\frac{\partial^m \theta(\eta;q)}{\partial q^m}\bigg|_{q=0}, \tag{7.30}$$

$$\bar{\phi}(\eta;q) = \phi_0(\eta) + \sum_{m=1}^{\infty} \phi_m(\eta)q^m, \qquad \phi_m(\eta) = \frac{1}{m!}\frac{\partial^m \phi(\eta;q)}{\partial q^m}\bigg|_{q=0}. \tag{7.31}$$

94

Auxiliary parameters are chosen such that the series $(7.30) - (7.32)$ converge at $q = 1$. Hence we have

$$f(\eta) = f_0(\eta) + \sum_{m=1}^{\infty} f_m(\eta), \tag{7.32}$$

$$\theta(\eta) = \theta_0(\eta) + \sum_{m=1}^{\infty} \theta_m(\eta), \tag{7.33}$$

$$\phi(\eta) = \phi_0(\eta) + \sum_{m=1}^{\infty} \phi_m(\eta). \tag{7.34}$$

Explicit mth-order deformation problems $(7.19 - 7.21)$ are

$$\mathcal{L}_f \left[f_m(\eta) - \chi_m f_{m-1}(\eta) \right] = \hbar_f \mathcal{R}_m^f(\eta), \tag{7.35}$$

$$\mathcal{L}_\theta \left[\theta_m(\eta) - \chi_m \theta_{m-1}(\eta) \right] = \hbar_\theta \mathcal{R}_m^\theta(\eta), \tag{7.36}$$

$$\mathcal{L}_\phi \left[\phi_m(\eta) - \chi_m \phi_{m-1}(\eta) \right] = \hbar_\phi \mathcal{R}_m^\phi(\eta), \tag{7.37}$$

$$f_m(0) = 0, \ f_m(1) = 0, \ f_m'(1) = 0, \ f_m''(0) = 0,$$
$$\theta_m(0) = 0, \ \theta_m'(0) = 0, \ \phi_m(1) = 0, \ \phi_m'(0) = 0, \tag{7.38}$$

$$\mathcal{R}_m^f(\eta) = f_{m-1}^{(iv)} - S_q \left(\eta f_{m-1}''' + 3 f_{m-1}'' \right) - K f_{m-1}^{(vi)}$$
$$- S_q \sum_{k=0}^{m-1} \left[f_{m-1-k}' f_k'' - f_{m-1-k} f_k''' \right], \tag{7.39}$$

$$\mathcal{R}_m^\theta(\eta) = \theta_{m-1}'' - PrS_q \eta \theta_{m-1}' + PrS_q \sum_{k=0}^{m-1} f_{m-1-k} \theta_k'$$
$$+ PrEc \sum_{k=0}^{m-1} \left[f_{m-1-k}'' f_k'' + 4\delta^2 f_{m-1-k}' f_k' + K \left(\delta^2 f_{m-1-k}'' f_k'' + f_{m-1-k}''' f_k''' \right) \right], \tag{7.40}$$

$$\mathcal{R}_m^\phi(\eta) = \phi_{m-1}'' - ScS_q \eta \phi_{m-1}' - Sc\gamma \phi_{m-1} + ScS_q \sum_{k=0}^{m-1} f_{m-1-k} \phi_k', \tag{7.41}$$

$$\chi_m = \begin{cases} 0, & m \leq 1, \\ 1, & m > 1. \end{cases} \tag{7.42}$$

The general solutions of Eqs. $(7.24) - (7.26)$ are given by

$$f_m(\eta) = f_m^*(\eta) + C_1 + C_2\eta + C_3\eta^2 + C_4\eta^3, \tag{7.43}$$

$$\theta_m(\eta) = \theta_m^*(\eta) + C_5 + C_6\eta, \tag{7.44}$$

$$\phi_m(\eta) = \phi_m^*(\eta) + C_7 + C_8\eta, \tag{7.45}$$

where $f_m^*(\eta)$, $\phi_m^*(\eta)$, and $\theta_m^*(\eta)$ denotes the special solutions.

7.3 Convergence of the homotopy solutions

The convergence of series solutions $(7.24 - 7.26)$ contains the parameters $\hbar_f$, $\hbar_\theta$ and $\hbar_\phi$ for the functions f, θ and ϕ respectively. These parameters help in controlling and adjusting the convergence of the solutions. To find the ranges of admissible values of $\hbar_f$, $\hbar_\theta$ and $\hbar_\phi$ of the functions $f''(1)$, $\theta'(1)$ and $\phi'(1)$, we have plotted the $\hbar_f$ and $\hbar_\phi-$curves for 15th-order of approximations and 20th order of approximation for $\hbar_\theta-$curve. From Figs. (7.1) and (7.2) it is clear that the ranges for the admissible values of $\hbar_f$, $\hbar_\theta$ and $\hbar_\phi$ are $-1.70 \leq \hbar_f \leq -0.3$, $-1.6 \leq \hbar_\theta \leq -0.5$, and $-1.20 \leq \hbar_\phi \leq -0.20$ respectively. In Figs. $(7.3 - 7.5)$ the $\hbar-$curves for residual error of f, θ and ϕ are sketched in order to get the admissible ranges for $\hbar$. Here we found that by selecting the values of $\hbar$ from this range we get the correct result upto 6th decimal place. It is observed that the lowest possible error of f, θ and ϕ for $\hbar_f \in [-1.25, -0.25]$, $\hbar_\theta \in [-0.8, -0.4]$ and $\hbar_\phi \in [-1.0, -0.4]$ respectively. Residual errors increase as we move away from the line parallel to the $\hbar-$axis. Therefore it shows oscillatory/divergent behavior. Table 7.1 shows that 15th$-$ order of approximations are enough for convergence solutions of f and ϕ
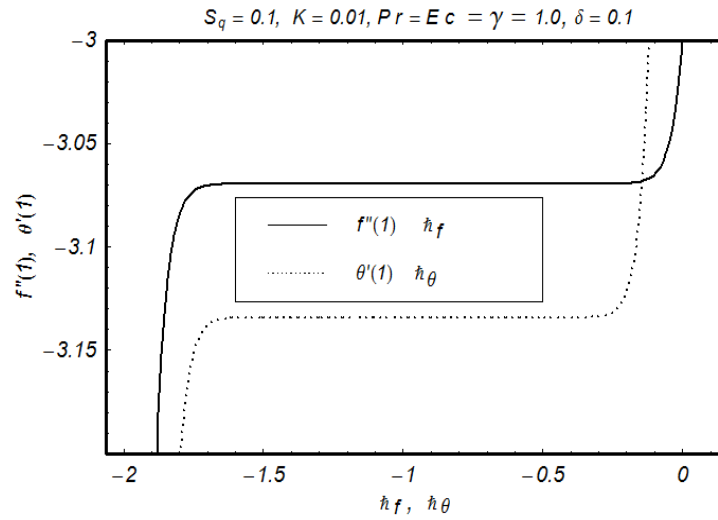
and 20th order approximations for θ.

Fig.7.1: Convergence region for the functions f and θ.
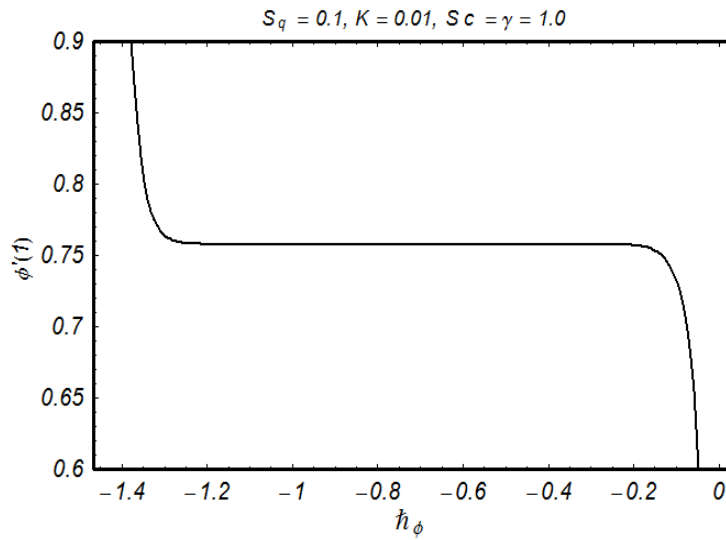

Fig.7.2: Convergence region for the function ϕ.
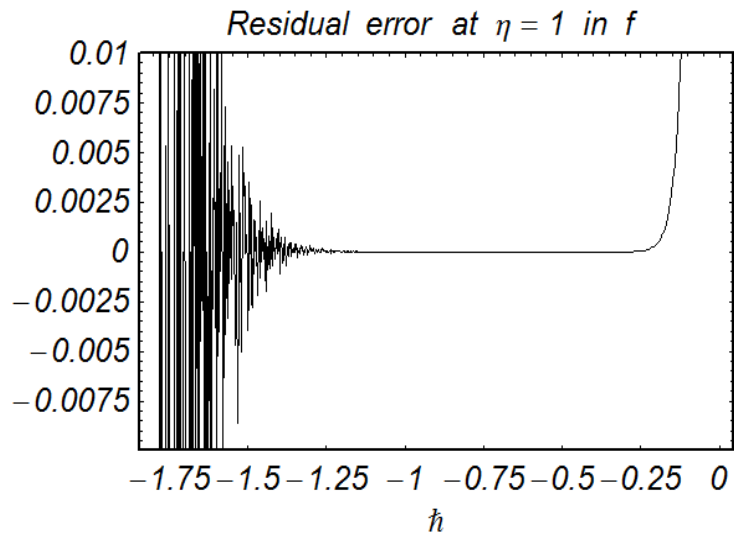
Fig. 7.3: Convergence region for residual error in $f(\eta)$.
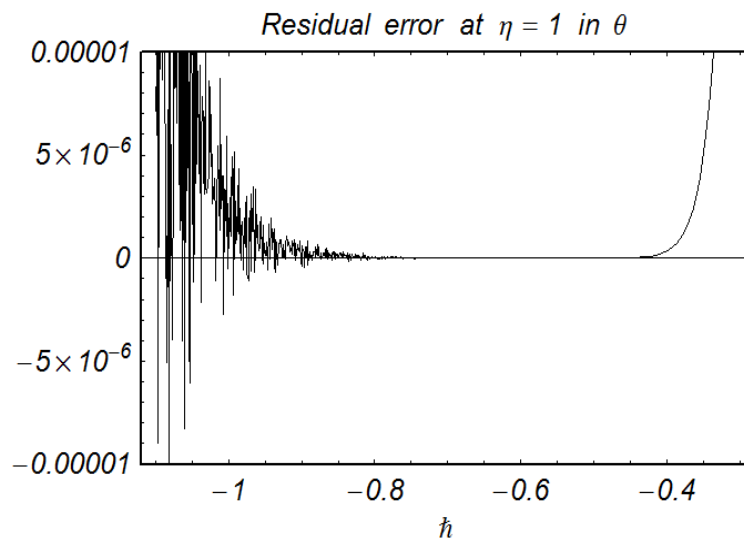

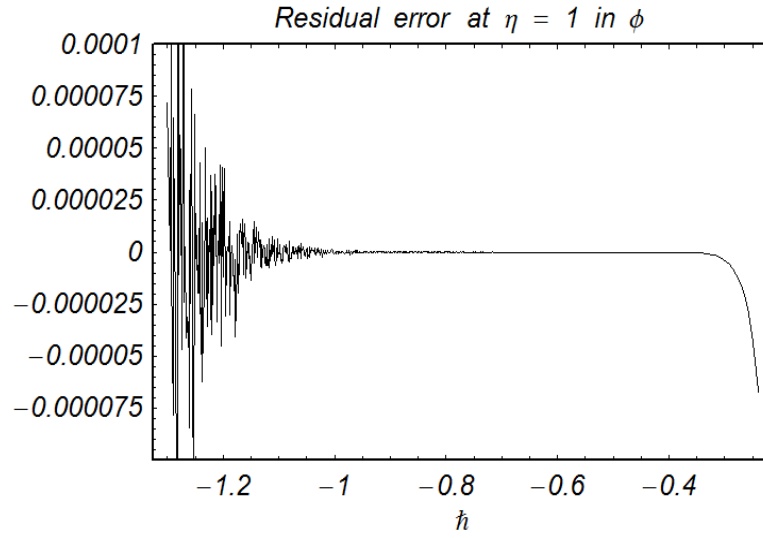Fig. 7.4: Convergence region for residual error in $\theta(\eta)$.

Fig.7.5: Convergence region for residual error in $\phi(\eta)$.

Table 7.1. Series solution's convergence by HAM for different order of approximations when $S_q = 0.1$, $K = 0.01$ and $\mathrm{Pr} = Ec = Sc = \gamma = \delta = 1.0$.

Order of approximations	$-f''(1)$	$-\theta'(1)$	$\phi'(1)$
1	3.042857	1.882980	0.600000
5	3.068946	3.102037	0.756355
10	3.069559	3.133750	0.757933
15	3.069565	3.134080	0.757946
20	3.069565	3.134083	0.757946
25	3.069565	3.134083	0.757946
30	3.069565	3.134083	0.757946
40	3.069565	3.134083	0.757946
50	3.069565	3.134083	0.757946

7.4 Discussion

In this section we discuss the influence of physical parameters on the velocity, temperature and concentration profiles. Hence we have plotted the Figs. $7.6 - 7.13$. In Figs. 7.6 and 7.7, we have discussed the influence of couple stress parameter K and squeezing parameter S_q on the velocity profile f'. From Fig. 7.6 it is clear that when we increase the couple stress parameter K then the velocity profile increases initially from $\eta = 0$ to $\eta = 0.45$ and it decreases from $\eta = 0.45$ to $\eta = 1$. Similar behavior is observed for the squeezing parameter S_q in Fig. 7.7. In Fig. 7.8, we explored the effects of Eckert number Ec on temperature profile θ. Obviously the temperature profile increases when the Eckert number Ec is increased. This is because of the fact that the presence of viscous dissipation effect significantly increases the temperature θ. Effects of Prandtl number Pr on the temperature profile θ is displayed in Fig. 7.9. This Fig. shows that an increase in Prandtl number heats up the fluid. It is also noticed that the temperature is gradually increasing from the walls towards the middle of the channel. The combined effects of squeezing parameter S_q on the temperature profile θ is discussed in Fig. 7.10. The temperature decreases from $\eta = 0$ to $\eta = 1$ for fixed values of other parameters. Considerable reduction occurs in the temperature field θ for higher values of S_q. It is found that the temperature is comparatively high when the plates are moving to each other. An increase in S_q can be related with the reduction in kinematic viscosity which consequently depends upon the velocity and the distance between the plates. Reduction appears in the concentration for larger values of chemical reaction parameter ($\gamma > 0$). Further enhancement is noted in the concentration field for higher values of generative chemical reaction parameter ($\gamma < 0$). Higher values of γ result in the enhancement of concentration at the lower wall. Influence of Schmidt number (Sc) on the concentration field ϕ is characterized in Fig. 7.12. Thinner boundary layer is analyzed due to small molecular diffusivity when Schmidt number Sc is increased. Effect of S_q on concentration field is discussed in Fig. 7.13. The concentration field also increases when S_q is increased. Tables ($7.2 - 7.4$) are presented for the numerical values of skin friction coefficient, local Nusselt and Sherwood numbers for different parameters. In Table 7.2, when we increase the squeezing parameter S_q, the skin friction coefficient increases while local Nusselt number and local Sherwood number decrease. The skin friction coefficient, local Nusselt number and local Sherwood number decrease when couple stress parameter is increased. Numerical values

of local Nusselt number for different parameters are discussed in Table 7.3. With the increase of Pr, Ec, and δ, the local Nusselt number also increases. Numerical values of local Sherwood number for different parameters are shown in Table 7.4. Local Sherwood number is increasing function of Sc. Tables 7.5 and 7.6 provides the comparison for viscous case. Here the comparison is excellent.
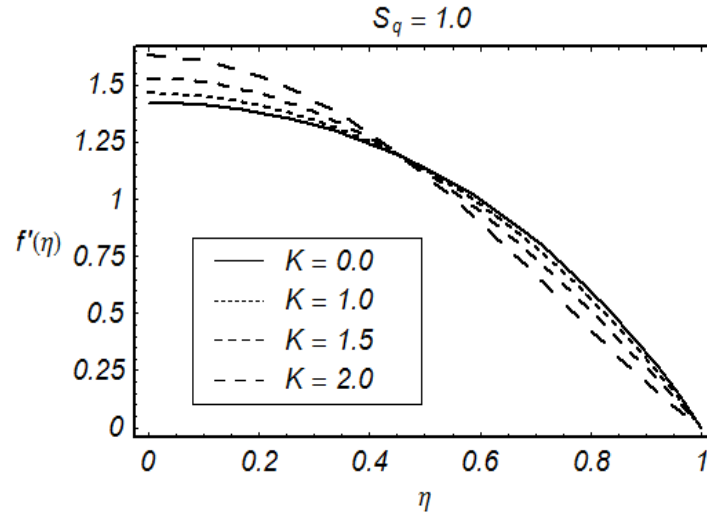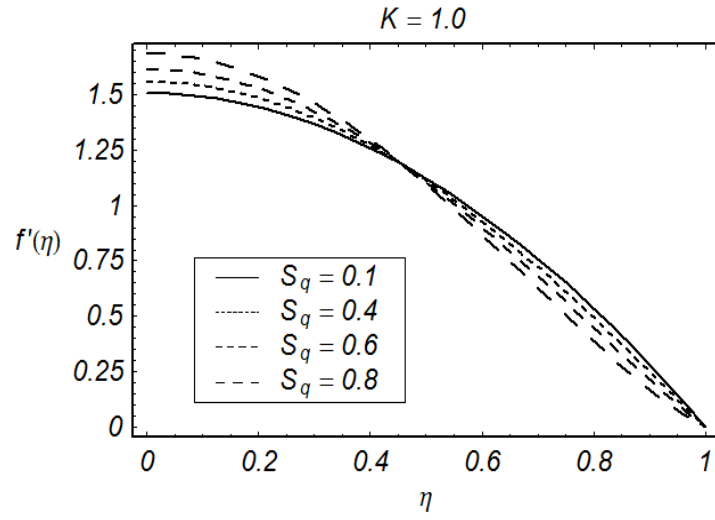

Fig. 7.6: Influence of K on f'.
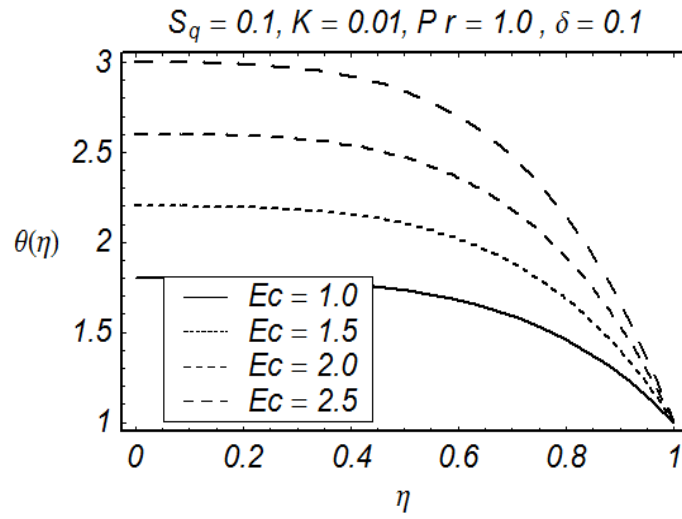
Fig. 7.7: Influence of S_q on f'.

Fig. 7.8: Influence of Ec on θ.
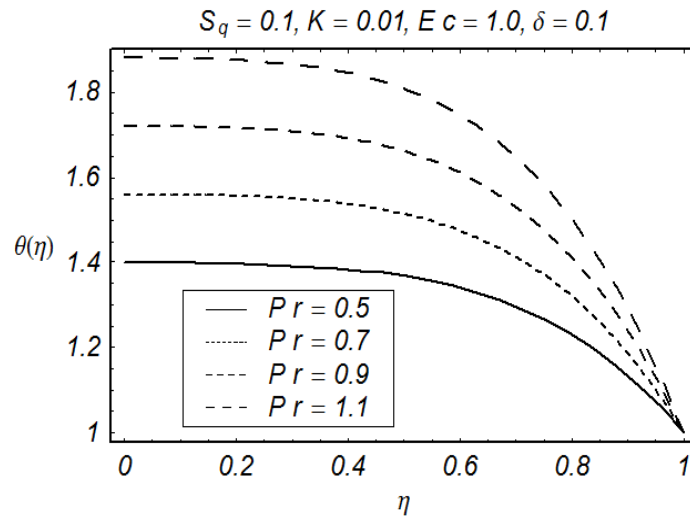
Fig. 7.9: Influence of Pr on θ.
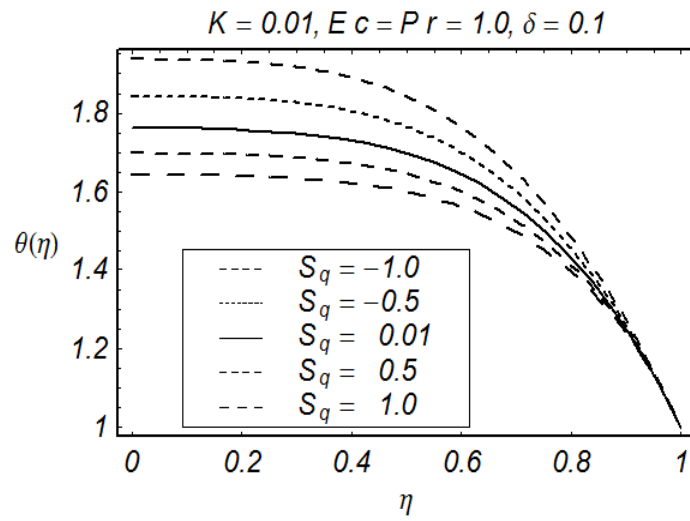
Fig. 7.10: Influence of S_q on θ.
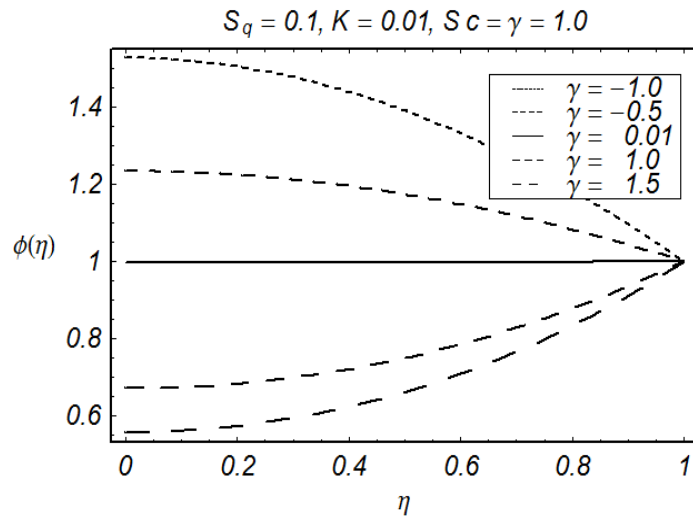
Fig. 7.11: Influence of γ on ϕ.
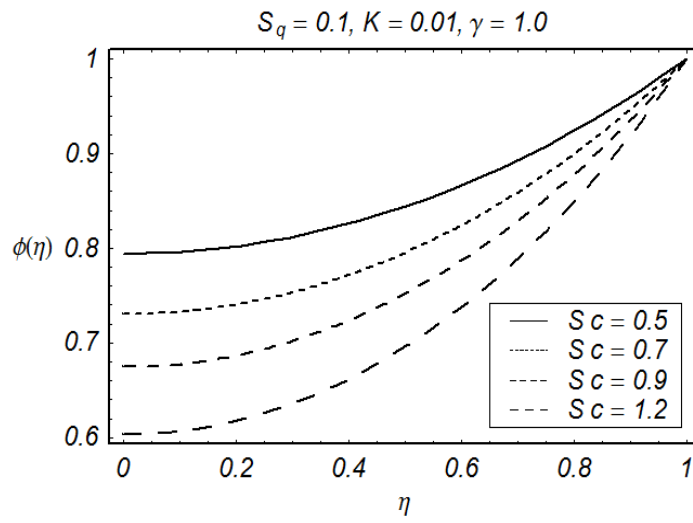

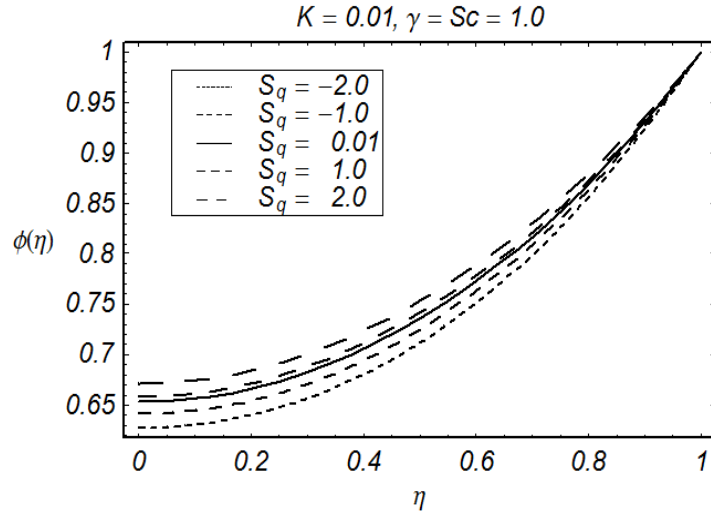Fig. 7.12: Influence of Sc on ϕ.

Fig. 7.13: Influence of S_q on ϕ.

Table 7.2. Values of skin friction coefficient, local Nusselt number and local Sherwood number for different values of S_q and K when $Pr = Ec = Sc = \gamma = 1.0$.

S_q	K	$-k(1)$	$-\theta(1)$	$-\phi(1)$
-0.1	0.01	2.937676	3.145330	0.765336
-0.01		2.993850	3.138872	0.761964
0.01		3.006131	3.137755	0.761225
0.1		3.060523	3.134083	0.757946
0.5		3.286238	3.140897	0.744223
0.01	0.01	3.006131	3.137755	0.761225
	0.02	3.005165	3.228405	0.761225
	0.03	3.004234	3.319040	0.761225
	0.04	3.003340	3.409661	0.761225

Table 7.3. Values of local Nusselt number for different values of Pr, δ and Ec when $S_q = 0.1$ and $K = 0.01$.

P_r	E_c	δ	$-\theta'(1)$
0.3	1.0	0.1	0.942163
0.5			1.569348
1.0			3.134083
1.5			4.694227
1.0	0.01	0.1	0.0313408
	0.5		1.567042
	0.8		2.507267
	1.5		4.701125
1.0	1.0	0.0	3.086392
		0.5	4.278670
		1.0	7.855504
		1.5	13.81689
		2.0	22.16283

Table 7.4. Values of local Sherwood number for different values of Sc and γ when $Pr = Ec = 1.0$, $\delta = 0.1$

S_c	γ	$\phi'(1)$
0.1	1.0	0.0967333
0.2		0.1874234
0.7		0.5702172
1.2		0.8703312
1.5		1.0235430
1.0	−0.5	0.5993247
	−0.3	0.3316206
	0.1	0.0961821
	0.3	0.2715976
	0.5	0.4281469

Table 7.5. Comparison of skin friction coefficient, local Nusselt number and local Sherwood number when $K = 0$, $Pr = Ec = Sc = \gamma = 1.0$ and $\delta = 0.1$.

	Mustafa et al.[23]			Present		
S_q	$-f''(1)$	$-\theta'(1)$	$-\phi'(1)$	$-f''(1)$	$-\theta'(1)$	$-\phi'(1)$
-1.0	2.170090	3.319899	0.804558	2.17009087	3.31989927	0.80455875
-0.5	2.614038	3.129491	0.781402	2.61740384	3.12949108	0.78140233
0.01	3.007134	3.047092	0.761225	3.00713375	3.04709193	0.76122521
0.5	3.336449	3.026324	0.744224	3.33644946	3.02632354	0.74422428
2.0	4.167389	3.118551	0.701813	4.16738918	3.11855069	0.70181323

Table 7.6: Comparison between HAM and HPM solutions [69]

S	$f''(1)$	
	HPM [69]	HAM (Present results)
0.1	2.97682	2.97682
0.5	–	2.89177
1.0	–	2.80242
1.5	–	2.73094

7.5 Main results

Here the effects of heat and mass transfer in squeezing flow of incompressible couple stress fluid are analyzed. The main observations are put into the following points.

- Velocity profile $f'(\eta)$ increases near the lower plate while it decreases near the upper plate when couple stress and squeezing parameters are increased.

- Effects of Prandtl number Pr and Eckert number Ec have increasing behavior for the temperature $\theta(\eta)$.

- Increase in squeezing parameter Sq decreases the temperature $\theta(\eta)$.

- Concentration field $\phi(\eta)$ increases when squeezing parameter is increased.

- Concentration field $\phi(\eta)$ is higher for larger values of Schmidt number (Sc).

- Destructive and generative chemical reaction parameters $(\gamma > 0, \gamma < 0)$ have opposite effects for concentration field ϕ.

- Increasing the squeezing parameter S_q, the skin friction coefficient increases while local Nusselt number and local Sherwood number decrease.

- The skin friction coefficient, local Nusselt number and local Sherwood number decrease when couple stress parameter is increased.

Chapter 8

MHD unsteady squeezing flow of second grade fluid over a porous stretching plate

This chapter is concerned with the unsteady squeezing flow of non-Newtonian fluid between two parallel plates. Rheological equation of second grade fluid is used. The consider fluid model can predict the normal stress effect. The fluid is electrically conducting in the presence of constant applied magnetic field. Transformation procedure reduces the partial differential equations into the ordinary differential equations. A series solution is developed using a modern mathematical scheme. The solution expressions for velocity components are computed and discussed. In addition the skin friction coefficient is analyzed through the tabular values.

8.1 Mathematical formulation

We consider the flow of second grade (a subclass of differential type of non-Newtonian) fluid between the two walls. The porous lower wall (situated at $y = 0$) is stretching in an unsteady manner with the velocity $ax/1 - bt$ ($t < 1/b$). Note that for $b = 0$, steady state case of linearly stretching is recovered (see [98, 101]). Further the lower wall is porous with $V_0 > 0$ for suction and $V_0 < 0$ corresponds to injection case. Here the porosity of the plate is also taken in an unsteady manner. The upper wall situated at $y = h(t)$ is squeezing towards the lower wall and

this generate the squeezing flow. The squeezing velocity is taken V_h. The lower plate is situated at $y = 0$ and the upper moving plate located at $h(t) = \sqrt{\nu(1 - bt)/a}$ moves with velocity V_h. Note that $\sqrt{\frac{\nu}{a}}$ has a dimension of length which is a constant. When $t = 0$, then $h(t) = \sqrt{\frac{\nu}{a}}$ and when $t = \frac{1}{b}$ then $h(t) = 0$. Infect $h(t) = 0$ means that there is no other plate which provides a contradiction to the present flow configuration. Hence $t \neq \frac{1}{b}$ in present case. Therefore the flow domain $0 \leq h(t) < \sqrt{\frac{\nu}{a}}$ represents a finite interval. A magnetic field $B_0/(1 - bt)$ is applied along the $y-$axis. The induced magnetic and electric fields are neglected. The governing equations for two-dimensional flow of second grade fluid are

$$\frac{\partial u}{\partial x} + \frac{\partial v}{\partial y} = 0, \tag{8.1}$$

$$\frac{\partial u}{\partial t} + u\frac{\partial u}{\partial x} + v\frac{\partial u}{\partial y} = -\frac{1}{\rho}\frac{\partial p}{\partial x} + \nu\left[\frac{\partial^2 u}{\partial x^2} + \frac{\partial^2 u}{\partial y^2}\right] - \frac{\sigma B_0^2}{\rho(1 - bt)}u$$
$$+ \frac{\alpha_1}{\rho}\left[\frac{\partial^3 u}{\partial t\partial x^2} + \frac{\partial^3 u}{\partial t\partial y^2} + 2\frac{\partial v}{\partial y}\frac{\partial^2 v}{\partial x\partial y} + 2\frac{\partial v}{\partial x}\frac{\partial^2 v}{\partial x^2} + u\left(\frac{\partial^3 u}{\partial x^3} + \frac{\partial^3 u}{\partial x\partial y^2}\right)\right.$$
$$\left. + v\left(\frac{\partial^3 u}{\partial x^2\partial y} + \frac{\partial^3 u}{\partial y^3}\right) + \frac{\partial u}{\partial x}\left(3\frac{\partial^2 u}{\partial x^2} + \frac{\partial^2 u}{\partial y^2}\right) + \frac{\partial u}{\partial y}\left(\frac{\partial^2 u}{\partial x\partial y} + \frac{\partial^2 v}{\partial x^2}\right)\right], \tag{8.2}$$

$$\frac{\partial v}{\partial t} + u\frac{\partial v}{\partial x} + v\frac{\partial v}{\partial y} = -\frac{1}{\rho}\frac{\partial p}{\partial y} + \nu\left[\frac{\partial^2 v}{\partial x^2} + \frac{\partial^2 v}{\partial y^2}\right]$$
$$+ \frac{\alpha_1}{\rho}\left[\frac{\partial^3 v}{\partial t\partial x^2} + \frac{\partial^3 v}{\partial t\partial y^2} + 2\frac{\partial u}{\partial y}\frac{\partial^2 u}{\partial y^2} + u\left(\frac{\partial^3 v}{\partial x^3} + \frac{\partial^3 v}{\partial x\partial y^2}\right)\right.$$
$$\left. + v\left(\frac{\partial^3 v}{\partial y^3} + \frac{\partial^3 v}{\partial x^2\partial y}\right) + \frac{\partial v}{\partial x}\left(\frac{\partial^2 u}{\partial y^2} + \frac{\partial^2 v}{\partial x\partial y}\right) + \frac{\partial v}{\partial y}\left(\frac{\partial^2 v}{\partial x^2} + 3\frac{\partial^2 v}{\partial y^2}\right)\right]. \tag{8.3}$$

Here u denotes the velocity in the $x-$direction and v the velocity in the $y-$direction and ρ, ν, p and $\alpha_1(> 0)$ are the fluid density, the kinematic viscosity, pressure and the material parameter respectively.

The boundary conditions are

$$u(x, y, t) = U_0 = \frac{ax}{1 - \gamma t}, \quad V_0(x, y, t) = -\frac{w_0}{1 - \gamma t}, \quad \text{at} \quad y = 0,$$

$$u(x, y, t) = 0, \quad v(x, y, t) = V_h = -\frac{\gamma}{2}\sqrt{\frac{\nu}{a(1 - \gamma t)}} \quad \text{at} \quad y = h(t), \tag{8.4}$$

where 'a' denotes the stretching rate of the lower plate, $w_0 > 0$ indicates the suction and $w_0 < 0$

for the injection/blowing velocity. Eliminating pressure gradient from Eqs. (8.2−8.3) and using

$$u = U_0 f'(\eta), \ v = -\sqrt{\frac{a\upsilon}{1-bt}} f(\eta), \ \eta = \frac{y}{h(t)}. \tag{8.5}$$

we arrive at

$$f^{(iv)} - f'f'' + ff''' - \frac{S_q}{2}\left(\eta f''' + 3f''\right)$$
$$+\beta\left[f'f^{(iv)} - ff^{(v)} + \frac{S_q}{2}\left(5f^{(iv)} + \eta f^{(iv)}\right)\right] - M^2 f'' = 0. \tag{8.6}$$

The corresponding boundary conditions can be written in the form

$$f(0) = S, \ f'(0) = 1, \ f(1) = \frac{S_q}{2}, \ f'(1) = 0. \tag{8.7}$$

where squeezing parameter S_q, the second grade parameter α^*, the suction/injection parameter S and the magnetic parameter M have the following definitions:

$$S_q = \frac{\gamma}{a}, \quad \alpha^* = \frac{a\alpha_1}{\mu(1-at)}, \quad S = \frac{w_0}{ah}, \quad M^2 = \frac{\sigma B_0^2}{\rho a}. \tag{8.8}$$

Note that the upper plate moves downward with velocity $V_h < 0$ for $S_q > 0$. For $S_q < 0$ the upper plate moves apart with respect to the plane $y = 0$ and $S_q = 0$ corresponds to the steady case or stationary upper plate. The skin friction coefficient is given by

$$C_f = \frac{(\tau_{xy})_{y=h(t)}}{\rho v_h^2} \tag{8.9}$$

with

$$\begin{aligned}\tau_{xy} &= \mu\left(\frac{\partial u}{\partial y} + \frac{\partial v}{\partial x}\right) + \alpha_1\left[\frac{\partial^2 u}{\partial t \partial y} + \frac{\partial^2 v}{\partial t \partial x} + u\left(\frac{\partial^2 u}{\partial x \partial y} + \frac{\partial^2 v}{\partial x^2}\right)\right.\\ &\left. + v\left(\frac{\partial^2 u}{\partial y^2} + \frac{\partial^2 v}{\partial x \partial y}\right) + \frac{\partial u}{\partial x}\left(\frac{\partial u}{\partial y} - \frac{\partial v}{\partial x}\right) + \frac{\partial v}{\partial y}\left(\frac{\partial v}{\partial x} - \frac{\partial u}{\partial y}\right)\right]. \end{aligned} \tag{8.10}$$

Dimensionless form of Eq. (8.9) is

$$2\,\mathrm{Re}^{\frac{1}{2}} C_f = f''(1) + \alpha^*\left[S_q\left\{3f''(1) + f'''(1)\right\} + 4f'(1)f''(1) - 2f(1)f'''(1)\right]. \tag{8.11}$$

8.2 Homotopy analysis procedure

8.2.1 Zeroth order deformation problems

To find the series solution through homotopy analysis method (HAM), the velocity field is written by a set of base functions

$$\left\{ \eta^k \mid k \geq 0 \right\} \tag{8.12}$$

in the form

$$f(\eta) = \sum_k a_k \eta^{2k+1} \tag{8.13}$$

in which a_k are the coefficients. The initial approximation $f_0(\eta)$ and the auxiliary operator $\mathcal{L}_f$ are chosen in the forms:

$$f_0(\eta) = \eta - 2\eta^2 + \eta^3 + S\left(1 - 3\eta^2 + 2\eta^3\right) + S_q \eta^2 \left(\frac{3}{2} - \eta\right), \tag{8.14}$$

$$\mathcal{L}_f = f^{(iv)}. \tag{8.15}$$

The operator $\mathcal{L}_f$ has the property

$$\mathcal{L}_f\left(C_1 + C_2\eta + C_3\eta^2 + C_4\eta^3\right) = 0, \tag{8.16}$$

where $C_i(i = 1 - 4)$ are the arbitrary constants and the nonlinear operator is

$$\begin{aligned}
\mathcal{N}_f\left[\bar{f}(\eta,p)\right] &= \frac{\partial^4 \bar{f}}{\partial \eta^4} - \frac{\partial \bar{f}}{\partial \eta}\frac{\partial^2 \bar{f}}{\partial \eta^2} + \bar{f}\frac{\partial^3 \bar{f}}{\partial \eta^3} - \frac{S_q}{2}\left(\eta\frac{\partial^3 \bar{f}}{\partial \eta^3} + 3\frac{\partial^2 \bar{f}}{\partial \eta^2}\right) - M^2\frac{\partial^2 \bar{f}}{\partial \eta^2} \\
&\quad + \alpha^* \left[\frac{\partial \bar{f}}{\partial \eta}\frac{\partial^4 \bar{f}}{\partial \eta^4} - \bar{f}\frac{\partial^5 \bar{f}}{\partial \eta^5} + \frac{S_q}{2}\left(5\frac{\partial^4 \bar{f}}{\partial \eta^4} + \eta\frac{\partial^5 \bar{f}}{\partial \eta^5}\right)\right].
\end{aligned} \tag{8.17}$$

The zeroth order problem has the definition

$$(1-q)\mathcal{L}_f\left[\bar{f}(\eta,q) - F_0(\eta)\right] = q\hbar_f \mathcal{N}_f\left[\bar{f}(\eta,q)\right], \tag{8.18}$$

$$\bar{f}(0,q) = S, \ \bar{f}'(0,q) = 1, \ \bar{f}(1,q) = \frac{S_q}{2}, \ \bar{f}'(1,q) = 0, \tag{8.19}$$

where $\hbar_f$ is an auxiliary parameter and $0 \leq q \leq 1$ is embedding parameter. It is observed that, when q changes from 0 to 1, then $f(\eta, q)$ varies from $f_0(\eta)$ to $f(\eta)$. For $q = 0$ and $q = 1$, one

obtains

$$\bar{f}(\eta, 0) = f_0(\eta), \ \bar{f}(\eta, 1) = f(\eta).$$ (8.20)

By applying the Taylor series on $f(\eta)$ one can write

$$f(\eta) = f_0(\eta) + \sum_{m=1}^{\infty} f_m(\eta) q^m,$$ (8.21)

$$f_m(\eta) = \frac{1}{m!} \frac{\partial^m \bar{f}(\eta, q)}{\partial q^m} \bigg|_{q=0}.$$ (8.22)

The convergence of the series solution is dependent upon $\hbar_f$. We choose $\hbar_f$ in such a way that the series (8.21) converges at $q = 1$ and hence

$$f(\eta) = f_0(\eta) + \sum_{m=1}^{\infty} f_m(\eta).$$ (8.23)

8.2.2 mth-order deformation problems

The mth-order deformation equations are obtained by differentiating the equations (8.18) and (8.19) with respect to q ($m-$times) and then putting $q = 0$ i.e.

$$\mathcal{L}_f \left[f_m(\eta) - \chi_m f_{m-1}(\eta) \right] = \hbar_f \mathcal{R}_m(\eta),$$ (8.24)

$$f_m(0) = f'_m(0) = f_m(1) = f'_m(1) = 0,$$ (8.25)

$$\chi_m = \begin{cases} 0, & m \leq 1, \\ 1, & m > 1, \end{cases}$$ (8.26)

$$\mathcal{R}_m(\eta) = f_{m-1}^{(iv)} - M^2 f''_{m-1} - \frac{S_q}{2} \left[\eta f'''_{m-1} + 3 f''_{m-1} - \alpha^* \left(5 f_{m-1}^{(iv)} + \eta f_{m-1}^{(v)} \right) \right]$$

$$+ \sum_{k=0}^{m-1} \left\{ \alpha^* \left(f'_{m-1-k} f_k^{(iv)} - f_{m-1-k} f_k^{(v)} \right) - f'_{m-1-k} f''_k + f_{m-1-k} f'''_k \right\}.$$ (8.27)

The above equations have a solution

$$f_m(\eta) = f_m^*(\eta) + C_1 + C_2 \eta + C_3 \eta^2 + C_4 \eta^3,$$ (8.28)

in which f_m^* represents a special solution.

8.2.3   Convergence analysis

The series solution (8.23) contains the auxiliary parameter $\hbar_f$. This auxiliary parameter can adjust the convergence of the obtained series solution. Fig. 8.1 shows the $h-$curve of the function f for $S_q = M = 1.0$ and $\alpha^* = 0.1$. The permissible values of auxiliary parameter $\hbar_f$ are $-1.1 \leq \hbar_f \leq -0.2$ and $-1.1 \leq \hbar_f \leq -0.25$ for both suction and injection respectively. Table 8.1 helps in making a guess that how much order of approximations are necessary for a convergent solution. This table shows that the $13th$ and $11th$ order of approximations are enough for the convergent solution of suction and injection respectively. We have performed all computations regarding the convergence of the derived series solutions. It is noted that the obtained solutions converge for $\beta = 0.5, 1.0, 1.5, 2.0$. Now it is obvious that values of $\hbar_f$ are admissible for which the plots are parallel to $\hbar_f-$curve. For example in Figs. (a), (b), (c), (d) the admissible values for $\hbar_f$ are $-0.3 \leq \hbar_f \leq -0.05$, $-0.16 \leq \hbar_f \leq -0.03$, $-0.08 \leq \hbar_f \leq -0.02$, $-0.09 \leq \hbar_f \leq -0.01$.
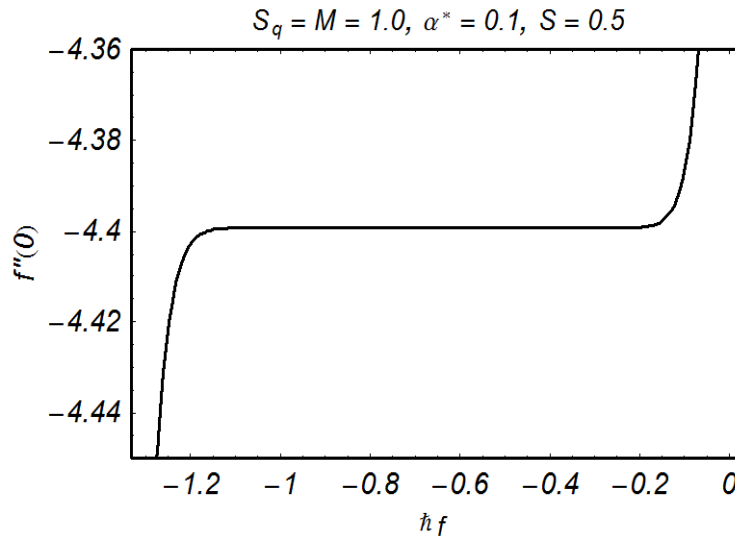

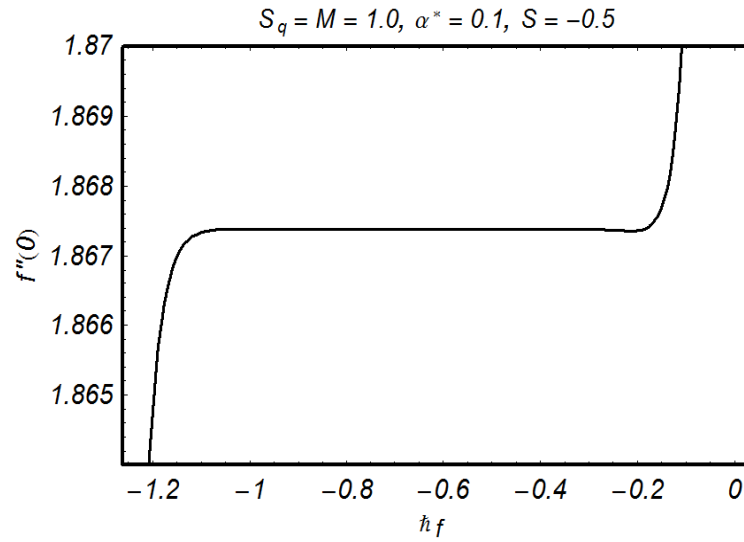Fig.8.1: Convergence region of f at $\eta = 0$ for suction.

Fig.8.2: Convergence region of f'' at $\eta = 0$ for blowing.

Table 8.1. Series solution's convergence by HAM for different order of approximations when $S_q = M = 1.0$, $S = 0.5$ and $\alpha^* = 0.1$.

Order of approximations	$-f''(0)$ for suction	$f''(0)$ for injection
1	4.284524	1.890476
5	4.399092	1.867194
10	4.399209	1.867386
11	4.399207	1.867388
13	4.399205	1.867388
20	4.399205	1.867388
25	4.399205	1.867388
30	4.399205	1.867388
35	4.399205	1.867388
40	4.399205	1.867388

115

8.3 Graphical results and analysis

In this section, we discuss the influence of embedding parameters on the velocity profiles f' and f. Effects of second grade parameter (α^*) on f' and f are discussed in the Figs. $(8.3, 8.4)$. It is reported that f' increases initially when α^* is increased whereas for $\eta \geq 0.4$, there is decrease in velocity profile f' (Fig. 8.3). As expected the higher magnitude of velocity field is observed for larger α^*. This is because of the fact that viscoelastic effect and wall permeability lead to enhance the velocity f. Effects of suction parameter S on f' and f are shown in the Figs. (8.5, 8.6). Increase in suction parameter S yields a decrease in velocity field f'. Reverse flow occurs due to reduction in the velocity f' for larger suction. Such reverse flow is more dominant near the upper plate in comparison to the lower plate. Physically this is due to the considerable adverse pressure gradient produced by fluid particles fleeing from the lower wall. Fig. 8.6 shows that larger suction gives increase in f. Also variation in the velocity profile is confined in vicinity of lower plate. Figs. $(8.7, 8.8)$ illustrate the effects of parameter S_q on f' and f. It is noticed that the velocity increases by increasing S_q. It is also observed that the higher value of S_q depreciate the reverse flow. Fig. 8.8 shows the effects of S_q on f. Here f increases with the increase of S_q. Fig. $(8.9, 8.10)$ plots the effects of magnetic parameter (M) on horizontal and vertical velocities f' and f respectively for suction case. With increase of M, the velocity profile f' decreases for $0 \leq \eta \leq 0.4$ and it increases when $0.4 \leq \eta \leq 1$. In fact Lorentz force increases with the magnetic parameter M which is a resistive force. So horizontal velocity profile decreases and vertical velocity increases. Figs. $(8.11 - 8.16)$ are devoted to examine the effects of α^*, S_q and M on f' and f for the injection case. Opposite behavior is seen in the case of blowing/injection from the suction case. Combined effects of suction and injection on the velocity fields f' and f for different values of α^* are shown in the Figs. $(8.17, 8.18)$. Figs. $(8.19, 8.20)$ present the simultaneous effects of suction and blowing on velocity fields f' and f for various values of M. Simultaneous effects of suction and injection on velocity fields f' and f for different values of S_q are displayed in Fig. $(8.21, 8.22)$. Figs. 8.17 and 8.19 show that the velocity f' increases near the lower and upper plate while it decreases at the centre of the channel by increasing α^* and M (for injection case $S < 0$). Reverse behavior is seen in the case of suction. Fig. 8.18 shows that when we increases α^*, the velocity f increases for suction and it decreases for injection. Fig. 8.20 shows that the magnitude of the vertical

velocity f reduces due to suction while it increases for injection case with the increase of M. Fig. 8.21 shows that magnitude of velocity f' decreases for the suction while it increases for the injection when we increase squeezing parameter S_q. Fig 8.22 shows that the magnitude of velocity f increases for suction case. However the magnitude of f decreases for injection case. Table 8.2 includes numerical values of skin friction for different parameters. With the increase of suction parameter S and second grade parameter α^*, the skin friction coefficient increases while it decreases by increasing the squeezing parameter S_q and M.
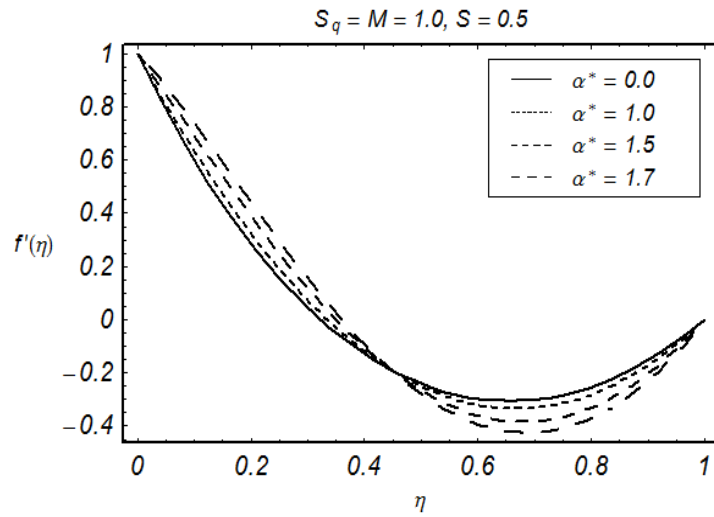
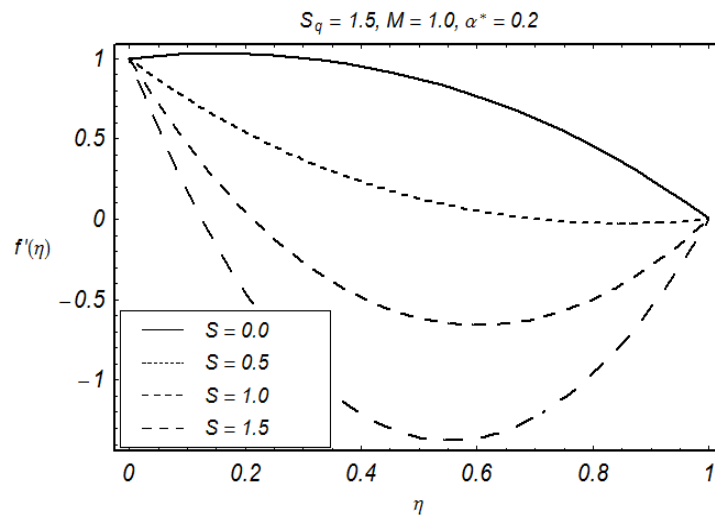Fig. 8.3: Influence of α^* on f'.
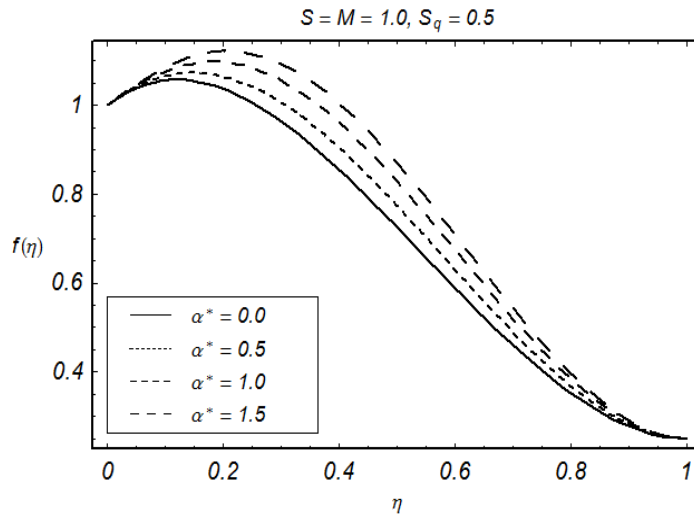
Fig. 8.4: Influence of α^* on f.
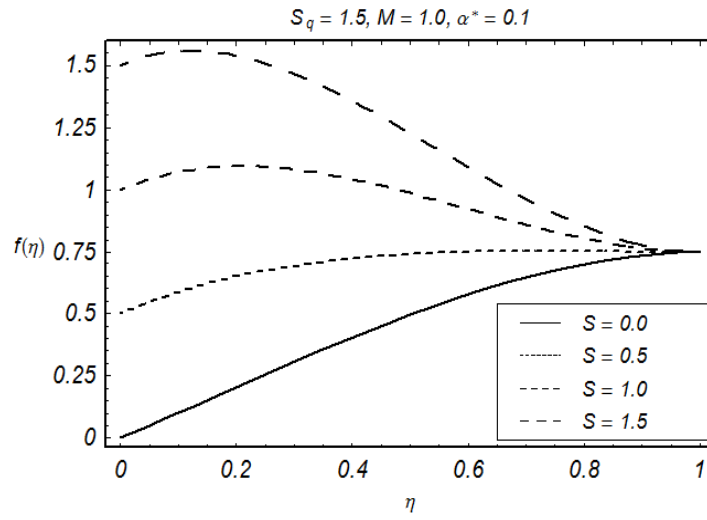

Fig. 8.5: Influence of S on f'.

Fig. 8.6: Influence of S on f.

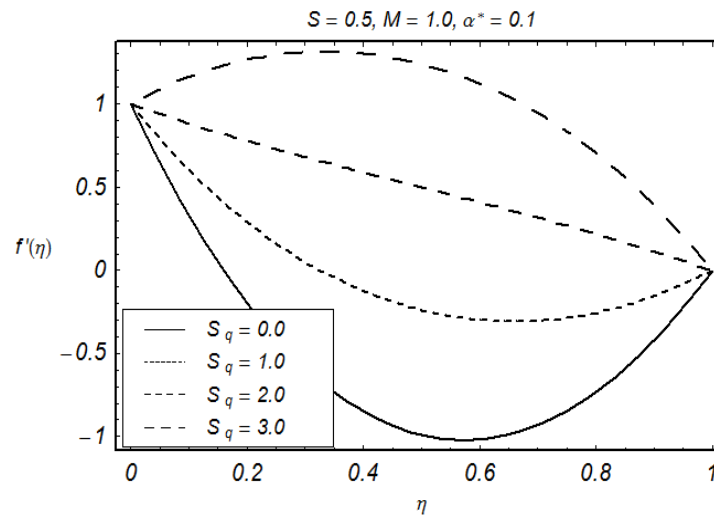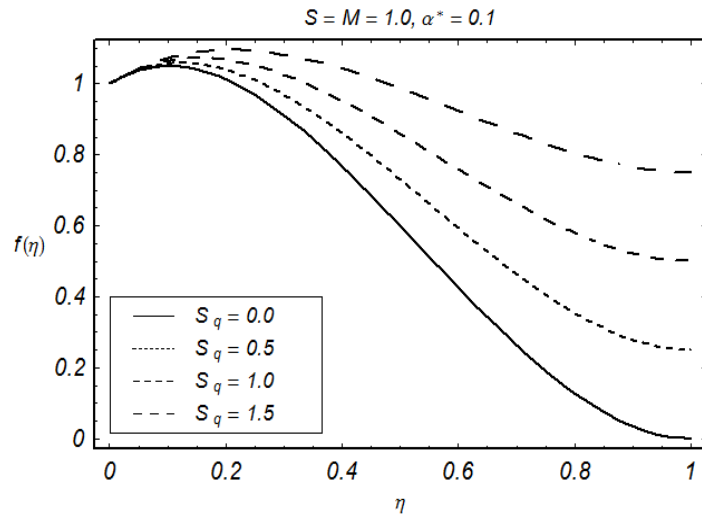
Fig. 8.7: Influence of S_q on f'.
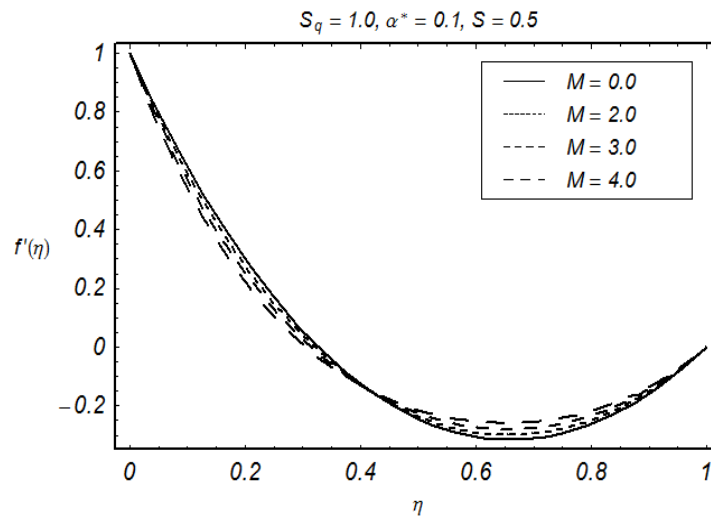
Fig. 8.8: Influence of S_q on f.

Fig. 8.9: Influence of M on f'.
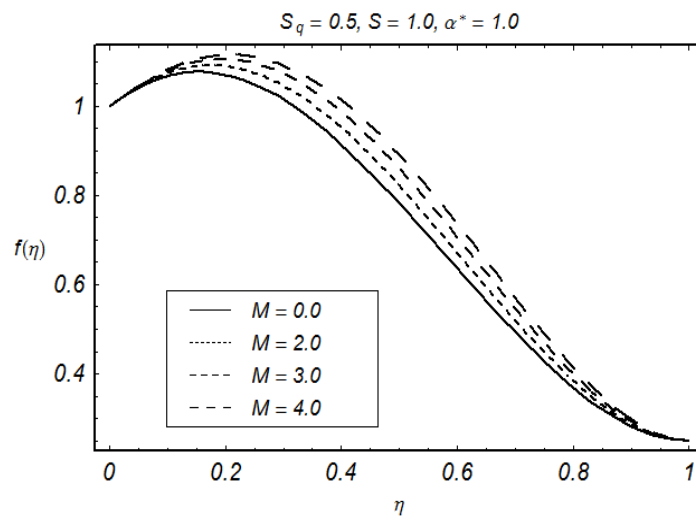
Fig. 8.10: Influence of M on f.

Fig. 8.11: Influence of α^* on f'.
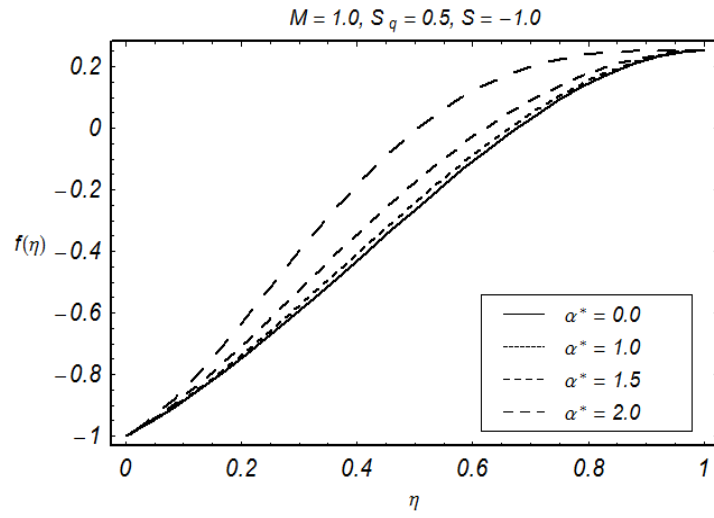
Fig. 8.12: Influence of α^* on f.

Fig. 8.13: Influence of S_q on f'.

Fig. 8.14: Influence of S_q on f.

Fig. 8.15: Influence of M on f'.
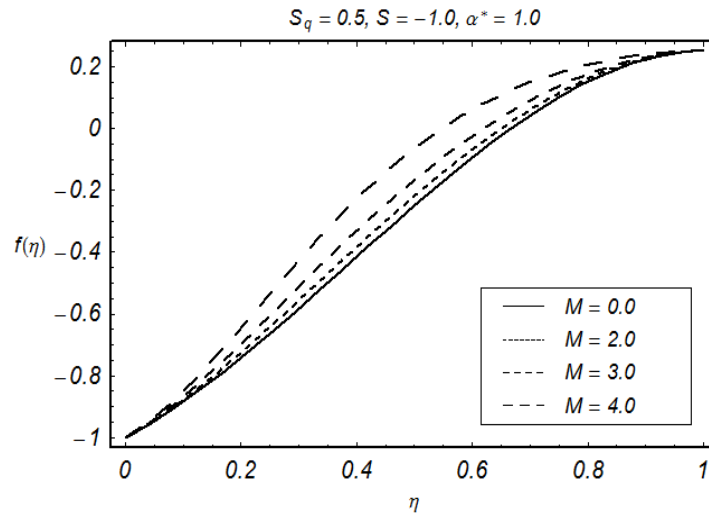
Fig. 8.16: Influence of M on f.
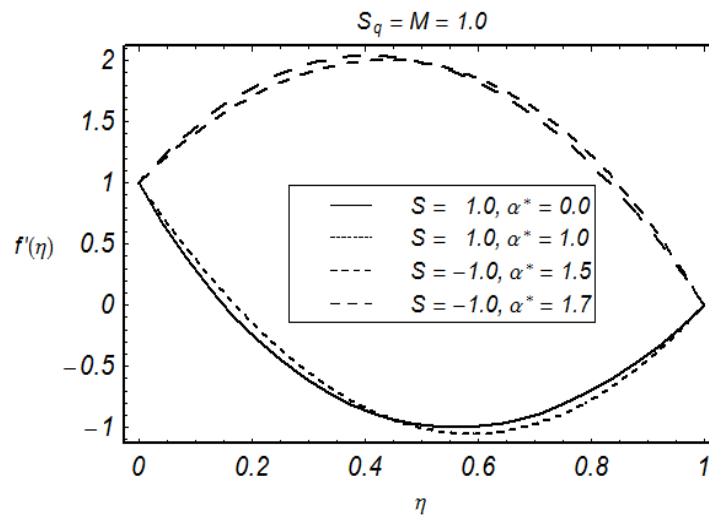
Fig. 8.17: Influence of α^* on f'.
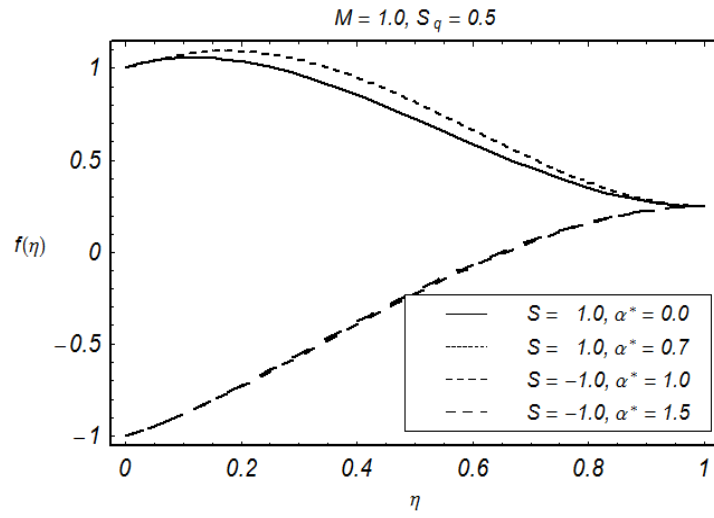
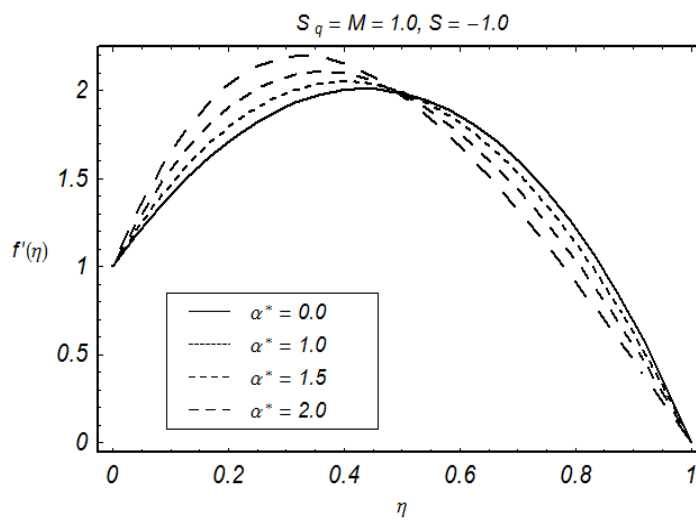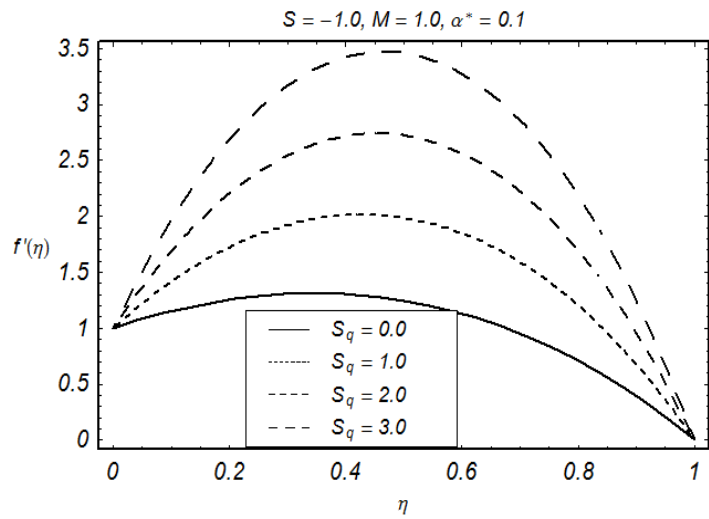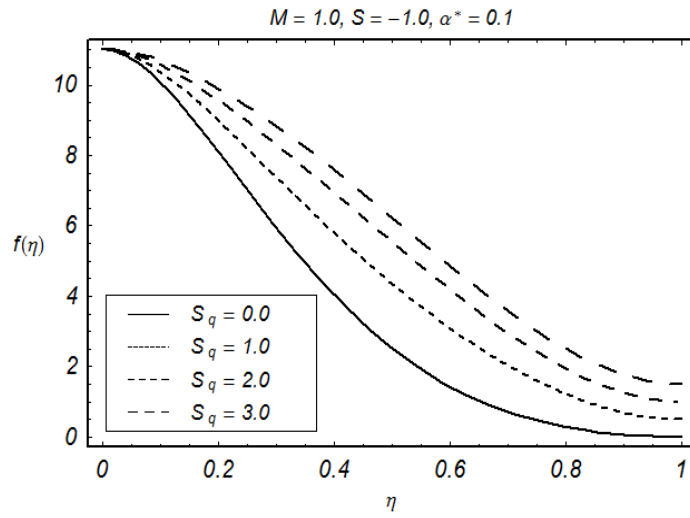Fig. 8.18: Influence of α^* on f.
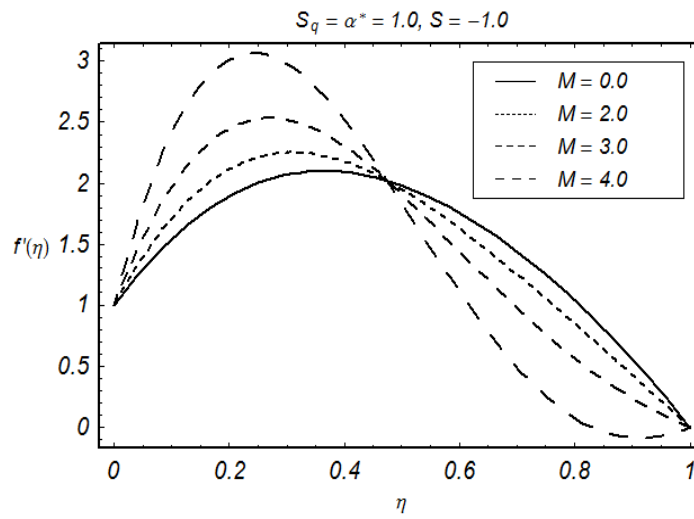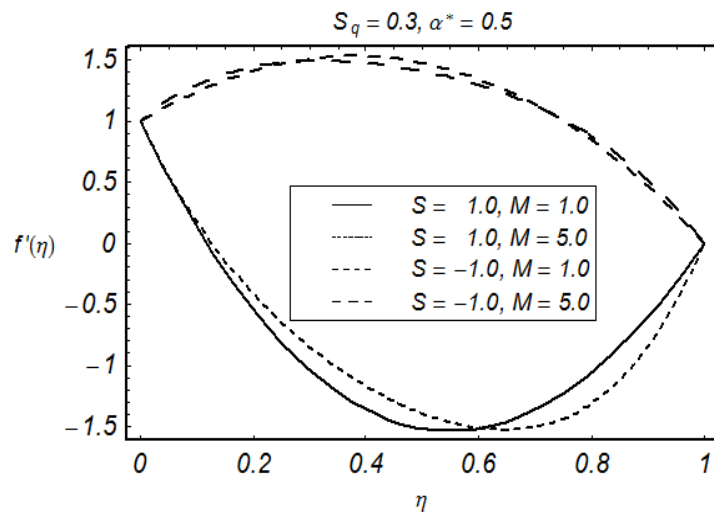

Fig. 8.19: Influence of M on f'.
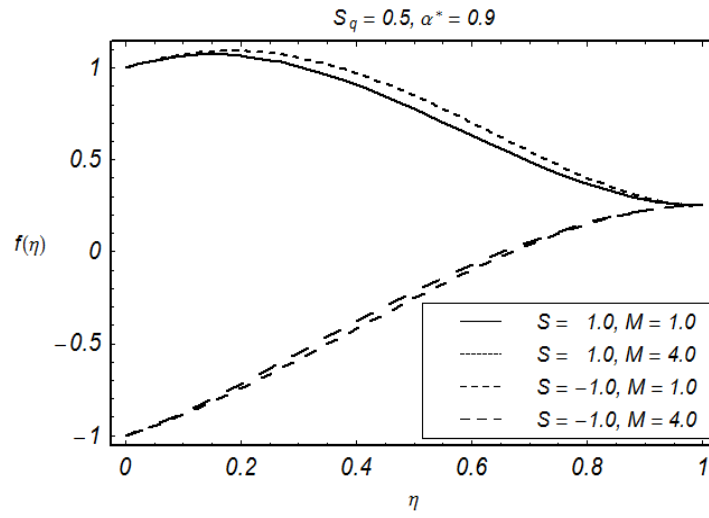
Fig. 8.20: Influence of M on f.
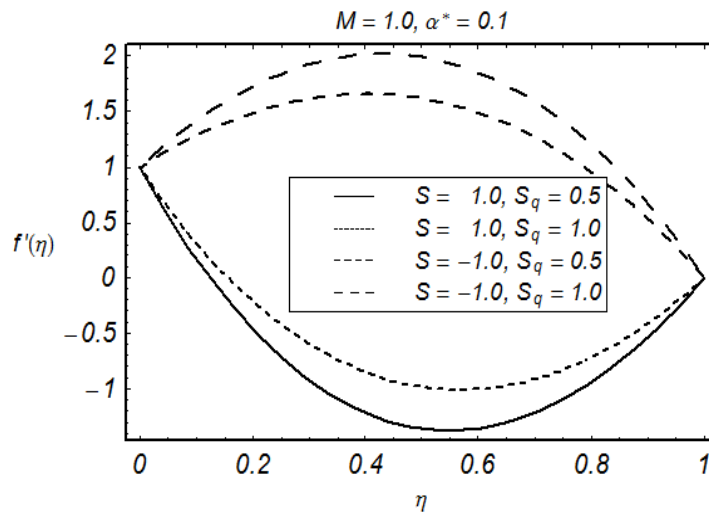
Fig. 8.21: Influence of S_q on f'.

126
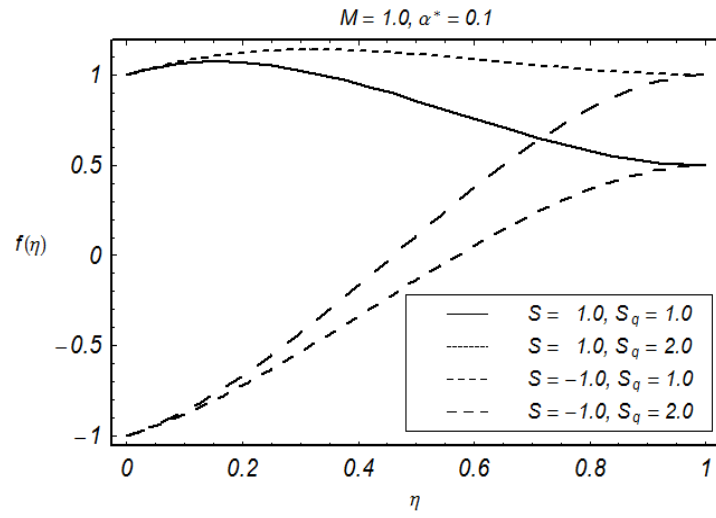
Fig. 8.22: Influence of S_q on f.

Table 8.2. Values of skin friction coefficient for different values of S, S_q, M and α^*.

S	S_q	M	β	$2R_e^{\frac{1}{2}}C_f$
-0.5	0.5	0.3	0.1	-3.040855
0.1				1.177707
0.3				2.518978
0.5				3.824939
0.1	0.0	0.3	0.1	2.522514
	0.2			2.044922
	0.3			1.775929
	0.5			1.177707
	0.6			0.848527
0.1	0.5	0.0	0.1	1.181439
		0.1		1.181024
		0.3		1.177707
		0.5		1.171101
		0.6		1.166581
0.1	0.5	0.3	0.00	1.008879
			0.01	1.025835
			0.03	1.059691
			0.05	1.093479
			0.08	1.144053
			0.09	1.160886

8.4 Key findings

The squeezing flow of second grade fluid is studied in this chapter. The main outcomes are as follows:

- The second grade parameter α^* has opposite effects on the velocity profile $f'(\eta)$ in both suction and injection cases.

- Vertical velocity $f(\eta)$ for suction and injection has opposite behavior when second grade parameter α^* is increased .

- Horizontal velocity $f'(\eta)$ decreases while vertical velocity $f(\eta)$ increases with the increase of suction parameter.

- Horizontal and vertical velocities have opposite effects for suction and injection when Hartman number is increased.

- Larger values of suction parameter S and second grade parameter α^*, the skin friction coefficient increases while it decreases by increasing the squeezing parameter S_q and M.

Chapter 9

MHD squeezing flow of second grade fluid with thermal-diffusion and diffusion-thermo effects

The combined effects of heat and mass transfer in the magnetohydrodynamic (MHD) squeezing flow of second grade fluid between the two parallel plates are investigated. Simultaneous effects of thermal-diffusion (Soret), diffusion-thermo (Dufour) and viscous dissipation are considered. Suitable variables are utilized for the conversion of partial differential system into an ordinary differential system. Series solution is obtained by homotopy analysis method (HAM). Various physical results are shown to present the effects of involved sundry parameters. A comparative study with the already published results shows an excellent agreement.

9.1   Mathematical analysis

We examine the heat and mass transfer analyses in the time-dependent squeezing flow of an incompressible second grade fluid. Thermal diffusion (Soret) and diffusion thermo (Dufour) effects have been considered. Fluid is electrically conducting in the presence of constant magnetic field B_0. The flow is bounded by two parallel plates at $z = \pm H \left(1 - at\right)^{\frac{1}{2}} = \pm h(t)$. Note that $a > 0$ corresponds to the squeezing of two plates whereas $a < 0$ means the separation of the plates. The governing flow problem is modeled in the presence of viscous dissipation.

Mass transfer is also considered in the presence of first order chemical reaction. The governing equations from the laws of conservation of mass, linear momentum, energy and concentration are given by

$$\frac{\partial u}{\partial x} + \frac{\partial v}{\partial y} = 0, \tag{9.1}$$

$$\frac{\partial u}{\partial t} + u\frac{\partial u}{\partial x} + v\frac{\partial u}{\partial y} = -\frac{1}{\rho}\frac{\partial p}{\partial x} + \nu\left[\frac{\partial^2 u}{\partial x^2} + \frac{\partial^2 u}{\partial y^2}\right] - \frac{\sigma}{\rho(1-at)}B_0^2 u \tag{9.2}$$

$$+\frac{\alpha_1}{\rho}\left[\begin{array}{c} \frac{\partial^3 u}{\partial t\partial x^2} + \frac{\partial^3 u}{\partial t\partial y^2} + 2\frac{\partial v}{\partial y}\frac{\partial^2 v}{\partial x\partial y} + 2\frac{\partial v}{\partial x}\frac{\partial^2 v}{\partial x^2} + u\left(\frac{\partial^3 u}{\partial x^3} + \frac{\partial^3 u}{\partial x\partial y^2}\right) \\ +v\left(\frac{\partial^3 u}{\partial x^2\partial y} + \frac{\partial^3 u}{\partial y^3}\right) + \frac{\partial u}{\partial x}\left(3\frac{\partial^2 u}{\partial x^2} + \frac{\partial^2 u}{\partial y^2}\right) + \frac{\partial u}{\partial y}\left(\frac{\partial^2 u}{\partial x\partial y} + \frac{\partial^2 v}{\partial x^2}\right) \end{array}\right], \tag{9.3}$$

$$\frac{\partial v}{\partial t} + u\frac{\partial v}{\partial x} + v\frac{\partial v}{\partial y} = -\frac{1}{\rho}\frac{\partial p}{\partial y} + \nu\left[\frac{\partial^2 v}{\partial x^2} + \frac{\partial^2 v}{\partial y^2}\right]$$

$$+\frac{\alpha_1}{\rho}\left[\begin{array}{c} \frac{\partial^3 v}{\partial t\partial x^2} + \frac{\partial^3 v}{\partial t\partial y^2} + 2\frac{\partial u}{\partial y}\frac{\partial^2 u}{\partial y^2} + u\left(\frac{\partial^3 v}{\partial x^3} + \frac{\partial^3 v}{\partial x\partial y^2}\right) \\ +v\left(\frac{\partial^3 v}{\partial y^3} + \frac{\partial^3 v}{\partial x^2\partial y}\right) + \frac{\partial v}{\partial x}\left(\frac{\partial^2 u}{\partial y^2} + \frac{\partial^2 v}{\partial x\partial y}\right) + \frac{\partial v}{\partial y}\left(\frac{\partial^2 v}{\partial x^2} + 3\frac{\partial^2 v}{\partial y^2}\right) \end{array}\right], \tag{9.4}$$

$$\frac{\partial T}{\partial t} + u\frac{\partial T}{\partial x} + v\frac{\partial T}{\partial y} = \frac{K_c}{\rho c_p}\left(\frac{\partial^2 T}{\partial x^2} + \frac{\partial^2 T}{\partial y^2}\right) + \frac{\nu}{c_p}\left[4\left(\frac{\partial u}{\partial x}\right)^2 + \left(\frac{\partial u}{\partial y} + \frac{\partial v}{\partial x}\right)^2\right]$$

$$-\frac{\alpha_1}{\rho c_p}\left[\frac{\partial v}{\partial x}\left(-\frac{\partial^2 u}{\partial y\partial t} - v\frac{\partial^2 u}{\partial y^2}\right) - \frac{\partial v}{\partial x}\left(u\frac{\partial^2 u}{\partial x\partial y} + v\frac{\partial^2 v}{\partial x\partial y} + u\frac{\partial^2 v}{\partial x^2} + \frac{\partial^2 v}{\partial x\partial t}\right)\right.$$

$$-2\frac{\partial u}{\partial x}\left(\frac{\partial^2 u}{\partial x\partial t} + v\frac{\partial^2 u}{\partial x\partial y} + u\frac{\partial^2 u}{\partial x^2}\right) - 2\frac{\partial v}{\partial y}\left(\frac{\partial^2 v}{\partial y\partial t} + v\frac{\partial^2 v}{\partial y^2} + u\frac{\partial^2 v}{\partial x\partial y}\right)$$

$$\left.-\frac{\partial u}{\partial y}\left\{\frac{\partial^2 u}{\partial y\partial t} + \frac{\partial^2 v}{\partial x\partial t} + v\left(\frac{\partial^2 u}{\partial y^2} + \frac{\partial^2 v}{\partial x\partial y}\right) + u\left(\frac{\partial^2 u}{\partial x\partial y} + \frac{\partial^2 v}{\partial x^2}\right)\right\}\right]$$

$$+\frac{DK_T}{C_s c_p}\left(\frac{\partial^2 C}{\partial x^2} + \frac{\partial^2 C}{\partial y^2}\right), \tag{9.5}$$

$$\frac{\partial C}{\partial t} + u\frac{\partial C}{\partial x} + v\frac{\partial C}{\partial y} = D\left(\frac{\partial^2 C}{\partial x^2} + \frac{\partial^2 C}{\partial y^2}\right) - K_1(t)C + \frac{DK_T}{T_m}\left(\frac{\partial^2 T}{\partial x^2} + \frac{\partial^2 T}{\partial y^2}\right), \tag{9.6}$$

where u denotes the velocity in the $x-$direction, v the velocity in the $y-$direction and T, C, p, ρ, ν, K_c, C_p, D, T_m, K_T and $K_1(t) = \frac{k_1}{1-at}$ are the temperature, the concentration, the pressure, the fluid density, the kinematic viscosity, the thermal conductivity, the specific heat, the coefficient of mass diffusivity, mean fluid temperature, thermal diffusion ratio and the time-dependent reaction rate respectively.

The boundary conditions can be expressed as follows:

$$u = 0, \ v = v_w = \frac{dh}{dt}, \ T = T_H, \ C = C_H \ \text{at} \ y = h(t),$$

$$v = \frac{\partial u}{\partial y} = \frac{\partial T}{\partial y} = \frac{\partial C}{\partial y} = 0 \quad \text{at} \ y = 0. \tag{9.7}$$

Eliminating pressure gradient from Eqs. (9.2) and (9.3) and using the transformations

$$\eta = \frac{y}{H\sqrt{1-at}}, \ u = \frac{ax}{2(1-at)}f'(\eta), \ v = \frac{-aH}{2\sqrt{1-at}}f(\eta),$$

$$\theta = \frac{T}{T_H}, \ \phi = \frac{C}{C_H} \tag{9.8}$$

we get

$$f^{(iv)} - S_q(\eta f''' + 3f'' + f'f'' - ff''')$$

$$+\frac{\beta}{2}\left(\eta f^{(v)} + 5f^{(iv)} + f'f^{(iv)} - ff^{(v)}\right) - M^2 f'' = 0, \tag{9.9}$$

$$\theta'' + PrS_q\left(f\theta' - \eta\theta'\right) + PrEc\left(f''^2 + 4\delta^2 f'^2\right)$$

$$+\frac{PrEc\beta}{2}\left\{-3f''^2 - f'f''^2 - \eta f'''f'' + ff''f'''\right.$$

$$\left.-\delta\left(-2f'^2 - \eta f'f'' + ff'f''\right)\right\}, \tag{9.10}$$

$$\phi'' + ScS_q\left(f\phi' - \eta\phi'\right) + Sc\gamma\phi + SrSc\theta'' = 0, \tag{9.11}$$

$$f(0) = 0, \ f(1) = 1, \ f'(1) = 0, \ f''(0) = 0,$$

$$\theta(1) = 1 = \phi(1), \ \theta'(0) = 0 = \phi'(0), \tag{9.12}$$

where the squeezing parameter S_q, the second grade parameter α^*, the Prandtl number Pr, the Eckert number Ec, the Schmidt number Sc, the chemical reaction parameter γ, the Hartman

number M, the Soret number Sr and the Dufour number Df have the following definitions:

$$
\begin{aligned}
S_q &= \frac{aH^2}{2\nu}, \qquad \alpha^* = \frac{a\alpha_1}{\mu(1-at)}, \qquad Pr = \frac{\mu c_p}{K_c}, \\
Ec &= \frac{1}{T_H C_p}\left(\frac{ax}{2(1-at)}\right)^2, \quad Sc = \frac{\nu}{D}, \quad \gamma = \frac{k_1 H^2}{\nu}, \quad \delta^2 = \frac{H^2(1-at)}{x^2}, \\
M^2 &= \frac{\sigma B_0^2}{\rho a}, \quad Sr = \frac{DK_T T_H}{\nu C_H T_m}, \quad Df = \frac{DK_T C_H}{\nu c_p C_s T_H}.
\end{aligned}
\tag{9.13}
$$

Note that the plate movement is described by the squeezing parameter S_q. When $S_q > 0$, the plates are moving away from each other and when $S_q < 0$, the plates are moving towards each other. For $Ec = 0$, the viscous dissipation effect are absent. Moreover $\gamma > 0$ represents the destructive chemical reaction and $\gamma < 0$ characterizes the generative chemical reaction. Here $\alpha^* = 0$ corresponds to the viscous fluid case. The skin friction coefficient, Nusselt number and Sherwood numbers are given by

$$
C_f = \frac{(\tau_{xy})_{y=h(t)}}{\rho v_w^2}, \quad Nu = \frac{-HK_c\left(\frac{\partial T}{\partial y}\right)_{y=h(t)}}{K_c T_H}, \quad Sh = \frac{-HD_m\left(\frac{\partial C}{\partial y}\right)_{y=h(t)}}{D_m C_H}.
\tag{9.14}
$$

Using Eq. (9.7) in Eq. (9.13) we get

$$
\begin{aligned}
\frac{H^2}{x^2}(1-at)\operatorname{Re}_x C_f &= f''(1) + \frac{\alpha^*}{2}\left[f'''(1) + 3f''(1) + 3f'(1)f''(1) - f(1)f'''(1)\right], \\
\sqrt{1-at}\,Nu &= -\theta'(1), \quad \sqrt{1-at}\,Sh = \phi'(1).
\end{aligned}
\tag{9.15}
$$

9.2   Solution of the problem

9.2.1   Zeroth order deformation problems

We express $f(\eta)$, $\theta(\eta)$ and $\phi(\eta)$ are expressed by a set of base functions

$$
\left\{\eta^k \mid k \geq 0\right\}
\tag{9.16}
$$

in the forms

$$
f(\eta) = \sum_k a_k \eta^{2k+1}, \quad \theta(\eta) = \sum_k b_k \eta^{2k+1}, \quad \phi(\eta) = \sum_k c_k \eta^{2k+1}
\tag{9.17}
$$

in which a_k, b_k and c_k are the coefficients. The initial guesses $f_0(\eta)$, $\theta_0(\eta)$, $\phi_0(\eta)$ and the auxiliary operators $\mathcal{L}_f$, $\mathcal{L}_\theta$, $\mathcal{L}_\phi$ are chosen in the forms:

$$f_0(\eta) = \frac{1}{2}\left(3\eta - \eta^3\right),\ \theta_0(\eta) = 1,\ \phi_0(\eta) = 1, \tag{9.18}$$

$$\mathcal{L}_f = f^{(iv)},\ \mathcal{L}_\theta = \theta'',\ \mathcal{L}_\phi = \phi''. \tag{9.19}$$

The operators $\mathcal{L}_f$, $\mathcal{L}_\theta$ and $\mathcal{L}_\phi$ have the properties

$$\mathcal{L}_f\left(C_1 + C_2\eta + C_3\eta^2 + C_4\eta^3\right) = 0,\ \mathcal{L}_\theta\left(C_5 + C_6\eta\right) = 0,\ \mathcal{L}_\phi\left(C_7 + C_8\eta\right) = 0, \tag{9.20}$$

where $C_i(i = 1 - 8)$ are the arbitrary constants and the nonlinear operators are

$$\mathcal{N}_f\left[\bar{f}(\eta, q)\right] = \frac{\partial^4 \bar{f}}{\partial \eta^4} - S_q\left(\eta\frac{\partial^3 \bar{f}}{\partial \eta^3} + 3\frac{\partial^2 \bar{f}}{\partial \eta^2} + \frac{\partial \bar{f}}{\partial \eta}\frac{\partial^2 \bar{f}}{\partial \eta^2} - \bar{f}\frac{\partial^3 \bar{f}}{\partial \eta^3}\right) - M^2\frac{\partial^2 \bar{f}}{\partial \eta^2}$$
$$+ \frac{\alpha^*}{2}\left[\eta\frac{\partial^5 \bar{f}}{\partial \eta^5} + 5\frac{\partial^4 \bar{f}}{\partial \eta^4} + \frac{\partial \bar{f}}{\partial \eta}\frac{\partial^4 \bar{f}}{\partial \eta^4} - \bar{f}\frac{\partial^5 \bar{f}}{\partial \eta^5}\right], \tag{9.21}$$

$$\mathcal{N}_\theta\left[\bar{f}(\eta, q), \bar{\theta}(\eta, q), \bar{\phi}(\eta, q)\right] = \frac{\partial^2 \bar{\theta}}{\partial \eta^2} + PrS_q\left(\bar{f}\frac{\partial \bar{\theta}}{\partial \eta} - \eta\frac{\partial \bar{\theta}}{\partial \eta}\right) + PrEc\left[\left(\frac{\partial^2 \bar{f}}{\partial \eta^2}\right)^2 + 4\delta^2\left(\frac{\partial \bar{f}}{\partial \eta}\right)^2\right]$$

$$+ \frac{PrEc\alpha^*}{2}\left[-3\left(\frac{\partial^2 \bar{f}}{\partial \eta^2}\right)^2 - \frac{\partial \bar{f}}{\partial \eta}\left(\frac{\partial^2 \bar{f}}{\partial \eta^2}\right)^2 - \eta\frac{\partial^3 \bar{f}}{\partial \eta^3}\frac{\partial^2 \bar{f}}{\partial \eta^2} + \bar{f}\frac{\partial^2 \bar{f}}{\partial \eta^2}\frac{\partial^3 \bar{f}}{\partial \eta^3}\right. \tag{9.22}$$

$$\left. - \delta\left\{-2\left(\frac{\partial \bar{f}}{\partial \eta}\right)^2 - \eta\frac{\partial \bar{f}}{\partial \eta}\frac{\partial^2 \bar{f}}{\partial \eta^2} + \bar{f}\frac{\partial \bar{f}}{\partial \eta}\frac{\partial^2 \bar{f}}{\partial \eta^2}\right\}\right] + PrDf\frac{\partial^2 \bar{\phi}}{\partial \eta^2}, \tag{9.23}$$

$$\mathcal{N}_\phi\left[\bar{f}(\eta, q), \bar{\theta}(\eta, q), \bar{\phi}(\eta, q)\right] = \frac{\partial^2 \bar{\phi}}{\partial \eta^2} + ScS_q\left(\bar{f}\frac{\partial \bar{\phi}}{\partial \eta} - \eta\frac{\partial \bar{\phi}}{\partial \eta}\right) + Sc\gamma\bar{\phi} + SrSc\frac{\partial^2 \bar{\theta}}{\partial \eta^2}. \tag{9.24}$$

The zeroth order problems have the following statements:

$$(1 - q)\mathcal{L}_f\left[\bar{f}(\eta, q) - F_0(\eta)\right] = q\hbar_f\mathcal{N}_f\left[\bar{f}(\eta, q)\right], \tag{9.25}$$

$$\bar{f}(0, q) = S,\ \bar{f}'(0, q) = 1,\ \bar{f}(1, q) = \frac{S_q}{2},\ \bar{f}'(1, q) = 0, \tag{9.26}$$

$$(1-q)\,\mathcal{L}_\theta\left[\bar{\theta}\left(\eta,q\right)-\theta_0\left(\eta\right)\right]=q\hbar_\theta\mathcal{N}_\theta\left[\bar{f}(\eta,q),\bar{\theta}(\eta,p),\bar{\phi}(\eta,q)\right], \tag{9.27}$$

$$\bar{\theta}'\left(0,q\right)=0,\bar{\theta}\left(1,q\right)=1, \tag{9.28}$$

$$(1-q)\,\mathcal{L}_\phi\left[\bar{\phi}\left(\eta,q\right)-\phi_0\left(\eta\right)\right]=q\hbar_\phi\mathcal{N}_\phi\left[\bar{f}(\eta,q),\bar{\theta}(\eta,q),\bar{\phi}(\eta,q)\right], \tag{9.29}$$

$$\bar{\phi}'\left(0,q\right)=0,\bar{\phi}\left(1,q\right)=1, \tag{9.30}$$

where $\hbar_f$, $\hbar_\theta$ and $\hbar_\phi$ denote the auxiliary parameters and $0 \leq q \leq 1$ shows embedding parameter. It is observed that when q changes from 0 to 1, then $f(\eta,q)$, $\theta(\eta,q)$ and $\phi(\eta,q)$ vary from $f_0\left(\eta\right)$ to $f(\eta)$, $\theta_0\left(\eta\right)$ to $\theta(\eta)$ and $\phi_0\left(\eta\right)$ to $\phi(\eta)$. When $q=0$ and $q=1$, one obtains

$$\begin{aligned}
\bar{f}(\eta,0) &= f_0(\eta),\ \bar{f}(\eta,1)=f(\eta), \tag{9.31}\\
\bar{\theta}(\eta,0) &= \theta_0(\eta),\ \bar{\theta}(\eta,1)=\theta(\eta), \tag{9.32}\\
\bar{\phi}(\eta,0) &= \phi_0(\eta),\ \bar{\phi}(\eta,1)=\phi(\eta). \tag{9.33}
\end{aligned}$$

Taylor series for $f(\eta)$, $\theta(\eta)$ and $\phi(\eta)$ yields

$$\begin{aligned}
f(\eta) &= f_0(\eta)+\sum_{m=1}^{\infty}f_m(\eta)q^m,\ f_m(\eta)=\frac{1}{m!}\left.\frac{\partial^m\bar{f}(\eta,q)}{\partial q^m}\right|_{q=0}, \tag{9.34}\\
\theta(\eta) &= \theta_0(\eta)+\sum_{m=1}^{\infty}\theta_m(\eta)q^m,\ \theta_m(\eta)=\frac{1}{m!}\left.\frac{\partial^m\bar{\theta}(\eta,q)}{\partial q^m}\right|_{q=0}, \tag{9.35}\\
\phi(\eta) &= \phi_0(\eta)+\sum_{m=1}^{\infty}\phi_m(\eta)q^m,\ \phi_m(\eta)=\frac{1}{m!}\left.\frac{\partial^m\bar{\phi}(\eta,q)}{\partial q^m}\right|_{q=0}. \tag{9.36}
\end{aligned}$$

The convergence of the series solutions are dependent upon $\hbar_f$, $\hbar_\theta$ and $\hbar_\phi$. We choose $\hbar_f$, $\hbar_\theta$ and $\hbar_\phi$ in such a way that the series $(9.33-9.35)$ converge at $q=1$ and hence

$$\begin{aligned}
f(\eta) &= f_0(\eta)+\sum_{m=1}^{\infty}f_m(\eta), \tag{9.37}\\
\theta(\eta) &= \theta_0(\eta)+\sum_{m=1}^{\infty}\theta_m(\eta), \tag{9.38}\\
\phi(\eta) &= \phi_0(\eta)+\sum_{m=1}^{\infty}\phi_m(\eta). \tag{9.39}
\end{aligned}$$

135

9.2.2 mth-order deformation problems

The mth-order deformation equations are found by differentiating the equations (9.24), (9.26)and (9.28) with respect to q ($m-$times) and then putting $q = 0$ we obtain:

$$\mathcal{L}_f \left[f_m(\eta) - \chi_m f_{m-1}(\eta) \right] = \hbar_f \mathcal{R}_m^f(\eta),$$
$$f_m(0) = f_m'(0) = f_m(1) = f_m'(1) = 0, \tag{9.40}$$

$$\mathcal{L}_\theta \left[\theta_m(\eta) - \chi_m \theta_{m-1}(\eta) \right] = \hbar_\theta \mathcal{R}_m^\theta(\eta),$$
$$\theta_m'(0) = 0, \ \theta_m(1) = 0 \tag{9.41}$$

$$\mathcal{L}_\phi \left[\phi_m(\eta) - \chi_m \phi_{m-1}(\eta) \right] = \hbar_\phi \mathcal{R}_m^\phi(\eta),$$
$$\phi_m'(0) = 0, \ \phi_m(1) = 0, \tag{9.42}$$

$$\chi_m = \begin{cases} 0, & m \leq 1, \\ 1, & m > 1, \end{cases}$$

$$\mathcal{R}_m^f(\eta) = f_{m-1}^{(iv)} - M^2 f_{m-1}'' - \frac{S_q}{2} \left[\eta f_{m-1}''' + 3 f_{m-1}'' - \frac{\alpha^*}{2} \left(\eta f_{m-1}^{(v)} + 5 f_{m-1}^{(iv)} \right) \right]$$
$$+ \sum_{k=0}^{m-1} \left\{ \frac{\alpha^*}{2} \left(f_{m-1-k}' f_k^{(iv)} - f_{m-1-k} f_k^{(v)} \right) - f_{m-1-k}' f_k'' + f_{m-1-k} f_k''' \right\}, \tag{9.43}$$

$$\mathcal{R}_m^\theta(\eta) = \theta_{m-1}'' - Pr S_q \eta \theta_{m-1}' + Pr Df \phi_{m-1}''$$
$$+ \sum_{k=0}^{m-1} \left[Pr S_q f_{m-1-k} \theta_k' + Pr Ec \left(f_{m-1-k}'' f_k'' + 4\delta^2 f_{m-1-k}' f_k' \right) \right.$$
$$+ \frac{Pr Ec \alpha^*}{2} \left\{ -3 f_{m-1-k}'' f_k'' - \eta f_{m-1-k}''' f_k'' - \delta \left(-2 f_{m-1-k}' f_k' - \eta f_{m-1-k}' f_k'' \right) \right.$$
$$\left. \left. - f_{m-1-k}' \sum_{l=0}^{k} f_{k-l}'' f_l'' + f_{m-1-k} \sum_{l=0}^{k} f_{k-l}'' f_l'' - \delta f_{m-1-k} \sum_{l=0}^{k} f_{k-l}' f_l'' \right\} \right], \tag{9.44}$$

$$\mathcal{R}_m^\phi(\eta) = \phi_{m-1}'' - ScS_q\eta\phi_{m-1}' + Sc\gamma\phi_{m-1} + SrSc\theta_{m-1}'' + ScS_q\sum_{k=0}^{m-1} f_{m-1-k}\phi_k'. \qquad (9.45)$$

The general solutions of equations (8.24) and (8.25) can be expressed as

$$f_m(\eta) = f_m^*(\eta) + C_1 + C_2\eta + C_3\eta^2 + C_4\eta^3, \qquad (9.46)$$

$$\theta_m(\eta) = \theta_m^*(\eta) + C_5 + C_6\eta, \qquad (9.47)$$

$$\phi_m(\eta) = \phi_m^*(\eta) + C_7 + C_8\eta, \qquad (9.48)$$

in which f_m^*, θ_m^* and ϕ_m^* represent the special solutions.

9.2.3 Convergence analysis

The convergence of the series solutions $(9.36 - 9.38)$ strongly depends upon the auxiliary parameters $(\hbar_f, \hbar_\theta$ and $\hbar_\phi)$ for the functions $(f, \theta$ and $\phi)$ respectively. These auxiliary parameters adjust the convergence of the obtained series solutions. Figs. $(9.1 - 9.3)$ show the $h-$curves of the functions f, θ and ϕ for $\alpha^* = 0.5$, $S_q = Pr = Ec = Sc = 1.0$, $Df = M = 0.2$, $Sr = 0.3$ and $\delta = 0.1$. The permissible values of these auxiliary parameters $\hbar_f$, $\hbar_\theta$ and $\hbar_\phi$ are $-0.6 \leq \hbar_f \leq -0.2$, $-0.61 \leq \hbar_\theta \leq -0.46$ and $-0.7 \leq \hbar_\phi \leq -0.35$ respectively. Table 9.1 is useful in making a guess that how much order of approximations are necessary for the convergent solutions. This table shows that the $6th$, $35th$ and $33th$ order of approximations are adequate

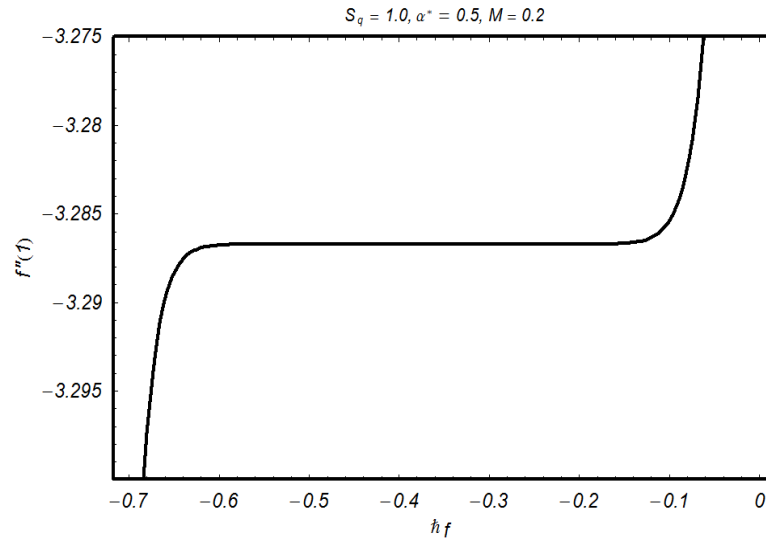for the convergent solutions of f, θ and ϕ respectively.

Fig. 9.1: Convergence region for the function f.
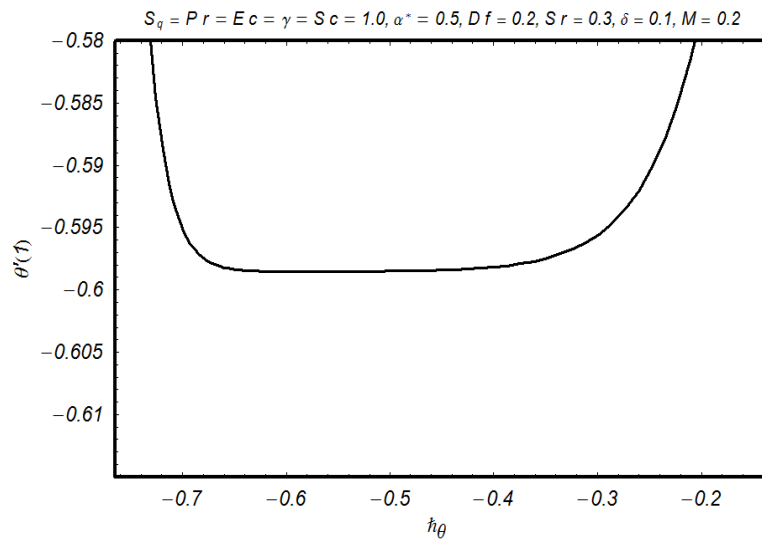
Fig. 9.2: Convergence region for the function θ.
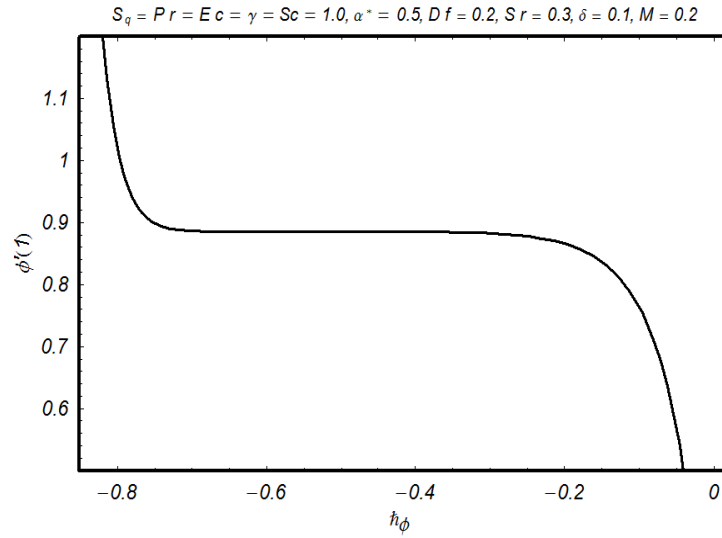
Fig. 9.3: Convergence region for the function ϕ.

Table 9.1. Series solution's convergence by HAM for different order of approximations when $\alpha^* = 0.5$, $M = 0.2$, $S_q = Pr = Ec = Sc = \gamma = 1.0$, $Df = 0.2$, $Sr = 0.3$ and $\delta = 0.1$.

Order of approximations	$-f''(1)$	$-\theta'(1)$	$\phi'(1)$
1	3.288914	0.157714	0.400000
5	3.286721	0.510613	0.805592
6	3.286720	0.540208	0.831707
10	3.286720	0.586933	0.874009
15	3.286720	0.596898	0.883754
25	3.286720	0.598494	0.885423
30	3.286720	0.598525	0.885457
33	3.286720	0.598529	0.885462
35	3.286720	0.598531	0.885462
40	3.286720	0.598531	0.885462
50	3.286720	0.598531	0.885462

9.3 Analysis

This section explains the influence of emerging physical parameters on the velocity, temperature and concentration profiles. For this purpose, we have plotted the Figs. $9.4 - 9.11$. In Figs. 9.4 and 9.5, we have discussed the influences of Hartman number (M) and squeezing parameter (S_q) on the velocity profile f'. From Fig. 9.4 it is clear that when we increase the Hartman number (M), the velocity profile decreases initially in the range $(0 \leq \eta \leq 0.45)$ and it increases after that $(0.45 \leq \eta \leq 1)$. Notice that when magnetic field is applied to any fluid then the apparent viscosity of the fluid increases to the point of becoming a viscoelastic solid. Magnetic field intensity can be used to adjust and control the fluid's yield stress as a result force transmission ability of the fluids increases/decreases. It is used in the practical life applications to design electromagnetic casting of metals, MHD power generation and MHD ion propulsion etc. Finally near the plate the magnetic field strength is greater which retards the flow and as the distance increases from the plate the magnetic field strength is weaker whereas the squeezing effects are dominant in that portion which finally causes an increase in velocity. From Fig. 9.5, it is seen that f' decreases when $0 \leq \eta \leq 0.45$ and it increases with the increase of S_q when $0.45 \leq \eta \leq 1$. Simultaneous effects of Soret (Sr) and Dufour (Df) on the temperature field (θ) and concentration (ϕ) are discussed in the Figs. 9.6 and 9.7 when the product of (Sr) and (Df) remains constant. We observed from these Figs. that the effects of (Sr) and (Df) are opposite. In Fig. 9.8 we discuss the effects of chemical reaction parameter (γ) on the concentration field ϕ. Higher values of destructive $(\gamma > 0)$ and generative $(\gamma < 0)$ chemical reaction parameters result in the reduction and enhancement of concentration field (ϕ) respectively. Concentration field at the lower plate is higher for constructive chemical reaction when compared with the destructive chemical reaction. Effects of Hartman number (M) on the temperature (θ) and concentration fields (ϕ) are discussed in the Figs. 9.9 and 9.10. The effects of Hartman number (M) on the temperature and concentration fields are quite opposite. Effects of Eckert number (Ec) on temperature is displayed in Fig. 9.11. There is an increase in temperature when Eckert number (Ec) increases. It is due to the fact that presence of viscous dissipation effects significantly increases the temperature (θ). Tables 9.2 and 9.3 are prepared to show the numerical values of skin friction coefficient, local Nusselt and Sherwood numbers for different physical parameters. From Table 9.2 it is noticed that when we increase the squeezing parameter (S_q), the

second grade parameter (α^*) and the Hartman number (M), the magnitude of the skin friction coefficient increases. The local Nusselt and local Sherwood numbers are decreased when the squeezing parameter (S_q) and the second grade parameter (α^*) increase while these increase with the increase of Hartman number (M). Numerical values of rate of heat transfer (local Nusselt number) and rate of mass transfer (local Sherwood number) for various parameters are discussed in Table 9.3. With the increase of Ec and γ the rate of heat and mass transfer increase. By increasing (Sr) and decreasing (Df), the local Nusselt number decreases but local Sherwood number increases. Table 9.4 is prepared to show a comparison for viscous case (Ref. [71]). This comparison confirms the validity of present flow analysis.
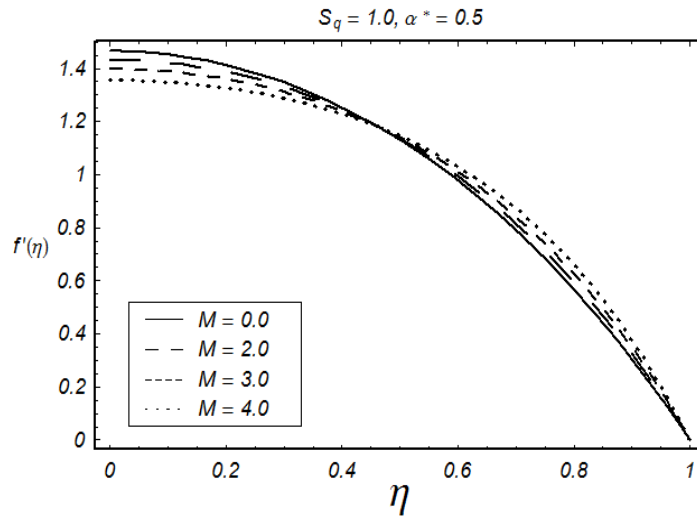
Fig. 9.4: Influence of M on $f'(\eta)$.
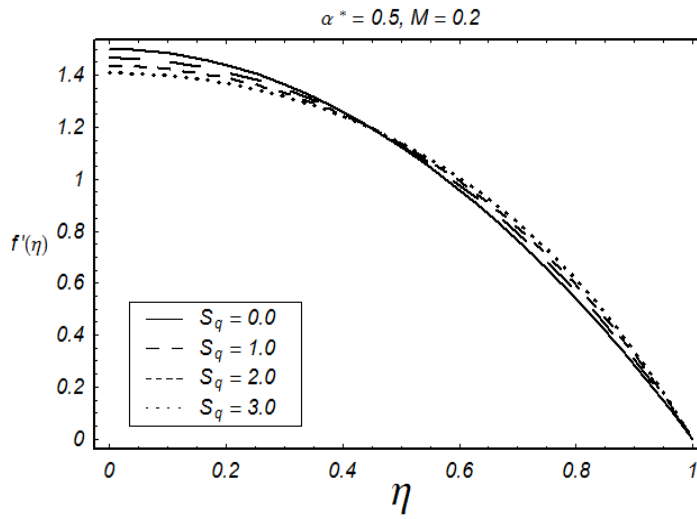
Fig. 9.5: Influence of S_q on $f'(\eta)$.
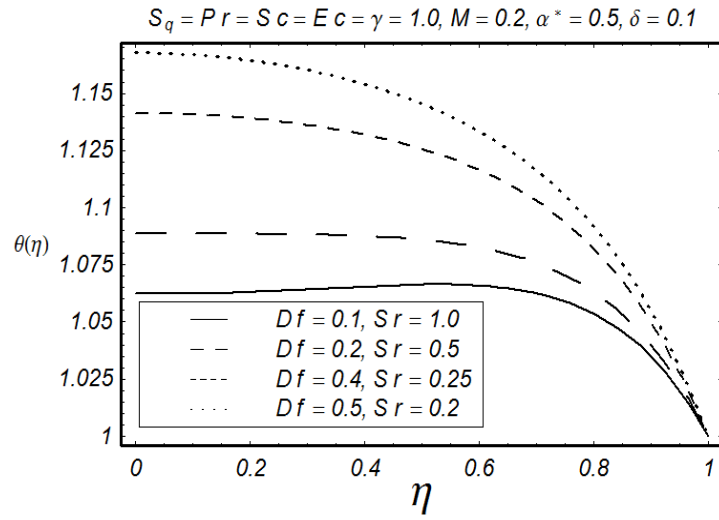
Fig. 9.6: Effects of Df and Sr on $\theta(\eta)$.

Fig. 9.7: Effects of Df and Sr on $\phi(\eta)$.

143

$S_q = P r = S c = E c = \gamma = 1.0, D f = M = 0.2, S r = 0.3, \alpha^* = 0.5, \delta = 0.1$

Fig. 9.8: Influence of γ on $\phi(\eta)$.

$S_q = P r = S c = E c = \gamma = 1.0, D f = S r = 0.2, \alpha^* = 0.5, \delta = 0.1$
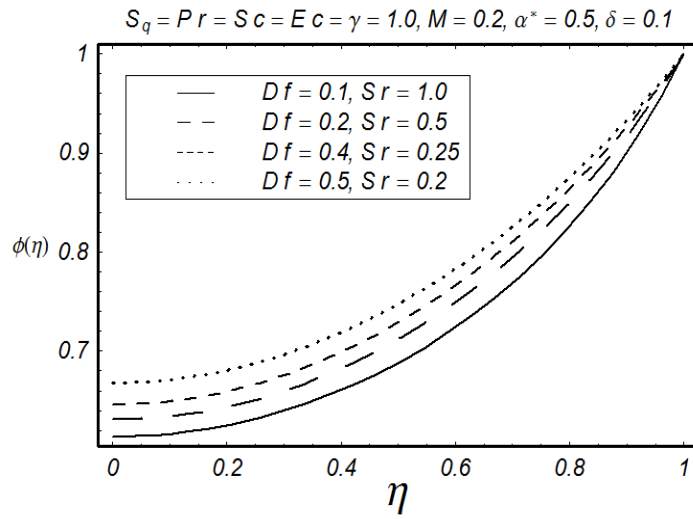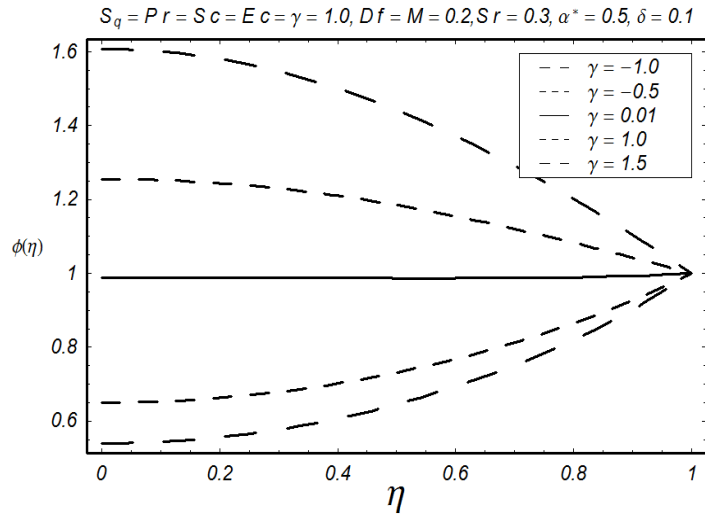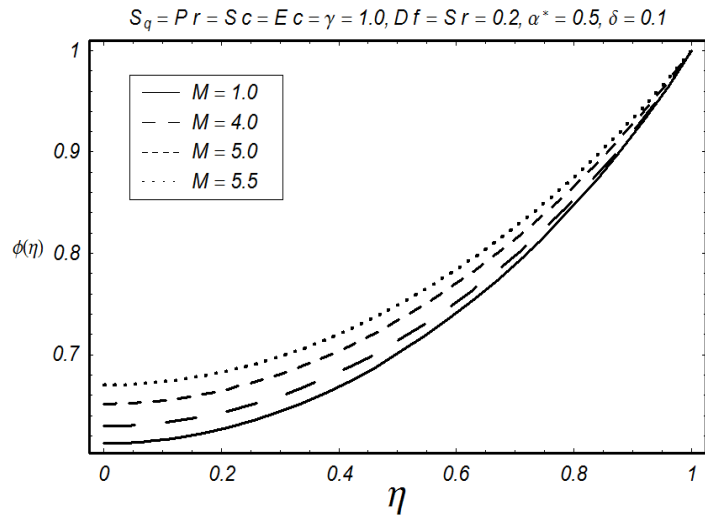
Fig. 9.9: Influence of M on $\phi(\eta)$.
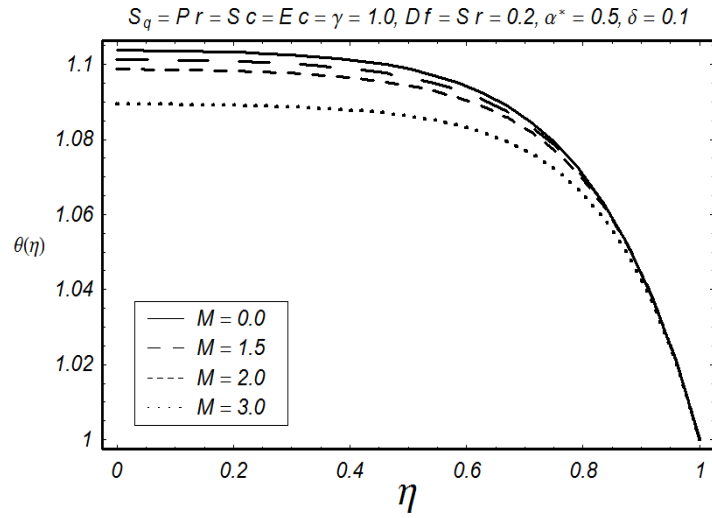
Fig. 9.10: Influence of M on $\theta(\eta)$.
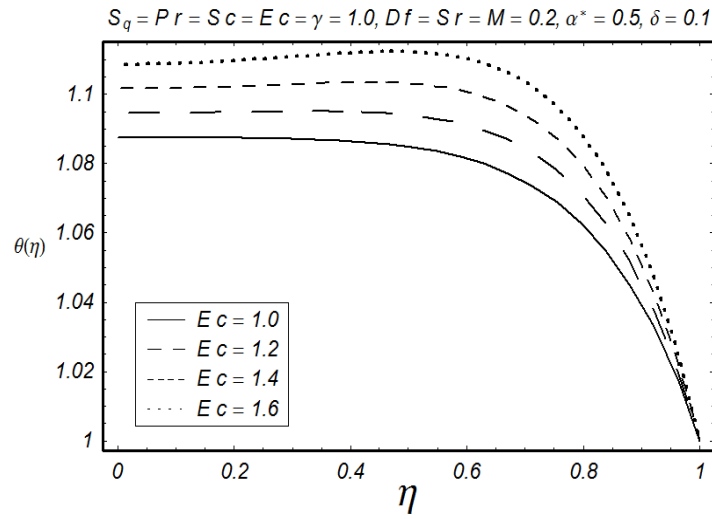
Fig. 9.11: Influence of Ec on $\theta(\eta)$.

145

Table 9.2. Values of skin friction coefficient, local Nusselt number and local Sherwood number for different values of S_q, α^* and M when $Pr = Ec = Sc = \gamma = 1.0$, $Df = 0.2$, $Sr = 0.3$ and $\delta = 0.1$.

S_q	α^*	M	$\frac{l^2(1-at)}{x^2}\,\mathrm{Re}_x\,C_f$	$-\theta'(1)$	$-\phi'(1)$
0.1	0.5	0.2	-5.307561	0.579811	-0.911588
0.5			-5.509490	0.588261	-0.899520
1.0			-5.751760	0.598530	-0.885463
1.5			-5.983845	0.608522	-0.872431
0.5	0.1	0.2	-3.762730	2.65571	-1.43215
	0.4		-5.067670	1.10424	-1.03162
	0.8		-6.843277	-0.959052	-0.504731
0.5	0.5	0.1	-5.505274	0.587931	-0.899418
		0.2	-5.509490	0.588262	-0.899521
		0.4	-5.526328	0.589576	-0.899926

Table 9.3. Values of local Nusselt number and local Sherwood number for different values of Ec, Df, Sr and γ when $S_q = Pr = Sc = 1.0$, $\alpha^* = 0.5$ and $M = 0.2$

Ec	Df	Sr	γ	$-\theta'(1)$	$-\phi'(1)$
0.3	0.2	0.3	1.0	0.279789	-0.796915
0.5				0.370857	-0.822213
0.9				0.552995	-0.872813
1.5				0.826203	-0.948711
1.0	0.1	0.2	1.0	0.726798	-0.859097
	0.025	0.8		0.674634	-1.22408
	0.02	1.0		0.671156	-1.34573
	0.01	2.0		0.664201	-1.95403
1.0	0.2	0.3	-0.5	0.576609	0.379749
			-0.3	0.625264	0.118924
			0.5	0.764753	-0.624207
			1.0	0.826203	-0.948711

Table 9.4. Comparison of skin friction coefficient, local Nusselt number and local Sherwood number when $\alpha^* = M = Df = Sr = 0$, $Pr = Ec = Sc = \gamma = 1.0$ and $\delta = 0.1$.

	Mustafa et al.[71]			Present		
S_q	$-f''(1)$	$-\theta'(1)$	$-\phi'(1)$	$-f''(1)$	$-\theta'(1)$	$-\phi'(1)$
-1.0	2.170090	3.319899	0.804558	2.17009087	3.31989927	0.80455875
-0.5	2.614038	3.129491	0.781402	2.61740384	3.12949108	0.78140233
0.01	3.007134	3.047092	0.761225	3.00713375	3.04709193	0.76122521
0.5	3.336449	3.026324	0.744224	3.33644946	3.02632354	0.74422428
2.0	4.167389	3.118551	0.701813	4.16738918	3.11855069	0.70181323

9.4 Concluding remarks

The combined effects of thermal-diffusion, diffusion-thermo, viscous dissipation and chemical reaction in MHD flow of second grade fluid between parallel plates are discussed. Computations

are analyzed for the nonlinear analysis. Main findings are mentioned below.

- Effects of Hartman number M and squeezing parameter S_q are similar in a qualitative sense.

- Temperature profile $\theta(\eta)$ increases throughout the domain with the increase of Soret and Dufour numbers.

- Temperature profile $\theta(\eta)$ is decreasing function of Hartman number M.

- Concentration profile $\phi(\eta)$ is an increasing function of Soret and Dufour numbers.

- Concentration field $\phi(\eta)$ is a decreasing function of destructive chemical reaction parameter $(\gamma > 0)$ and an increasing function of generative chemical reaction parameter $(\gamma < 0)$.

- Magnitude of the skin friction coefficient increases for larger squeezing parameter S_q, the second grade parameter α^* and the Hartman number M.

- The local Nusselt and local Sherwood numbers are decreased when the squeezing parameter S_q and the second grade parameter α^* increase. However Hartman number M leads to an increase in the local Nusselt and Sherwood number.

- With the increase of Ec and γ, the rate of heat and mass transfer increase. By increasing Sr and decreasing Df, the local Nusselt number decreases but local Sherwood number increases.

Chapter 10

Axisymmetric squeezing flow of third grade fluid

This chapter addresses the time-dependent flow of an incompressible third grade fluid between the squeezing disks. The relevant equations of thermodynamic compatible third grade fluid are modeled. The considered fluid model can predict the shear thinning and shear thickening effects even in study flow situation. Transformation procedure reduces the partial differential system to the ordinary differential system. Solution to the nonlinear problem is computed in series form. The presented graphical results illustrate the influence of emerging parameters in the considered problem.

10.1 Mathematical formulation and analysis

We consider axisymmetric flow of third grade fluid between two parallel disks separated by a distance $H(1 - at)^{\frac{1}{2}}$. The upper disk at $z = h(t) = H(1 - at)^{\frac{1}{2}}$ is moving with velocity $\frac{-aH(1-at)^{-\frac{1}{2}}}{2}$. The lower porous disk at $z = 0$ is fixed. In absence of body forces, the laws of conservation of mass and linear momentum are

$$\frac{\partial u}{\partial r} + \frac{u}{r} + \frac{\partial w}{\partial z} = 0, \tag{10.1}$$

$$\rho \frac{d\mathbf{V}}{dt} = \text{div } \mathbf{T}, \tag{10.2}$$

149

where the Cauchy stress tensor in third grade fluid is defined as

$$\mathbf{T} = -p\mathbf{I} + \mathbf{S}, \quad \mathbf{S} = \mu\mathbf{A}_1 + \alpha_1\mathbf{A}_2 + \alpha_2\mathbf{A}_1^2 + \beta_3(tr\mathbf{A}_1^2)\mathbf{A}_1, \tag{10.3}$$

with

$$\mathbf{A}_1 = \mathbf{L} + \mathbf{L}^T, \ \mathbf{A}_2 = \frac{d\mathbf{A}_1}{dt} + \mathbf{A}_1\mathbf{L} + \mathbf{L}^T\mathbf{A}_1, \ \mathbf{L} = \text{grad}\,\mathbf{V}, \tag{10.4}$$

in which d/dt denotes the material time differentiation, $\mathbf{A}_i$ $(i = 1, 2)$ first two Rivlin-Ericksen tensors, $\mathbf{V}$ the velocity field, u the velocity component along radial direction (r), w the velocity component along axial direction (z), ρ the fluid density, p the pressure, $\mathbf{I}$ the identity tensor, μ the dynamic viscosity and α_i $(i = 1, 2)$ and β_3 the material parameters of third grade fluid.

Using Eqs. (10.3) and (10.4) in Eq. (10.2), we have the following scalar equations

$$
\begin{aligned}
&\frac{\partial u}{\partial t} + u\frac{\partial u}{\partial r} + w\frac{\partial u}{\partial z} = -\frac{1}{\rho}\frac{\partial p}{\partial r} + \nu\left(\frac{\partial^2 u}{\partial r^2} + \frac{\partial^2 u}{\partial z^2} + \frac{1}{r}\frac{\partial u}{\partial r} - \frac{u}{r^2}\right) \\
&+ \frac{\alpha_1}{\rho}\left[2\frac{\partial^3 u}{\partial t\partial r^2} + \frac{2}{r}\frac{\partial^2 u}{\partial t\partial r} + \frac{\partial^3 u}{\partial t\partial z^2} + \frac{\partial^3 w}{\partial z\partial t\partial r} + u\left(2\frac{\partial^3 u}{\partial r^3} + \frac{2}{r}\frac{\partial^2 u}{\partial r^2} + \frac{\partial^3 u}{\partial r\partial z^2} + \frac{\partial^3 w}{\partial z\partial r^2}\right)\right. \\
&+ w\left(2\frac{\partial^3 u}{\partial z\partial r^2} + \frac{2}{r}\frac{\partial^2 u}{\partial z\partial r} + \frac{\partial^3 u}{\partial z^3} + \frac{\partial^3 w}{\partial r\partial z^2} - \frac{2}{r^2}\frac{\partial u}{\partial z}\right) + \frac{\partial u}{\partial z}\left(2\frac{\partial^2 w}{\partial r^2} + 4\frac{\partial^2 u}{\partial r\partial z} + \frac{\partial^2 w}{\partial r^2} + \frac{\partial^2 w}{\partial z^2}\right) \\
&+ \frac{\partial u}{\partial r}\left(10\frac{\partial^2 u}{\partial r^2} + 3\frac{\partial^2 u}{\partial z^2} + \frac{\partial^2 w}{\partial r\partial z} + \frac{4}{r}\frac{\partial u}{\partial r} - \frac{2u}{r^2}\right) + \frac{\partial w}{\partial z}\left(2\frac{\partial^2 u}{\partial z^2} + \frac{\partial^2 w}{\partial z\partial r}\right) - \frac{2}{r^2}\frac{\partial u}{\partial t} \\
&\left. + \frac{\partial w}{\partial r}\left(2\frac{\partial^2 u}{\partial z\partial r} + 4\frac{\partial^2 w}{\partial r^2} + 2\frac{\partial^2 u}{\partial z\partial r} + \frac{2}{r}\left(\frac{\partial u}{\partial z} + \frac{\partial w}{\partial r}\right) + 3\frac{\partial^2 w}{\partial z^2} + \frac{\partial^2 u}{\partial r\partial z}\right)\right] \\
&+ \frac{\alpha_2}{\rho}\left[\frac{\partial u}{\partial r}\left(8\frac{\partial^2 u}{\partial r^2} + \frac{4}{r}\frac{\partial u}{\partial r} + 2\frac{\partial^2 u}{\partial z^2} + 2\frac{\partial^2 w}{\partial z\partial r}\right) + \frac{\partial w}{\partial r}\left(4\frac{\partial^2 u}{\partial r\partial z} + 2\frac{\partial^2 w}{\partial r^2} + 2\frac{\partial^2 w}{\partial z^2} + \frac{1}{r}\frac{\partial w}{\partial r}\right)\right. \\
&\left. + \frac{\partial u}{\partial z}\left(4\frac{\partial^2 u}{\partial r\partial z} + 2\frac{\partial^2 w}{\partial r^2} + 2\frac{\partial^2 w}{\partial z^2} + \frac{1}{r}\frac{\partial u}{\partial z} + \frac{2}{r}\frac{\partial w}{\partial r}\right) + 2\frac{\partial w}{\partial z}\left(\frac{\partial^2 u}{\partial z^2} + \frac{\partial^2 w}{\partial r\partial z}\right) - \frac{4u^2}{r^3}\right] \\
&+ \frac{\beta_3}{\rho}\left[2\frac{\partial u}{\partial r}\left(4\frac{\partial u}{\partial z}\frac{\partial^2 u}{\partial r\partial z} + \frac{8u}{r^2}\frac{\partial u}{\partial r} - \frac{8u^2}{r^3}\right)\right. \\
&+ \left(\frac{2}{r}\frac{\partial u}{\partial r} + \frac{\partial^2 u}{\partial z^2} - \frac{2u}{r^2}\right)\left\{4\left(\frac{\partial u}{\partial r}\right)^2 + 2\left(\frac{\partial u}{\partial z}\right)^2 + 4\left(\frac{\partial w}{\partial z}\right)^2 + \frac{4u^2}{r^2}\right\} \\
&\left. + \frac{\partial u}{\partial z}\left(8\frac{\partial u}{\partial r}\frac{\partial^2 u}{\partial r\partial z} + 4\frac{\partial u}{\partial z}\frac{\partial^2 u}{\partial z^2} + 8\frac{\partial w}{\partial z}\frac{\partial^2 w}{\partial z^2} + \frac{8u}{r^2}\frac{\partial u}{\partial z}\right)\right], \tag{10.5}
\end{aligned}
$$

$$\frac{\partial w}{\partial t} + u\frac{\partial w}{\partial r} + w\frac{\partial w}{\partial z} = -\frac{1}{\rho}\frac{\partial p}{\partial z} + \nu\left(\frac{\partial^2 w}{\partial r^2} + \frac{\partial^2 w}{\partial z^2} + \frac{1}{r}\frac{\partial w}{\partial r}\right)$$

$$+ \frac{\alpha_1}{\rho}\left[\frac{\partial^3 w}{\partial t\partial r^2} + \frac{\partial^3 w}{\partial t\partial z^2} + \frac{1}{r}\frac{\partial^2 w}{\partial t\partial r} + \frac{\partial u}{\partial r}\left(4\frac{\partial^2 u}{\partial r\partial z} + 2\frac{\partial^2 w}{\partial r^2} + \frac{3}{r}\frac{\partial u}{\partial z} + \frac{1}{r}\frac{\partial w}{\partial r}\right)\right.$$

$$+ u\left(\frac{\partial^3 u}{\partial r^2\partial z} + \frac{\partial^3 w}{\partial r^3} + \frac{1}{r}\frac{\partial^2 u}{\partial r\partial z} + \frac{1}{r}\frac{\partial^2 w}{\partial r^2} + 2\frac{\partial^3 w}{\partial r\partial z^2}\right) + w\left(\frac{\partial^3 w}{\partial r\partial z^2} + \frac{1}{r}\frac{\partial^2 w}{\partial r\partial z} + \frac{\partial^3 w}{\partial z^3}\right)$$

$$+ \frac{\partial w}{\partial r}\left(3\frac{\partial^2 u}{\partial z^2} + 4\frac{\partial^2 w}{\partial r\partial z} + \frac{\partial^2 u}{\partial r^2} + \frac{2}{r}\frac{\partial w}{\partial z}\right) + \frac{\partial u}{\partial z}\left(3\frac{\partial^2 u}{\partial r^2} + 3\frac{\partial^2 w}{\partial z\partial r} + 2\frac{\partial^2 w}{\partial r\partial z} + 4\frac{\partial^2 u}{\partial z^2}\right)$$

$$+ \frac{\partial w}{\partial z}\left(3\frac{\partial^2 w}{\partial r^2} + \frac{1}{r}\frac{\partial w}{\partial r} + 9\frac{\partial^2 w}{\partial z^2}\right)\right] + \frac{\alpha_2}{\rho}\left[\frac{\partial u}{\partial r}\left(2\frac{\partial^2 w}{\partial r^2} + 2\frac{\partial^2 u}{\partial r\partial z} + \frac{2}{r}\frac{\partial u}{\partial z} + \frac{2}{r}\frac{\partial w}{\partial r}\right)\right.$$

$$+ \frac{\partial u}{\partial z}\left(2\frac{\partial^2 u}{\partial r^2} + 4\frac{\partial^2 w}{\partial r\partial z} + 2\frac{\partial^2 u}{\partial z^2}\right) + \frac{\partial w}{\partial r}\left(2\frac{\partial^2 u}{\partial r^2} + 4\frac{\partial^2 w}{\partial r\partial z} + 2\frac{\partial^2 u}{\partial z^2}\right)$$

$$+ 2\frac{\partial w}{\partial z}\left(\frac{\partial^2 w}{\partial r^2} + 3\frac{\partial^2 w}{\partial z^2} + \frac{1}{r}\frac{\partial w}{\partial r}\right)\right] + \frac{\beta_3}{\rho}\left[\left(\frac{\partial u}{\partial z} + \frac{\partial w}{\partial r}\right)\left\{8\frac{\partial u}{\partial r}\frac{\partial^2 u}{\partial r^2} + 8\frac{\partial w}{\partial z}\frac{\partial^2 w}{\partial r\partial z}\right.\right.$$

$$+ 4\left(\frac{\partial u}{\partial z} + \frac{\partial w}{\partial r}\right)\left(\frac{\partial^2 u}{\partial r\partial z} + \frac{\partial^2 w}{\partial r^2}\right) + \frac{8u}{r^2}\frac{\partial u}{\partial r} - \frac{8u^2}{r^3}\right\}$$

$$+ \left(\frac{1}{r}\frac{\partial w}{\partial r} + \frac{\partial^2 w}{\partial r^2} + \frac{\partial^2 w}{\partial z^2}\right)\left\{4\left(\frac{\partial u}{\partial r}\right)^2 + 2\left(\frac{\partial u}{\partial z} + \frac{\partial w}{\partial r}\right)^2 + 4\left(\frac{\partial w}{\partial z}\right)^2 + \frac{4u^2}{r^2}\right\}$$

$$+ 2\frac{\partial w}{\partial z}\left\{8\frac{\partial u}{\partial r}\frac{\partial^2 u}{\partial r\partial z} + 4\left(\frac{\partial u}{\partial z} + \frac{\partial w}{\partial r}\right)\left(\frac{\partial^2 u}{\partial z^2} + \frac{\partial^2 w}{\partial z\partial r}\right) + 8\frac{\partial w}{\partial z}\frac{\partial^2 w}{\partial z^2} + \frac{8u}{r^2}\frac{\partial u}{\partial z}\right\}\right]. \tag{10.6}$$

The boundary conditions are

$$u = 0, \qquad w = \frac{\partial h}{\partial t}, \quad \text{at} \quad z = h(t),$$

$$u = 0, \qquad w = -w_0, \quad \text{at} \quad z = 0. \tag{10.7}$$

Using the following similarity transforms

$$u = \frac{ar}{2(1-at)}f'(\eta), \qquad w = -\frac{aH}{\sqrt{1-at}}f(\eta), \qquad \eta = \frac{z}{H\sqrt{1-at}}, \tag{10.8}$$

equation (10.1) is satisfied automatically and by eliminating pressure gradient, Eqs. (10.5) −

(10.7) give

$$
f^{(iv)} - S_q \left(\eta f''' + 3f'' - 2ff''' \right) + \frac{\alpha^*}{2} \left(\eta f^{(v)} + 5f^{(iv)} - 4f''f''' - 2f'f^{(iv)} - 2ff^{(v)} \right)
$$

$$
- \frac{\alpha_2^*}{2} (2f'f^{(iv)} + 4f''f''') + \alpha_3^* \left\{ Re \left(\frac{3}{2}(f'')^2 f^{(iv)} + 3f''(f''')^2 \right) \right.
$$

$$
\left. +6(f')^2 f^{(iv)} + 48f'f''f''' + 14(f'')^3 \right\} = 0, \tag{10.9}
$$

$$
f(0) = S, \qquad f'(0) = 0, \qquad f(1) = \frac{1}{2}, \qquad f'(1) = 0, \tag{10.10}
$$

where S denotes the suction/injection at the lower stationary disk. The squeeze parameter S_q, second grade parameters α^* and α_2^*, third grade parameter α_3^* and Reynolds number Re are introduced via the following definitions:

$$
S_q = \frac{aH^2}{2\nu}, \quad \alpha^* = \frac{a\alpha_1}{\mu\,(1 - at)}, \quad \alpha_2^* = \frac{a\alpha_2}{\mu\,(1 - at)}, \quad \alpha_3^* = \frac{a^2\beta_3}{\mu\,(1 - at)^2}, \quad Re = \frac{r^2}{H^2\,(1 - at)}. \tag{10.11}
$$

The skin friction coefficient in the present flow is

$$
C_{fr} = \frac{\tau_{rz}\,|_{z=h(t)}}{\rho \left(\frac{aH}{2(1-at)^{1/2}} \right)^2}, \tag{10.12}
$$

with

$$
\tau_{rz} = \mu \left(\frac{\partial u}{\partial z} + \frac{\partial w}{\partial r} \right) + \alpha_1 \left[\frac{\partial^2 u}{\partial t \partial z} + \frac{\partial^2 w}{\partial t \partial r} + u \left(\frac{\partial^2 u}{\partial r \partial z} + \frac{\partial^2 w}{\partial r^2} \right) \right.
$$

$$
\left. +w \left(\frac{\partial^2 u}{\partial z^2} + \frac{\partial^2 w}{\partial z \partial r} \right) + \frac{\partial u}{\partial r} \left(3\frac{\partial u}{\partial z} + \frac{\partial w}{\partial r} \right) + \frac{\partial w}{\partial z} \left(\frac{\partial u}{\partial z} + 3\frac{\partial w}{\partial r} \right) \right]
$$

$$
+\alpha_2 \left[2\frac{\partial u}{\partial r} \left(\frac{\partial u}{\partial z} + \frac{\partial w}{\partial r} \right) + 2\frac{\partial w}{\partial z} \left(\frac{\partial u}{\partial z} + \frac{\partial w}{\partial r} \right) \right]
$$

$$
+\beta_3 \left(\frac{\partial u}{\partial z} + \frac{\partial w}{\partial r} \right) \left[4\left(\frac{\partial u}{\partial r} \right)^2 + 2\left(\frac{\partial u}{\partial z} + \frac{\partial w}{\partial r} \right)^2 + 4w\left(\frac{\partial w}{\partial z} \right)^2 + \frac{4u^2}{r^2} \right]. \tag{10.13}
$$

Dimensionless form of Eq. (10.13) is

$$
\frac{H^2}{r^2} Re_r C_{fr} = \left(1 + \frac{3}{2}\alpha^* + \frac{1}{2}\alpha_3^* Re f''(1) \right) f''(1), \tag{10.14}
$$

where

$$R_{er}^{-1} = \frac{2\nu}{raH\left(1 - at\right)^{1/2}}.$$ (10.15)

10.2 Series expression

The initial guess is taken as

$$f_0(\eta) = S + \left(\frac{3}{2} - 3S\right)\eta^2 + (2S - 1)\,\eta^3,$$ (10.16)

while the auxiliary linear operator is defined by

$$\mathcal{L}_f = \frac{d^4}{d\eta^4}$$ (10.17)

which satisfy

$$\mathcal{L}_f\left[C_1 + C_2\eta + C_3\eta^2 + C_4\eta^3\right] = 0,$$ (10.18)

in which $C_i (i = 1 - 4)$ are the constants.

The zeroth order problem is

$$(1 - q)\mathcal{L}_f\left[\bar{f}(\eta, q) - f_0(\eta)\right] = q\hbar_f\mathcal{N}_f[\bar{f}(\eta, q)],$$

$$\bar{f}(0, q) = S,\ \bar{f}'(0, q) = 0,\ \bar{f}'(1, q) = \frac{1}{2},\ \bar{f}'(1, q) = 0,$$ (10.19)

in which the involved nonlinear operator $\mathcal{N}_f$ is given by

$$
\begin{aligned}
\mathcal{N}_f[\bar{f}(\eta, p)] = {} & \frac{\partial^5\bar{f}}{\partial\eta^5} - S_q\left[\eta\frac{\partial^3\bar{f}}{\partial\eta^3} + 3\frac{\partial^2\bar{f}}{\partial\eta^2} - 2\bar{f}(\eta, q)\frac{\partial^3\bar{f}}{\partial\eta^3}\right] \\
& + \frac{\alpha^*}{2}\left[\eta\frac{\partial^5\bar{f}}{\partial\eta^5} + 5\frac{\partial^4\bar{f}}{\partial\eta^4} - 4\frac{\partial^2\bar{f}}{\partial\eta^2}\frac{\partial^3\bar{f}}{\partial\eta^3} - 2\frac{\partial\bar{f}}{\partial\eta}\frac{\partial^4\bar{f}}{\partial\eta^4} - 2\bar{f}(\eta, p)\frac{\partial^5\bar{f}}{\partial\eta^5}\right] \\
& - \frac{\alpha_2^*}{2}\left[2\frac{\partial\bar{f}}{\partial\eta}\frac{\partial^4\bar{f}}{\partial\eta^4} + 4\frac{\partial^2\bar{f}}{\partial\eta^2}\frac{\partial^3\bar{f}}{\partial\eta^3}\right] + \alpha_3^*\left[Re\left(\frac{3}{2}\left(\frac{\partial^2\bar{f}}{\partial\eta^2}\right)^2\frac{\partial^4\bar{f}}{\partial\eta^4} + 3\frac{\partial^2\bar{f}}{\partial\eta^2}\left(\frac{\partial^3\bar{f}}{\partial\eta^3}\right)^2\right)\right. \\
& \left. + 6\left(\frac{\partial\bar{f}}{\partial\eta}\right)^2\frac{\partial^4\bar{f}}{\partial\eta^4} + 48\frac{\partial\bar{f}}{\partial\eta}\frac{\partial^2\bar{f}}{\partial\eta^2}\frac{\partial^3\bar{f}}{\partial\eta^3} + 14\left(\frac{\partial^2\bar{f}}{\partial\eta^2}\right)^2\right].
\end{aligned}
$$ (10.20)

where the embedding parameter is $q \in [0, 1]$. For $q = 0$ and $q = 1$, we have

$$\bar{f}(\eta, 0) = f_0(\eta), \ \bar{f}(\eta, 1) = f(\eta), \tag{10.21}$$

The problems at the mth order are

$$\mathcal{L}\left[f_m(\eta, q) - \chi_m f_{m-1}(\eta)\right] = \hbar_f \mathcal{R}_m(\eta),$$

$$f_m(0) = f'_m(0) = f_m(1) = f'_m(1) = 0, \tag{10.22}$$

with

$$\mathcal{R}_m(\eta) = f_{m-1}^{(5)} - S_q(\eta f'''_{m-1} + 3f''_{m-1}) + \frac{\alpha^*}{2}\left(\eta f_{m-1}^{(5)} + 5f_{m-1}^{(4)}\right)$$

$$+2S_q \sum_{k=0}^{m-1} f_{m-1-k}f'''_k - \frac{\alpha^*}{2}\sum_{k=0}^{m-1}\left(f''_{m-1-k}f'''_k + 2f'_{m-1-k}f_k^{(iv)} + 2f_{m-1-k}f_k^{(v)}\right)$$

$$-\frac{\alpha_2^*}{2}\sum_{k=0}^{m-1}\left(f'_{m-1-k}f_k^{(4)} + 4f''_{m-1-k}f'''_k\right) + \alpha_3^* \sum_{k=0}^{m-1}\sum_{l=0}^{k}\left[Re\left(\frac{3}{2}f''_{m-1-k}f''_{k-l}f_l^{(4)} + 3f''_{m-1-k}f'''_{k-l}f'''_l\right)\right.$$

$$\left. +6f'_{m-1-k}f'_{k-l}f_l^{(iv)} + 48f'_{m-1-k}f''_{k-l}f'''_l + 14f''_{m-1-k}f''_{k-l}f''_l\right], \tag{10.23}$$

where $\hbar_f$ is the auxiliary parameter and χ_m is defined by

$$\chi_m = \begin{cases} 0, m \leq 1 \\ 1, m > 1. \end{cases} \tag{10.24}$$

Use of Taylor series leads to the following expression

$$\bar{f}(\eta, q) = f_0(\eta) + \sum_{m=1}^{\infty} f_m(\eta)q^m, \ f_m(\eta) = \frac{1}{m!}\frac{\partial^m \bar{f}(\eta, q)}{\partial q^m}\bigg|_{p=0}. \tag{10.25}$$

Note that the values of $\hbar_f$ are selected in such a way that the series (10.22) converge for $q = 1$.
Hence

$$f(\eta) = f_0(\eta) + \sum_{m=1}^{\infty} f_m(\eta). \tag{10.26}$$

10.3 Convergence analysis

The series solution (10.22) contains the auxiliary parameter $\hbar_f$. This parameter is useful in adjusting and controlling the convergence of the obtained solution. In order to obtain the admissible values of auxiliary parameter, we have drawn Figs. $(10.1 - 10.2)$ at $\eta = 0$ and $\eta = 1$ respectively. It is established that range for admissible values of $\hbar_f$ is $-2.2 \leq \hbar_f \leq -0.7$. Further, the series solutions converge in the whole region of η $(0 < \eta < 1)$ when $\hbar_f = -1.7$. Table 10.1 is useful in making a guess that how much order of approximations are necessary for a convergent solution. This table shows that the $25th$ and $15th$ order of approximations are enough for the convergent solution for lower and upper disks for injection respectively
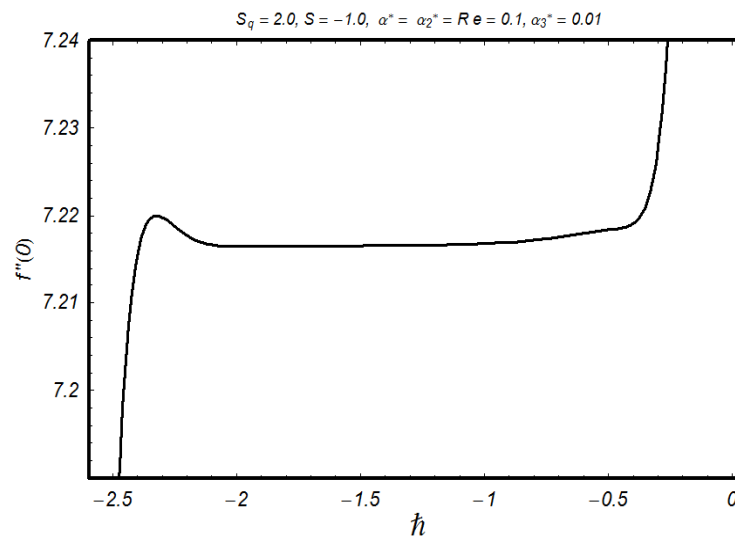

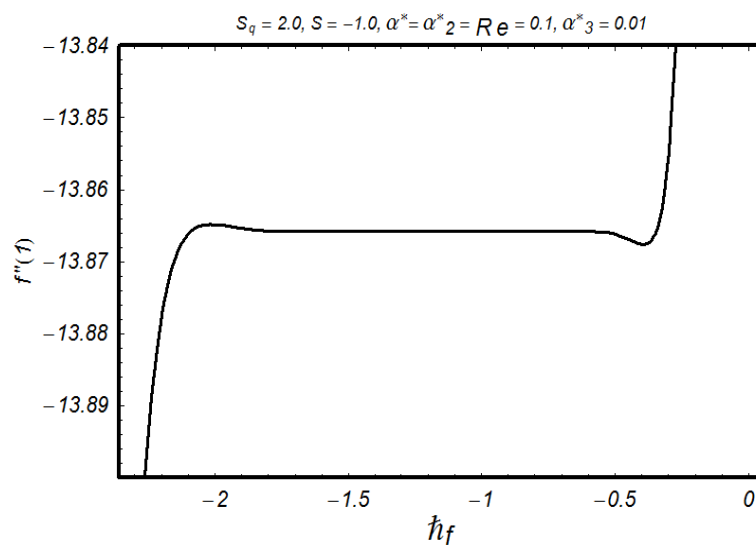Fig. 10.1: Convergence region for f at $\eta = 0$.

Fig. 10.2: Convergence region for f at $\eta = 1$.

Table 10.1: Series solution's convergence by HAM for different order of approximations when $S = -1.0$, $\alpha^* = \alpha_2^* = Re = 0.1$, $\alpha_3^* = 0.01$ and $S_q = 2.0$.

Order of approximation	$f''(0)$	$-f''(1)$
1	7.5600	12.1612
5	7.2198	13.8953
10	7.2178	13.8657
15	7.2169	13.8658
20	7.2166	13.8658
25	7.2165	13.8658
30	7.2165	13.8658
35	7.2165	13.8658
40	7.2165	13.8658

10.4   Graphical results and discussion

Our intention now is to describe the influences of the involved parameters on the velocity field $f'(\eta)$. Thus we plotted the Figs. $(10.3 - 10.10)$. Fig. 10.3 presents the influence of squeezing parameter S_q on f'. It is observed that squeezing S_q enhances the flow near the upper wall. Such increase in flow is compensated with the decrease in the lower part of channel in order to fulfil the condition of law of mass conservation. Influence of squeezing parameter S_q on the axial component of velocity f is plotted in Fig. 10.4. It is observed that axial velocity is a decreasing function of S_q. Influence of S on f' is shown in Fig. 10.5. It is observed that the velocity field f' increases with an increase in the magnitude of S. Effect of second grade parameters α^* and α_2^* on f' is investigated in Figs. 10.6 and 10.7. The velocity field f' decreases for $0 \leq \eta \leq 0.7$ and it increases for $0.7 \leq \eta \leq 1$ with the increase of α^* and α_2^*. Reverse flow has seen near the lower porous plate. Fig. 8 plots the effects of third grade parameter α_3^* on f'. It is noted from this Fig. that velocity of fluid increases near the lower and upper disks whereas it decreases at the center of channel. Since both S and S_q act as the boosting agents which always enhance the flow but at the center of the channel the third grade parameter α_3^* (being a viscoelastic parameter) is dominant. Thus it retards the flow at the central part. Effects of Reynolds number Re is plotted in Fig. 10.9. Opposite trends is noticed for f' when we increase Re (see Figs. 10.6 and 10.7).

Fig. 10.10 plots the influence of skin friction coefficient (drag force) $\frac{H^2}{r^2}R_{er}C_{fr}$ for different values of α_3^* vs Re. It is noticed that the magnitude of skin friction coefficient decreases by increasing α_3^*.

Table 10.2 presents the values of skin friction coefficient for different parameters. It is noted that skin friction coefficient increases with an increase in S whereas it decreases by increasing
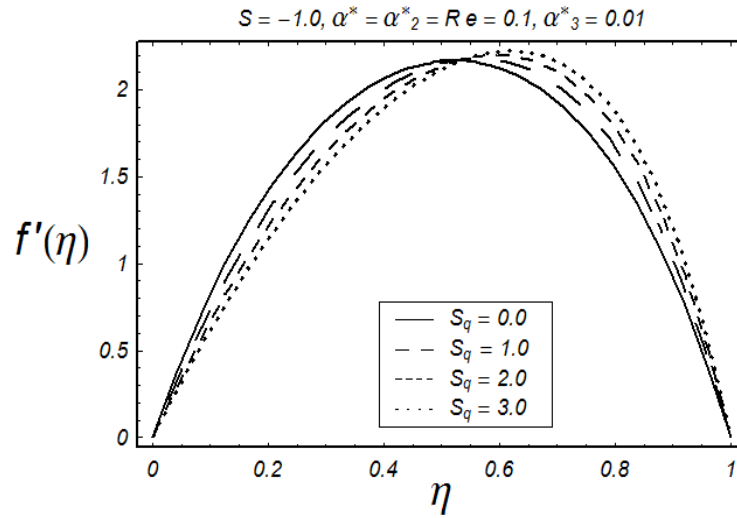
S_q and α_3^*.
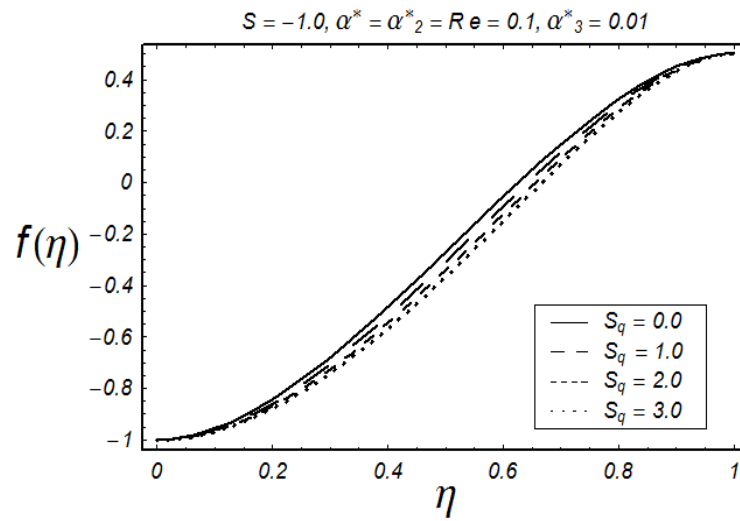

Fig. 10.3: Influence of S_q on f'.

Fig. 10.4: Influence of S_q on f.
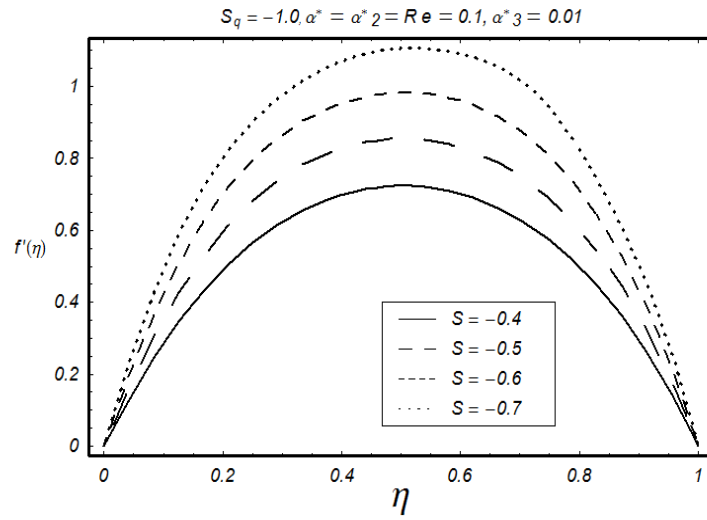
Fig. 10.5: Influence of S on f'.
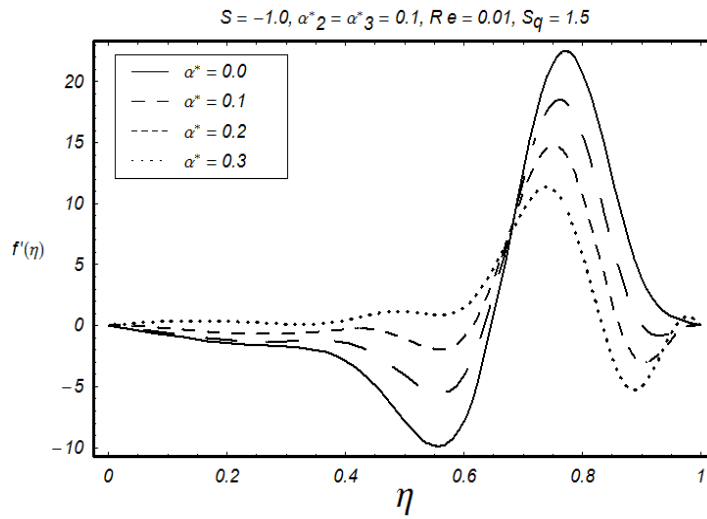
Fig. 10.6: Influence of α^* on f'.
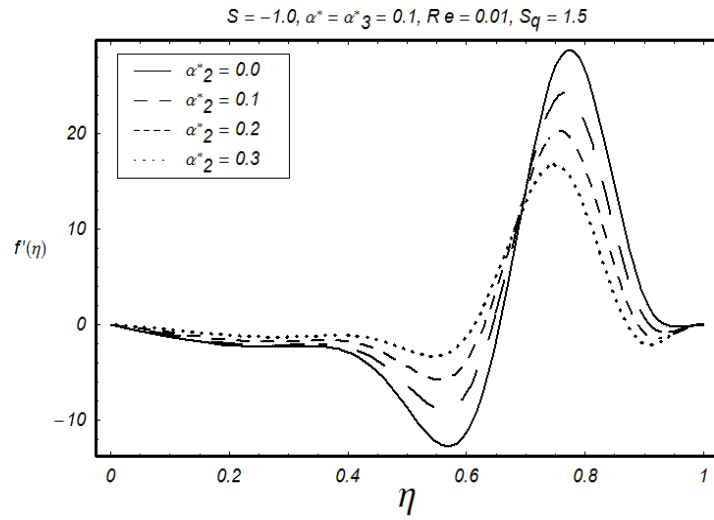
Fig. 10.7: Influence of α_2^* on f'.
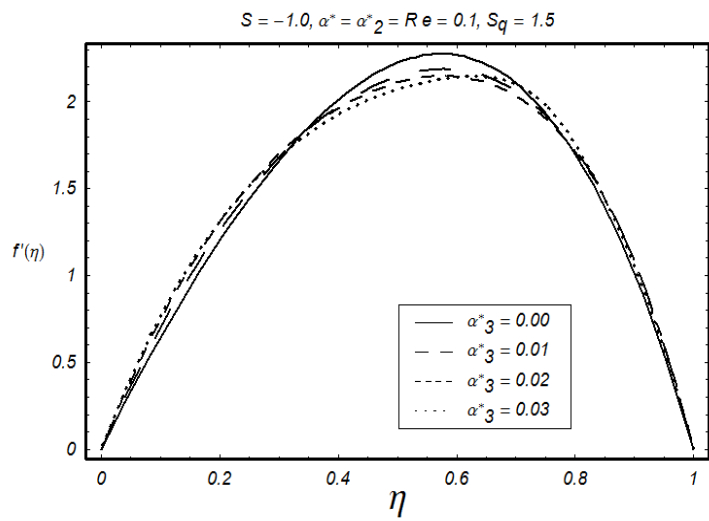
Fig. 10.8: Influence of α_3^* on f'.
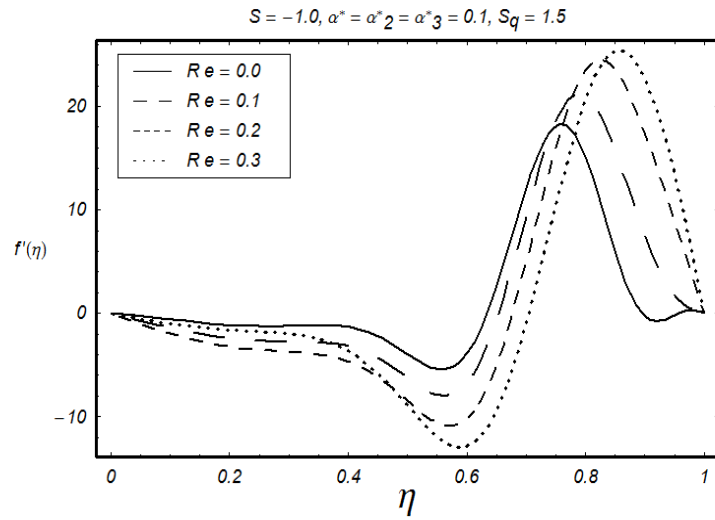
Fig. 10.9: Influence of Re on f'.
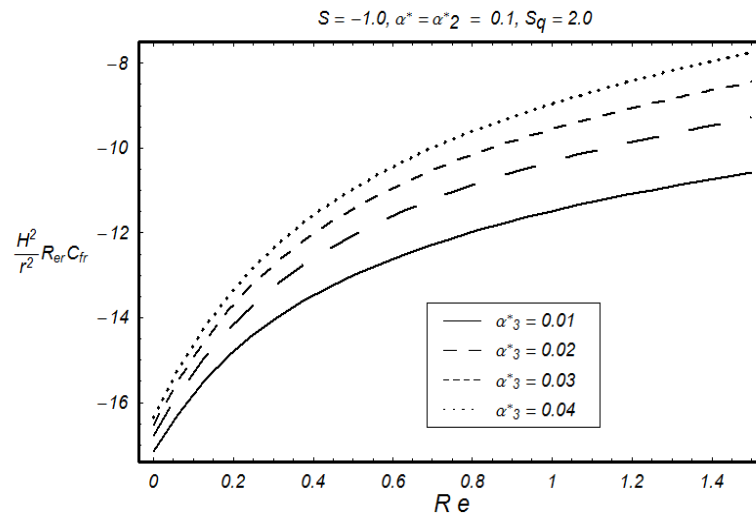
Fig. 10.10: Influence of α_3^* and Re on $\frac{H^2}{r^2}Re_r C_{fr}$.

161

Table 10.2: Values of skin friction coefficient $\frac{H^2}{r^2} R_{er} C_{fr}$ for different values of emerging parameters.

S	S_q	α_3^*	$\frac{H^2}{r^2} R_{er} C_{fr}$
-1.5	2.0	0.01	-23.97831
-1.0			-15.84972
-0.5			-9.073212
0.0			-3.870458
-1.0	0.0		-12.10583
	1.0		-14.03073
	2.0		-15.84972
	2.5		-16.70936
	2.0	0.00	-15.07652
		0.01	-15.84972
		0.02	-16.15729
		0.03	-16.25819

10.5 Key findings

Here axisymmetric squeezing flow of third grade fluid is studied. Main points of presented analysis are summarized below.

- Horizontal velocity $f'(\eta)$ decreases near the porous disk while it increases near the upper squeezing disk when squeezing parameter S_q increases.

- Vertical velocity $f(\eta)$ decreases through increase of squeezing parameter S_q.

- Velocity profile $f'(\eta)$ decreases with the increase of suction parameter S.

- Magnitude of velocity profile $f'(\eta)$ decreases for larger second grade parameters α^* and α_2^*.

- Velocity profile $f'(\eta)$ increases near the porous disk while it decreases near the upper disk when third grade parameter α_3^* increases.

- Skin friction coefficient increases with an increase in S whereas it decreases by increasing S_q and α_3^*.

Chapter 11

Summary

The research conducted in this thesis can be summarized through the contents of chapters two to ten. In fact chapter two describes the unsteady incompressible and axisymmetric flow of Jeffrey fluid between two parallel disks. The lower wall is static and subjected to the suction or injection while upper wall is squeezed towards the lower wall. The flow analysis is investigated without any body force. Pressure is eliminated from the governing momentum equations and then reduced to ordinary differential equation by using the suitable transformations. The resulting ordinary differential system is solved for the series solution. Convergence analysis of the series solution is explicitly discussed. Variations of pertinent parameters on velocity profile are shown graphically. Skin friction coefficient is also computed. It is found that the velocity profile is enhanced via larger porosity and squeezing parameters.

Chapter three extends the flow analysis of previous chapter through heat transfer characteristics. Conservation law of energy is used for the development of problem in addition to the conservation law of linear momentum. Thermal radiation effect is present to investigate the heat transfer behavior. Temperature at the lower and upper walls is assumed different. A system of ordinary differential equations is solved by homotopy analysis method. Behavior of various physical parameters on temperature distribution is examined for both the cases (i) suction (ii) blowing. It is analyzed that temperature distribution decreases for higher values of Prandtl number in both suction and blowing situations. However opposite effect is observed due to thermal radiation on the temperature profile in the cases of suction and blowing.

Chapter four focuses on the unsteady MHD incompressible squeezing flow of Jeffrey fluid

164

between two parallel plates. Simultaneous effects of heat and mass transfer are explored. The phenomena of Soret-Dufour and Joule heating are also considered to study the behavior of heat and mass transfer. Temperature and concentration at the lower and upper walls are assumed different. The fluid is electrically conducting in the presence of magnetic field. To find the series solutions by homotopy analysis method, the governing equations are first converted into ordinary differential equations using the appropriate transformations. The solution expressions for velocity, temperature and concentration fields are computed and discussed. In addition the skin friction coefficient, Nusselt number and Sherwood number are tabulated and analyzed.

Chapter five explores the simultaneous effects of heat and mass transfer in unsteady incompressible squeezing flow of Jeffrey fluid between parallel plates. The present analysis is investigated in the presence of viscous dissipation and first order chemical reaction. Temperature and concentration are assumed constant at the upper and lower plates. Series solution to the involved system is computed. Analysis is performed for residual errors of the series solutions. A parametric study of pertinent variables is conducted. The skin friction coefficient and local Nusselt and Sherwood numbers are computed and examined. It is examined that temperature profile is higher for larger values of Eckretnumber. Destructive and constructive chemical reactions have opposite effect on the concentration distribution.

The objective of chapter six is to revisit the flow analysis of chapter two by considering the couple stress fluid model. The considered fluid model here has distinct features through polar effects when compared with the other non-Newtonian fluid models. Specifically the present fluid model allows polar effects such as the presence of couple stress, body couple and non-symmetric tensors. The modeled nonlinear flow problem is reduced into the ordinary differential system. Computations have been carried out by homotopy analysis method (HAM). Effects of the squeezing and couple stress parameters on the velocity profile are discussed. Velocity profile increases in the lower and upper half of the channel while it decreases at the center of the channel for higher values of couple stress parameter.

Chapter seven discloses the behavior of simultaneous effects of heat and mass transfer in unsteady two-dimensional squeezing flow of couple stress fluid between the parallel plates. Characteristics of viscous dissipation and first order chemical reaction are analyzed. Appropriate transformation procedure is adopted to obtain a system of ordinary differential equations.

The governing problems are computed by homotopy analysis method (HAM). Convergence and residual errors of the series solutions are also analyzed. Quantities of interest are illustrated graphically. The skin friction coefficient and Nusselt and Sherwood numbers are computed and analyzed. Destructive and constructive chemical reactions have opposite effect on the concentration distribution.

Chapter eight is concerned with the unsteady squeezing flow of second grade fluid between two parallel plates. Rheological behavior of second grade fluid is analyzed in the magnetohydrodynamic flow. The considered fluid model can predict the normal stress effect. The fluid is assumed electrically conducting. The lower plate is stretched with linear velocity while the upper plate is squeezed. Transformation procedure reduces the partial differential equations into the ordinary differential equations. A series solution is developed using a modern mathematical scheme. The solution expressions for velocity components are computed and discussed. In addition the skin friction coefficient is analyzed through the tabulated values. It is analyzed that second grade parameter has opposite effects on the velocity profile in both suction and injection cases.

Chapter nine focuses on the combined effects of heat and mass transfer in the magnetohydrodynamic (MHD) squeezing flow of chemically reactive second grade fluid model. The flow analysis is performed between the two parallel plates. Simultaneous effects of thermal-diffusion (Soret), diffusion-thermo (Dufour) and viscous dissipation are considered. Suitable variables are utilized for the conversion of partial differential system into an ordinary differential system. Analytical solutions are obtained by homotopy analysis method (HAM). The behavior of involved sundry parameters on the velocity, temperature and concentration distributions are shown graphically. A comparative study with the already published results shows an excellent agreement. Concentration profile is an increasing function of Soret and Dufour numbers.

Chapter ten addresses the time-dependent flow of an incompressible third grade fluid between the squeezing disks. The relevant equations of thermodynamic compatible third grade fluid are modeled. The considered fluid model can predict the shear thinning and shear thickening effects along with the normal stress. Suitable transformations are used to get the system of ordinary differential equation. Solution to the nonlinear problem is computed in series form. The presented graphical results illustrate the influence of emerging parameters in the consid-

166

ered problem. It is analyzed that velocity distribution increases near the porous disk while it decreases near the upper disk when third grade parameter increases.

It is worthmentioning to point out that the outcomes of chapters two and three have been published in "**Chinese Physics Letters 29 (2012) 034701**" and "**The European Physical Journal Plus 128 (2013) 85**" respectively. The contents of chapters four and five are submitted for publication in "**Computers and Fluids**" and "**Applied and Computational Mathematics**". The materials of chapters six and seven are respectively submitted in "**The European Physical Journal Plus**" and "**Zeitschrift Natuforchung A**". Research presented in chapter eight is published in "**The European Physical Journal Plus 128 (2013) 157**" while the flow analysis of chapter nine is submitted in "**Heat Transfer Research**". Finally the results of chapter ten are submitted in "**Maejo International Journal of Science and Technology**".

The following problems will be discussed in future.

- Squeezing flow for Williamson fluid.

- Effects of melting heat transfer in squeezing flow of viscous and differential type fluids.

- Newtonian heating effects in squeezing flow of nanofluids.

Bibliography

[1] W. C. Tan and T. Masuoka, Stokes' first problem for a second grade fluid in a porous half-space with heated boundary, Int. J. Non-Linear Mech., 40 (2005) $515-522$.

[2] Q. Haitao and X. Mingyu, Unsteady flow of viscoelastic fluid with fractional Maxwell model in a channel, Mech. Research Comm., 34 (2007) $210-212$.

[3] C. Fetecau, C. Fetecau and M. Rana, General solutions for the unsteady flow of second-grade fluids over an infinite plate that applies arbitrary shear to the fluid, Z. Naturforsch. A (ZNA)., 66 (2011) $753-759$.

[4] M. Jamil, A. Rauf, C. Fetecau and N. A. Khan, Helical flows of second grade fluid due to constantly accelerated shear stresses, Comm. Nonlinear Sci. Num. Simulat., 16 (2011) $1959-1969$.

[5] M. Nazar, C. Fetecau, D. Vieru and C. Fetecau, New exact solutions corresponding to the second problem of Stokes for second grade fluids, Nonlinear Analysis: Real World Applications, 11 (2010) $584-591$.

[6] Y. Yao and Y. Liu, Some unsteady flows of a second grade fluid over a plane wall, Nonlinear Analysis: Real World Applications, 11 (2010) $4442-4450$.

[7] R. Ellahi and A. Zeeshan, A study of pressure distribution for a slider bearing lubricated with a second-grade fluid, Numerical Methods for Partial Differential Equations, 27 (2011) $1231-1241$.

[8] S. Nadeem, A. Rehman, C. Lee and J. Lee, Boundary layer flow of second grade fluid in a cylinder with heat transfer, Math. Problems Eng., doi:10.1155/2012/640289.

[9] F. Ali, M. Norzieha, S. Sharidan, I. Khan and T.Hayat, New exact solutions of Stokes' second problem for MHD second grade fluid in a porous space, Int. J. Non-Linear Mech., 47 (2012) 521 − 525.

[10] T. Hayat, A. Yousaf, M. Mustafa and S. Obaidat, MHD squeezing flow of second-grade fluid between two parallel disks, Int. J. Numer. Meth. Fluids, 69 (2012) 399 − 410.

[11] M. Khan, S. H. Ali and Q. Haitao, Exact solutions for some oscillating flows of a second grade fluid with a fractional derivative model, Math. Computer Modelling, 49 (2009) 1519 − 1530.

[12] C. Xue and J. Nie, Exact solutions of the Rayleigh-Stokes problem for a heated generalized second grade fluid in a porous half-space, App. Math. Modelling, 33 (2009) 524 − 531.

[13] M. Turkyilmazoglu, Dual and triple solutions for MHD slip flow of non-Newtonian fluid over a shrinking surface, Computers and Fluids, 70 (2012) 53 − 58.

[14] T. Hayat T, S. Iram, T. Javed and S. Asghar, Shrinking flow of second grade fluid in a rotating frame: an analytic solution. Comm. Nonlinear Sci. Numerical Simulat., 15 (2010) 2932 − 2941.

[15] T. Hayat, S. A. Shehzad, M. Qasim and S. Obaidat, Flow of a second grade fluid with convective boundary conditions, Thermal Sci., 15 (2011) 253 − 261.

[16] A. F. Dizaji, M. R. Salimpour and F. Jam, Flow field of a third-grade non-Newtonian fluid in the annulus of rotating concentric cylinders in the presence of magnetic field, J. Math. Anal. Appl., 337 (2008) 632 − 645.

[17] R. Ellahi, T. Hayat, F. M. Mahmood and A. Zeeshan, Fundamental flows with nonlinear slip condition: Exact solution, Z. Angew. Math. Phys., 61 (2010) 877 − 888.

[18] S. Abelman, E. Momoniat and T. Hayat, Couette flow of a third grade fluid with rotating frame and slip condition, Real World Applications, 10 (2009) 3329 − 3334.

[19] S. Abelman, E. Momoniat and T. Hayat, Steady MHD flow of a third grade fluid in a rotating frame and porous space, Non-Linear Analysis: Real World Applications, 10 (2009) 3322 − 3328.

[20] B. Sahoo and Y. Do, Effects of slip on sheet-driven flow and heat transfer of a third grade fluid past a stretching sheet, Int. Comm. Heat Mass Transfer, 37 (2010) $1064 - 1071$.

[21] S. Abbasbandy and T. Hayat, On series solution for unsteady boundary layer equations in a special third grade fluid, Comm. Nonlinear Sci. Numer. Simulat., 16 (2011) $3140 - 3146$.

[22] R. Narain and A. H. Kara, An analysis of the conservation laws for certain third-grade fluids, Non-Linear Analysis: Real World Applications, 11 (2010) $3236 - 3241$.

[23] M. Keimanesh, M. M. Rashidi, A. J. Chamkhab and R. Jafari, Study of a third grade non-Newtonian fluid flow between two parallel plates using the multi-step differential transform method, Comp. Math. Appli., 62 (2011) $2871 - 2891$.

[24] T. Hayat, S. Hina, A. A. Hendi and S. Asghar, Effect of wall properties on the peristaltic flow of a third grade fluid in a curved channel with heat and mass transfer, Int. J. Heat Mass Transfer, 54 (2011) $5126 - 5136$.

[25] R. Ellahi and S. Afzal, Effects of variable viscosity in a third grade fluid with porous medium: An analytic solution, Comm. Nonlinear Sci. Numer. Simulat., 14 (2009) $2056 - 2072$.

[26] M. Kothandapani and S. Srinivas, Peristaltic transport of a Jeffrey fluid under the effect of magnetic field in an asymmetric channel, Int. J. Non-Linear Mech., 43 (2008) $915 - 924$.

[27] T. Hayat and N. Ali, Peristaltic motion of a Jeffrey fluid under the effect of a magnetic field in a tube, Comm. Nonlinear Sci. Numer. Simulat., 13 (2008) $1343 - 1352$.

[28] T. Hayat, R. Sajjad and S. Asghar, Series solution for MHD channel flow of a Jeffery fluid, Comm. Nonlinear Sci. Numer. Simulat., 15 (2010) $2400 - 2406$.

[29] T. Hayat, S. Asad, M. Qasim and Awatif A. Hendi, Boundary layer flow of a Jeffrey fluid with convective boundary conditions, Int. J. Numer. Meth. Fluids, 69 (2012) $1350 - 1362$.

[30] T. Hayat, N. Ahmad and N. Ali, Effects of an endoscope and magnetic field on the peristalsis involving Jeffrey fluid. Comm. Nonlinear Sci. Numer. Simulat., 13 (2008) $1581 - 1591$.

[31] R. Ellahi, A. Riaz, S. Nadeem and M. Mushtaq, Series solutions of magnetohydrodynamic peristaltic flow of a Jeffrey fluid in eccentric cylinders, Appl. Math. Inf. Sci., 4 (2013) $1441 - 1449$.

[32] A. M. Siddiqui, A. A. Farooq, T. Haroon and B. S. Babcock, A variant of the classical von Karman flow for a Jeffrey fluid, Applied Mathematical Sciences, 7 (2013) $983 - 991$.

[33] V. K. Stokes, Couple stesses in fluids, Phy. of Fluids, 9 (1966) $1717 - 1715$.

[34] R. S. K. Lakshmana and T. K. V. Iyengar, Analytical and computational studies in couple stress fluid flows, U.G.C. Research project $C - 8 - 4/82\ SR\ III$, 1985.

[35] D. Srinivasacharya, Stokes flow of an incompressible couple stress fluid past an approximate sphere, Ph.D thesis, 1995.

[36] G. Ramanaiah, Squeeze films between finite plates lubricated by fluids with couple-stresses, Wear, 54 (1979) $315 - 320$.

[37] R. S. Gupta and R. L. Sharma, Analysis of couple stresses lubricant in hydrostatic thrust bearings, Wear, 48 (1988) $257 - 269$.

[38] T. Hayat, M. Awais, A. Safdar and A. A. Hendi, Unsteady three dimensional flow of couple stress fluid over a stretching surface with chemical reaction, Nonlinear Analysis: Modelling and Control, 17 (2012) $47 - 59$.

[39] D. Tripathi, A mathematical model for swallowing of food bolus through the oesophagus under the influence of heat transfer, Int. J. Ther. Sci. 51 (2012) $91 - 101$.

[40] S. Srinivas and M. Kothandapani, The influence of heat and mass transfer on MHD peristaltic flow through a porous space with compliant walls, Appl. Math. Comput., 213 (2009) $197 - 208$.

[41] T. Hayat, S. Noreen, M. S. Alhothuali, S. Asghar and A. Alhomaidan, Peristaltic flow under the effects of an induced magnetic field and heat and mass transfer, Int. J. Heat Mass Transfer, 55 (2012) $443 - 452$.

[42] T. Hayat and S. Hina, The influence of wall properties on the MHD peristaltic flow of a Maxwell fluid with heat and mass transfer, Nonlinear Analysis: Real World Applications, 11 (2010) 3155 − 3169.

[43] Kh. S. Mekheimer and Y. Abd elmaboud, The influence of heat transfer and magnetic field on peristaltic transport of a Newtonian fluid in a vertical annulus: Application of an endoscope, Physics Letters A, 372 (2008) 1657 − 1665.

[44] S. A. Shehzad, F. E. Alsaadi, S. J. Monaquel and T. Hayat, Soret and Dufour effects on the stagnation point flow of Jeffery fluid with convective boundary condition, Eur. Phys. J. Plus, 128 (2013) 56.

[45] T. Hayat, M. Awais, S. Asghar and S. Obaidat, Unsteady flow of third grade fluid with Soret and Dufour effects, J. Heat Transfer, 134 (2012) 062001.

[46] N. Islam and M. M. Alam, Dufour and Soret effects on steady MHD free convection and mass transfer fluid flow through a porous medium in a rotating system, J. Naval Arch. Marine Eng., 4 (2007) 43 − 55.

[47] M. M. Rashidi, T. Hayat, E. Erfani, S. A. Mohimanian Pour and Awatif A. Hendi, Simultaneous effects of partial slip and thermal-diffusion and diffusion-thermo on steady MHD convective flow due to a rotating disk, Comm. Nonlinear Sci. Numer. Simulat., 16 (2011) 4303 − 4317.

[48] T. Hayat, M. Mustafa and I. Pop, Heat and mass transfer for Soret and Dufour effects on mixed convection boundary layer flow over a stretching vertical surface in a porous medium filled with a viscoelastic fluid, Comm. Nonlinear Sci. Numer. Simulat., 15 (2009) 1183 − 1196.

[49] R. Tsai and J. S. Huang, Heat and mass transfer for Soret and Dufor's effects on Hiemenz flow through porous medium onto a stretching surface. Int J Heat Mass Transfer, 52 (2009) 2399 − 2406.

[50] A. A. Afify, Similarity solution in MHD: Effects of thermal diffusion and diffusion thermo on free convective heat and mass transfer over a stretching surface considering suction or injection, Comm. Nonlinear Sci. Numer. Simulat., 14 (2009) $2202 - 2214$.

[51] M. J. Stefan, Versuch über die scheinbare adhesion. Sitzungsber Sächs Akad Wiss Wein, Math-Nat Wiss Kl, 69 (1874) $713 - 721$.

[52] O. Reynolds, On the theory of lubrication and its application to Mr. Beauchamp Tower's experiments, including an experimental determination of the viscosity of olive oil, Philosophical Transactions of the Royal Society of London, 177 (1886) $157 - 234$.

[53] F. R. Archibald, Load capacity and time relations for squeeze films, J. Lubrication Technology, 78 (1956) $A231 - A245$.

[54] R. Usha and R. Sridharan, Arbitrary squeezing of a viscous fluid between elliptic plates, Fluid Dynamics Research, 18 (1996) $35 - 51$.

[55] H. M. Laun, M. Rady and O. Hassager, Analytical solutions for squeeze flow with partial wall slip, J. Non-Newtonian Fluid Mechanics, 81 (1999) $1 - 15$.

[56] D. C. Kuzma, Fluid inertia effects in squeeze films, Appl. Scientific Research, 18 (1968) $15 - 20$.

[57] R. J. Grimm, Squeezing flows of Newtonian liquid films an analysis include the fluid inertia, Appl. Scientific Research, 32 (1976) $149 - 166$.

[58] J. A. Tichy and W. O.Winer, Inertial considerations in parallel circular squeeze film bearings, J. Lubrication Technology, 92 (1970) $588 - 592$.

[59] C. Y. Wang and L. T. Watson, Squeezing flow of a viscous fluid between elliptic plates, Appl. Scientific Research, 35 (1979) $195 - 207$.

[60] J. D. Jackson, A study of squeezing flow, Appl. Sci. Research A, 11 (1962) $148 - 152$.

[61] P. T. Nhan, Squeeze flow of a viscoelastic solid, J. Non-Newtonian Fluid Mech., 95 (2000) $343 - 362$.

[62] C. Y. Wang, The squeezing of fluid between two plates, J. Appl. Mech., 43 (1976) 579−583.

[63] M. H. Hamdan and R. M. Baron, Analysis of the squeezing flow of dusty fluids, Appl. Scientific Research, 49 (1992) 345 − 354.

[64] W. E. Langlois, Isothermal squeeze films, Quarterly Appl. Math., 20 (1962) 131 − 150.

[65] R. L. Verma, A numerical solution for squeezing flow between parallel channels, Wear, 72 (1981) 89 − 95.

[66] E. A. Hamza, Suction and injection effects on a similar flow between parallel plates, Journal of Physics D: Applied Phys., 32 (1999) 656 − 663.

[67] K. R. Rajagopal and A. S. Gupta, On a class of exact solutions to the equations of motion of a second grade fluid, Int. J. Eng. Sci., 19 (1981) 1009 − 1014.

[68] M. M. Rashidi, H. Shahmohamadi and S. Dinarvand, Analytic approximate solutions for unsteady two-dimensional and axisymmetric squeezing flows between parallel plates, Mat. Prob. Eng., doi:10.1155/2008/935095

[69] G. Domairry and A. Aziz, Approximate analysis of MHD squeeze flow between two parallel disks with suction or injection by homotopy perturbation method, Math. Prob. Eng., 2009 (2009) 603916.

[70] M. Mahmood, S. Asghar and M. A. Hossain, Squeezed flow and heat transfer over a porous surface for viscous fluid, Heat and Mass Transfer, 44 (2007) 165 − 173.

[71] M. Mustafa, T.Hayat and S. Obaidat,On heat and mass transfer in the unsteady squeezing flow between parallel plates, Meccanica, 47 (2012) 1581 − 1589.

[72] T. Hayat, A. Yousaf, M. Mustafa and S. Asghar, Influence of heat transfer in the squeezing flow between parallel disks, Chem. Eng. Comm., 199 (2012) 1044 − 1062.

[73] A. Hussain, S. T. Mohyud-Din and T. A. Cheema, Analytical and numerical approaches to squeezing flow and heat transfer between two parallel disks with velocity slip and temperature jump, Chin. Phys. Lett., 29 (2012) 114705.

[74] A. R. A. Khaled and K. Vafai, Hydromagnetic squeezed flow and heat transfer over a sensor surface, Int. J. Eng. Sci., 42 (2004) $509 - 519$.

[75] M. Sheikholeslami, H. R. Ashorynejad, G. Domairry and I. Hashim, Flow and heat transfer of Cu-Water nanofluid between a stretching sheet and a porous surface in a rotating system, J. Appl. Math., 2012 (2012) 421320.

[76] H. M. Duwairi, B. Tashtoush and R. A. Damseh, On heat transfer effects of a viscous fluid squeezed and extruded between two parallel plates, Heat Mass Transfer, 41 (2004) $112 - 117$.

[77] E. A. Hamza, Unsteady flow between two disks with heat transfer in the presence of a magnetic field, J. Phys. D: Appl. Phys. 25 (1992) $1425 - 1431$.

[78] S. Bhattacharyya and A. Pal, Unsteady MHD squeezing flow between two parallel rotating discs, Mechanics Research Communications, 24 (1197) 615–623.

[79] E. Sweet, K. Vajravelu, R. A. Van Gorder and I. Pop, Analytical solution for the unsteady MHD flow of a viscous fluid between moving parallel plates, Comm. Nonlinear Sci. Numer. Simulat., 16 (2011) $266 - 273$.

[80] S. J. Liao, Beyond Perturbation: Introduction to homotopy analysis method, Chapman and Hall, CRC Press, Boca Raton (2003).

[81] H. S. Takhar, A. J. Chamkha and G. Nath, Flow and mass transfer on a stretching sheet with a magnetic field and chemically reactive species, Int. J. Eng. Sci., 38 (2000) $1303 - 1314$.

[82] T. Hayat, M. Mustafa and S. Obaidat, Soret and Dufour effects on the stagnation-point flow of a micropolar fluid toward a stretching sheet, ASME J. Fluid Engng. 133 (2011) 021202.

[83] B. Yao, Series solution of the temperature distribution in the Falkner-Skan wedge flow by the homotopy analysis method, Euro. J. Mech.B/Fluids, 28 (2009) $689 - 693$.

[84] D. Kumar, J. Singh and Sushila, Application of homotopy analysis transform method to fractional biological population model, Romanian Reports in Physics, 65 (2013) $63 - 75$.

[85] S. Abbasbandy, Homotopy analysis method for the Kawahara equation, Nonlinear Analysis: Real World Applications, 11 (2010) $307-312$.

[86] M. M. Rashidi, G. Domairry and S. Dinarvand, Approximate solutions for the Burger and regularized long wave equations by means of the homotopy analysis method, Comm. Nonlinear Sci. Numer. Simulat., 14 (2009) $708-717$.

[87] S. Abbasbandy, E. Shivanian and K. Vajravelu, Mathematical properties of h-curve in the frame work of the homotopy analysis method, Commun Nonlinear Sci Numer Simulat., 16 (2011) $4268-4275$.

[88] S. J. Liao, On the homotopy analysis method for nonlinear problems, Appl. Math. Comp., 147 (2004) $499-513$.

[89] M. M. Khader, S. Kumar and S. Abbasbandy, New homotopy analysis transform method for solving the discontinued problems arising in nanotechnology, Chin. Phys. B, 22 (2013) 110201.

[90] M. M. Khader, Numerical solution for discontinued problems arising in nanotechnology using HAM, J. Nano. Adv. Mat., 1 (2013) $59-67$.

[91] M. Turkyilmazoglu, Effective computation of exact and analytic approximate solutions to singular nonlinear equations of Lane-Emden-Flower type, Appl. Math. Modelling, 37 (2013) $7539-7548$.

[92] S. J. Liao, Homotopy Analysis Method in Nonlinear Differential Equations, Springer & Higher Education Press, 2012.

[93] T. Hayat and M. Mustafa, Influence of thermal radiation on the unsteady mixed convection flow of a Jeffrey fluid over a stretching sheet, Z. Naturforsch. (ZNA)., 65 (2010) $711-719$.

[94] M. M. Rashidi, M. T. Rastegari, M. Asadi and O. A. Bég, A study of non-Newtonian flow and heat transfer over a non-isothermal wedge using the homotopy analysis method, Chem. Eng. Comm., 199 (2012) $231-256$.

[95] S. Abbasbandy, M. S. Hashemi and I. Hashim, On convergence of homotopy analysis method and its application to fractional integro-differential equations, Quaestiones Mathematicae, 36 (2013) $93 - 105$.

[96] T. Hayat, R. Naz, A. Alsaedi and M. M. Rashidi, Hydromagnetic rotating flow of third grade fluid, Appl. Math. Mech. -Engl. Ed., 34 (2013) $1481 - 1494$.

[97] A. Lawal and D. M. Kalyon, Squeezing flow of viscoplastic fluids subject to wall slip, Polymer Processing Sci., 38 (1998) $1793 - 1804$.

[98] M. Ramzan, M. Farooq, A. Alsaedi and T. Hayat, MHD three-dimensional flow of couple stress fluid with Newtonian heating, Eur. Phys. J. Plus, 128 (2013) 49.

[99] S. Munawar, A. Mehmood and Asif Ali, Three-dimensional squeezing flow in a rotating channel of lower stretching porous wall, Comput. Math. Appl., 64 (2012) $1575 - 1586$.

[100] M. Turkyilmazoglu, Convergence of the homotopy perturbation method, Int. J. Nonlinear Sci. Numer. Simul., 12 (2011) $9 - 14$.

[101] A. Ishak, R. Nazar and I. Pop, Mixed convection on the stagnation point flow toward a vertical continuously stretching sheet, ASME J Heat Transfer, 129 (2007) $1087 - 1090$.

177